

CALIPSO Lidar Level 2 Profile Data Description Document

Version 5.00

Last Updated: October 5, 2025

Data Version: 5.00
Data Release Date: October 01, 2025
Data Date Range: June 12, 2006 to June 30, 2023

Introduction

The CALIPSO 5 km Cloud and Aerosol Profile Products (CPro and APro, respectively) report profiles of particulate extinction and backscatter coefficients along with additional parameters (e.g., particulate depolarization ratios) derived from these fundamental products. Layer optical depths are reported in the 5 km Cloud and Aerosol Layer Products. The layer optical depths are derived from the same retrievals used to compute the extinction profiles in the profile products. All of the extinction products are produced using the same fundamental algorithms ([Young and Vaughan, 2009](#); [Young et al., 2018](#)).

The cloud and aerosol profile products are reported at a uniform horizontal resolution of 5 km and over a nominal altitude range from 30 km to -0.5 km. Profile data for both tropospheric aerosol and stratospheric aerosol are reported in the aerosol profile product. Due to constraints imposed by the on-board data averaging scheme, the vertical resolution of the profile products varies as a function of altitude. In the tropospheric region between 20.2 km to -0.5 km, the profile products are reported at a resolution of 60 m vertically, while in the stratospheric region (above 20.2 km) the vertical resolution is 180 m.

Table of Contents

Introduction	1
Additional Documentation.....	5
Glossary and Acronym Dictionary	7
Data Product Descriptions	8
Scientific Data Sets: Measurement Altitudes.....	8
Lidar_Data_Altitudes (APro and CPro).....	8
Scientific Data Sets: Time and Position	8
Profile_Time (APro and CPro)	8
Profile_UTC_Time (APro and CPro).....	8
Day_Night_Flag (APro and CPro)	8
Profile_ID (APro and CPro).....	9
Latitude (APro and CPro).....	9
Longitude (APro and CPro).....	9
Scientific Data Sets: Column Integrated Parameters	9
Column_Integrated_Attenuated_Backscatter_532 (APro and CPro)	9
Column_IAB_Cumulative_Probability (APro and CPro)	10

Column_Optical_Depth_Cloud_532 (APro and CPro).....	10
Column_Optical_Depth_Cloud_Uncertainty_532 (APro and CPro)	10
Column_Optical_Depth_Tropospheric_Aerosols_532 (APro and CPro).....	11
Column_Optical_Depth_Tropospheric_Aerosols_1064 (APro and CPro).....	11
Column_Optical_Depth_Tropospheric_Aerosols_Uncertainty_532 (APro and CPro).....	12
Column_Optical_Depth_Tropospheric_Aerosols_Uncertainty_1064 (APro and CPro).....	12
Column_Optical_Depth_Stratospheric_Aerosols_532 (APro and CPro)	12
Column_Optical_Depth_Tropospheric_Aerosols_1064 (APro and CPro).....	12
Column_Optical_Depth_Stratospheric_Aerosols_Uncertainty_532 (APro and CPro)	12
Column_Optical_Depth_Stratospheric_Aerosols_Uncertainty_1064 (APro and CPro)	12
Column_Feature_Fraction (APro and CPro).....	12
Some Notes on Evaluating CALIOP Column Optical Properties	13
Scientific Data Sets: Profiles of Optical Properties	13
Total_Backscatter_Coefficient_532 (APro and CPro)	13
Total_Backscatter_Coefficient_Uncertainty_532 (APro and CPro)	14
Perpendicular_Backscatter_Coefficient_532 (APro and CPro).....	14
Perpendicular_Backscatter_Coefficient_Uncertainty_532 (APro and CPro).....	15
Particulate_Depolarization_Ratio_Profile_532 (APro and CPro).....	15
Particulate_Depolarization_Ratio_Uncertainty_532 (APro and CPro).....	16
Extinction_Coefficient_532 (APro and CPro)	16
Extinction_Coefficient_Uncertainty_532 (APro and CPro)	17
Backscatter_Coefficient_1064 (APro Only).....	18
Backscatter_Coefficient_Uncertainty_1064 (APro Only).....	18
Extinction_Coefficient_1064 (APro Only)	19
Extinction_Coefficient_Uncertainty_1064 (APro Only)	19
Ice_Water_Content_Profile (CPro Only).....	19
Ice_Water_Content_Profile_Uncertainty (CPro Only).....	20
Cloud_Multiple_Scattering_Profile_532 (CPro Only)	20
Aerosol_Multiple_Scattering_Profile_532 (APro Only)	21
Aerosol_Multiple_Scattering_Profile_1064 (APro Only)	21
Scientific Data Sets: Feature Type and Classification Confidence	21
Interpretation of 3-Dimensional SDSs.....	21
Atmospheric_Volume_Description (APro and CPro)	23
CAD_Score (APro and CPro)	24
Aerosol_Layer_Fraction (APro and CPro)	25
Cloud_Layer_Fraction (APro and CPro).....	26

Scientific Data Sets: Quality Assurance	26
Extinction_QC_Flag_532 (APro and CPro)	26
Extinction_QC_Flag_1064 (APro only)	26
Minimum_Laser_Energy_532 (APro and CPro)	27
Low_Energy_Mitigation_Column_QC_Flag (APro and CPro).....	27
Low_Energy_Mitigation_Feature_QC_Flag (APro and CPro).....	28
Unique_Layer_ID (APro and CPro)	28
Scientific Data Sets: Ancillary Meteorological Data	29
Molecular_Number_Density (APro and CPro)	29
Ozone_Number_Density (APro and CPro)	29
Temperature (APro and CPro).....	29
Pressure (APro and CPro)	29
Relative_Humidity (APro and CPro)	29
Surface_Wind_Speeds_02m (APro and CPro)	30
Tropopause_Height (APro and CPro)	30
Tropopause_Temperature (APro and CPro)	30
Scientific Data Sets: Surface Information.....	30
DEM_Surface_Elevation (APro and CPro)	30
IGBP_Surface_Type (APro and CPro)	30
Vgroup : Lidar_Surface_Detection	31
Surface_Top_Altitude_532	31
Surface_Top_Altitude_1064	31
Surface_Base_Altitude_532	31
Surface_Base_Altitude_1064	31
Surface_Integrated_Attenuated_Backscatter_532	32
Surface_Integrated_Attenuated_Backscatter_1064	32
Surface_532_Integrated_Depolarization_Ratio	32
Surface_1064_Integrated_Depolarization_Ratio	32
Surface_532_Integrated_Attenuated_Color_Ratio	32
Surface_1064_Integrated_Attenuated_Color_Ratio	32
Surface_Detection_Flags_532	32
Surface_Detection_Flags_1064	32
Surface_Overlying_Integrated_Attenuated_Backscatter_532	33
Surface_Overlying_Integrated_Attenuated_Backscatter_1064	33
Surface_Scaled_RMS_Background_532	33
Surface_Scaled_RMS_Background_1064	33

Surface_Peak_Signal_532	34
Surface_Peak_Signal_1064	34
Surface_Detections_333m_532.....	34
Surface_Detections_333m_1064.....	34
Surface_Detections_1km_532	34
Surface_Detections_1km_1064	34
Vgroup : Ocean_Derived_Column_Optical_Depth	34
ODCOD_Effective_Optical_Depth_532.....	34
ODCOD_Effective_Optical_Depth_532_Uncertainty.....	34
ODCOD_QC_Flag_532	35
ODCOD_Surface_Wind_Speeds_10m.....	35
ODCOD_Surface_Wind_Speed_Correction	35
Metadata Parameter Descriptions.....	36
Product_ID (APro and CPro).....	36
Date_Time_at_Granule_Start (APro and CPro)	36
Date_Time_at_Granule_End (APro and CPro).....	36
Date_Time_of_Production (APro and CPro)	36
Number_of_Bad_Profiles (APro and CPro)	36
Number_of_Good_Profiles (APro and CPro)	36
Initial_Subsatellite_Latitude (APro and CPro).....	36
Initial_Subsatellite_Longitude (APro and CPro).....	36
Final_Subsatellite_Latitude (APro and CPro)	36
Final_Subsatellite_Longitude (APro and CPro)	36
Orbit_Number_at_Granule_Start (APro and CPro)	37
Path_Number_at_Granule_Start (APro and CPro)	37
Rayleigh_Extinction_Cross-section_532 (APro and CPro)	37
Rayleigh_Extinction_Cross-section_1064 (APro and CPro)	37
Rayleigh_Backscatter_Cross-section_532 (APro and CPro).....	37
Rayleigh_Backscatter_Cross-section_1064 (APro and CPro).....	37
Ozone_Absorption_Cross-section_532 (APro and CPro).....	38
Ozone_Absorption_Cross-section_1064 (APro and CPro).....	38
Lidar_Level_1_Production_Date_Time (APro and CPro)	38
Ocean_Fresnel_Reflection_Coefficient_532 (APro and CPro).....	38
MERRA-2_Wind_Uncertainty (APro and CPro).....	38
AMSR_Wind_Correction_Uncertainty (APro and CPro)	38
Lidar_Data_Altitude (APro and CPro)	38

Initial_Lidar_Ratio_Clouds_532 (CPro only)	38
Initial_Lidar_Ratio_Tropospheric_Aerosols_532 (APro only)	38
Initial_Lidar_Ratio_Stratospheric_Aerosols_1064 (APro only)	38
Initial_Lidar_Ratio_Stratospheric_Aerosols_532 (APro only)	39
Initial_Lidar_Ratio_Tropospheric_Aerosols_1064 (APro only)	39
GEOS_Version (APro and CPro)	39
GMAO_Files_Used (APro and CPro)	39
Classifier_Coefficients_Version_Number (APro and CPro)	39
Classifier_Coefficients_Version_Date (APro and CPro)	39
Production_Script (APro and CPro)	39
CALIPSO Data Quality Information	39
Data Release Information	39
Relevant External Documentation	40
Data Release Information	42
Data Quality Summaries	43
Data Quality Statement for CALIPSO's Version 5.00 Lidar Level 2 Data Product Release	43
Data Quality Statement for CALIPSO's Version 4.51 Lidar Level 2 Data Product Release	58
Data Quality Statement for CALIPSO's Version 4.21 Lidar Level 2 Data Product Release	64
Data Quality Statement for CALIPSO's Version 4.20 Lidar Level 2 Data Product Release	64
Data Quality Statement for CALIPSO's Version 4.10 Lidar Level 2 Data Product Release	65
Data Quality Statement for CALIPSO's Version 3.41 Lidar Level 2 Data Product Release	74
Data Quality Statement for CALIPSO's Version 3.40 Lidar Level 2 Data Product Release	74
Data Quality Statement for CALIPSO's Version 3.30 Lidar Level 2 Data Product Release	74
Data Quality Statement for CALIPSO's Version 3.02 Lidar Level 2 Data Product Release	75
Data Quality Statement for CALIPSO's Version 3.01 Lidar Level 2 Data Product Release	75
Data Quality Statement for CALIPSO's Version 2.02 Lidar Level 2 Data Product Release	79
Data Quality Statement for CALIPSO's Version 2.01 Lidar Level 2 Data Product Release	80
Data Quality Statement for CALIPSO's Version 1.10 Lidar Level 2 Data Product Release	82
Appendix 1	82
References	84

Additional Documentation

Project Documentation

- CALIPSO Data Management Team: CALIPSO Data Products Catalog, PC-SCI-503, Release 5.00.

- Hostetler, C. A., Z. Liu, J. Reagan, M. Vaughan, D. Winker, M. Osborn, W. H. Hunt, K. A. Powell, and C. Trepte, 2006: CALIOP Algorithm Theoretical Basis Document: Calibration and Level 1 Data Products, PC-SCI-201 Release 1.0, <insert NTRS link here>
- Winker, D. M., C. A. Hostetler, M. A. Vaughan, and A. H. Omar, 2006: CALIOP Algorithm Theoretical Basis Document: Part 1 : CALIOP Instrument, and Algorithms Overview, PC-SCI-202 Part 1 Release 2.0, <insert NTRS link here>
- Vaughan, M. A., D. M. Winker, and K. A. Powell, 2005: CALIOP Algorithm Theoretical Basis Document Part 2: Feature Detection and Layer Properties Algorithms, PC-SCI-202 Part 2 Release 1.01, <insert NTRS link here>
- Liu, Z., A. H. Omar, Y. Hu, M. A. Vaughan, and D. M. Winker, 2005: CALIOP Algorithm Theoretical Basis Document: Part 3: Scene Classification Algorithms, PC-SCI-202 Part 3 Release 1.0, <insert NTRS link here>

Peer-Reviewed Algorithm Papers

- Avery, M. A., R. A. Ryan, B. J. Getzewich, M. A. Vaughan, D. M. Winker, Y. Hu, A. Garnier, J. Pelon, and C. A. Verhappen, 2020: "CALIOP V4 Cloud Thermodynamic Phase Assignment and the Impact of Near-Nadir Viewing Angles", *Atmos. Meas. Tech.*, **13**, 4539–4563, <https://doi.org/10.5194/amt-13-4539-2020>.
- Hunt, W. H., D. M. Winker, M. A. Vaughan, K. A. Powell, P. L. Lucker, and C. Weimer, 2009: CALIPSO Lidar Description and Performance Assessment, *J. Atmos. Oceanic Technol.*, **26**, 1214–1228, <https://doi.org/10.1175/2009JTECHA1223.1>.
- Kim, M.-H., A. H. Omar, J. L. Tackett, M. A. Vaughan, D. M. Winker, C. R. Trepte, Y. Hu, Z. Liu, L. R. Poole, M. C. Pitts, J. Kar, and B. E. Magill, 2018: The CALIPSO Version 4 Automated Aerosol Classification and Lidar Ratio Selection Algorithm, *Atmos. Meas. Tech.*, **11**, 6107–6135, <https://doi.org/10.5194/amt-11-6107-2018>.
- Liu, Z., J. Kar, S. Zeng, J. Tackett, M. Vaughan, M. Avery, J. Pelon, B. Getzewich, K.-P. Lee, B. Magill, A. Omar, P. Lucker, C. Trepte, and D. Winker, 2019: Discriminating Between Clouds and Aerosols in the CALIOP Version 4.1 Data Products, *Atmos. Meas. Tech.*, **12**, 703–734, <https://doi.org/10.5194/amt-12-703-2019>.
- Tackett, J. L., J. Kar, M. A. Vaughan, B. Getzewich, M.-H. Kim, J.-P. Vernier, A. H. Omar, B. Magill, M. C. Pitts, and D. Winker, 2023: "The CALIPSO version 4.5 stratospheric aerosol subtyping algorithm", *Atmos. Meas. Tech.*, **16**, 745–768, <https://doi.org/10.5194/amt-16-745-2023>.
- Vaughan, M., K. Powell, R. Kuehn, S. Young, D. Winker, C. Hostetler, W. Hunt, Z. Liu, M. McGill, and B. Getzewich, 2009: Fully Automated Detection of Cloud and Aerosol Layers in the CALIPSO Lidar Measurements, *J. Atmos. Oceanic Technol.*, **26**, 2034–2050, <https://doi.org/10.1175/2009JTECHA1228.1>.
- Winker, D. M., M. A. Vaughan, A. H. Omar, Y. Hu, K. A. Powell, Z. Liu, W. H. Hunt, and S. A. Young, 2009: Overview of the CALIPSO Mission and CALIOP Data Processing Algorithms, *J. Atmos. Oceanic Technol.*, **26**, 2310–2323, <https://doi.org/10.1175/2009JTECHA1281.1>.
- Young, S. A. and M. A. Vaughan, 2009: The retrieval of profiles of particulate extinction from Cloud Aerosol Lidar Infrared Pathfinder Satellite Observations (CALIPSO) data: Algorithm description, *J. Atmos. Oceanic Technol.*, **26**, 1105–1119, <https://doi.org/10.1175/2008JTECHA1221.1>.
- Young, S. A., M. A. Vaughan, R. E. Kuehn, and D. M. Winker, 2013: The Retrieval of Profiles of Particulate Extinction from Cloud-Aerosol Lidar Infrared Pathfinder Satellite Observations (CALIPSO) Data: Uncertainty and Error Sensitivity Analyses, *J. Atmos. Oceanic Technol.*, **30**, 395–428, <https://doi.org/10.1175/JTECH-D-12-00046.1>.
- Young, S. A., M. A. Vaughan, J. L. Tackett, A. Garnier, J. B. Lambeth, and K. A. Powell, 2018: Extinction and Optical Depth Retrievals for CALIPSO's Version 4 Data Release, *Atmos. Meas. Tech.*, **11**, 5701–5727, <https://doi.org/10.5194/amt-11-5701-2018>.

Glossary and Acronym Dictionary

Term	Meaning
AMSL	above mean sea level
AMSR	Advanced Microwave Scanning Radiometer
AOD	aerosol optical depth
APro	aerosol profile product
AVD	atmospheric volume description
CAD	cloud-aerosol discrimination
CALIOP	Cloud-Aerosol Lidar with Orthogonal Polarization
CALIPSO	Cloud-Aerosol Lidar and Infrared Pathfinder Satellite Observation
CERES	Clouds and the Earth's Radiant Energy System
CPro	cloud profile product
DEM	digital elevation model
FCF	feature classification flags
frame	a fundamental data averaging interval used extensively in CALIOP's level 1 and level 2 data processing. A frame consists of 15 consecutive single-shot profiles spanning an along-track distance of ~5 km. 15 shots is the least common multiple of the along-track averaging intervals defined by CALIOP's vertically varying onboard data averaging scheme (Hunt et al., 2009).
GMAO	Global Modeling and Assimilation Office
granule	continuous data segment in which all measurements were acquired while the lidar was configured for daytime data acquisition only or nighttime data acquisition only; each granule spans approximately one half of a full orbit, with daytime granules being slightly larger/longer than nighttime granules
HOI	horizontally oriented ice
HSRL	high spectral resolution lidar
IGBP	International Geosphere–Biosphere Programme
IIR	imaging infrared radiometer
L1B	level 1B
LEM	low energy mitigation
MERRA-2	Modern-Era Retrospective analysis for Research and Applications, Version 2
MHz	megahertz
N/A	not applicable
ODCOD	ocean-derived column optical depth
QC	quality control/quality assurance
RMS	root mean square
SNR	signal-to-noise ratio
SDS	scientific data set
sr	steradian
TAI	International Atomic Time
UTC	Coordinated Universal Time
WRS	Worldwide Reference System

Data Product Descriptions

Three main configurations of scientific data sets (SDSs) are reported in the CALIOP profile products. SDSs for optical properties (e.g., particulate extinction coefficients) are $N \times 399$ arrays, where N is the number of along-track 5 km columns in a granule and 399 is the number of altitude bins in each column. SDSs reporting column-specific information (e.g., latitude and longitude) are $N \times 1$ arrays. Finally, SDSs reporting feature classifications and/or diagnostic information at sub-range bin resolution (e.g., the atmospheric volume description) are reported as $N \times 399 \times 2$ matrices, where the first $N \times 399$ submatrix reports findings in the upper 30 m bin in each 60 m vertical average and the second $N \times 399$ submatrix reports findings in the lower 30 m bin. For altitudes above 8.2 km, where the vertical resolution of CALIOP's downlinked data is 60 m or larger, identical information is reported in the upper and lower submatrices.

Scientific Data Sets: Measurement Altitudes

Lidar_Data_Altitudes (APro and CPro)

Units: km

Format: Float_32

Valid range: -2.0000 30.0000

Dimensions: 399×1

Description: Altitudes (above mean sea level) that specify the midpoints of the 399 vertical bins in the CALIOP level 2 profile products. Vertical resolution is 60 m from -0.5 km to 20.2 km and 180 m at higher altitudes. This scientific data set (SDS) is only available in the V5.00 data release. In all prior versions, the lidar data altitude array was stored in the file metadata.

Scientific Data Sets: Time and Position

Profile_Time (APro and CPro)

Units: TAI seconds

Format: Float_64

Valid range: 420300000.0000 962300000.0000

Dimensions: number of profiles $\times 1$

Description: [International Atomic Time](#) (TAI) in elapsed seconds from January 1, 1993. Three values are reported: the time for the first pulse included in the 15 shot average; the time at the temporal midpoint (i.e., at the 8th of 15 consecutive laser shots); and the time for the final pulse.

Profile_UTC_Time (APro and CPro)

Units: yymmdd.ffffffff

Format: Float_64

Valid range: 60428.0000 230701.0000

Dimensions: number of profiles $\times 1$

Description: [Coordinated Universal Time \(UTC\)](#), formatted as yymmdd.ffffffff, where yy is a two digit data acquisition year number (06 to 23), mm is a month number (01 to 12), dd is a day number (1 to 31), and ffffffff is the elapsed fraction of the data acquisition day. Three values are reported: the time for the first pulse included in the 15 shot average; the time at the temporal midpoint (i.e., at the 8th of 15 consecutive laser shots); and the time for the final pulse.

Day_Night_Flag (APro and CPro)

Units: NoUnits

Format: Int_8

Valid range: 0 1

Dimensions: number of profiles × 1

Description: As CALIPSO approaches the terminator, the lidar is automatically reconfigured to adapt to changing lighting conditions that [directly impact signal-to-noise \(SNR\) levels](#). These changes occur at Sun-Earth-Satellite (SES) angles of 95° (day to night) and 265° (night to day), corresponding to changes in lighting conditions at an altitude of ~24 km above mean sea level. 0 indicates daytime measurement configuration, 1 indicates nighttime.

Profile_ID (APro and CPro)

Units: NoUnits

Format: Int_32

Valid range: 1 228630

Dimensions: number of profiles × 1

Description: Unique profile identifier generated sequentially for each lidar level 1b profile. Level 1b profile IDs are guaranteed to be unique within each granule but not unique over multiple granules. The level 2 profile products report the first and last profile IDs for the 15 consecutive lasers pulses averaged to create each 5 km profile product data record.

Latitude (APro and CPro)

Units: degrees_north

Format: Float_32

Valid range: -90.0000 90.0000

Dimensions: number of profiles × 1

Fill value: -9999

Description: Geodetic latitude of the laser footprint on the Earth's surface. Three values are reported: the footprint latitude for the first pulse included in the 15 shot average; the footprint latitude at the temporal midpoint (i.e., at the 8th of 15 consecutive laser shots); and the footprint latitude for the final pulse.

Longitude (APro and CPro)

Units: degrees_east

Format: Float_32

Valid range: -180.0000 180.0000

Dimensions: number of profiles × 1

Fill value: -9999

Description: Longitude of the laser footprint on the Earth's surface. Three values are reported: the footprint longitude for the first pulse included in the 15 shot average; the footprint longitude at the temporal midpoint (i.e., at the 8th of 15 consecutive laser shots); and the footprint longitude for the final pulse.

Scientific Data Sets: Column Integrated Parameters

Column_Integrated_Attenuated_Backscatter_532 (APro and CPro)

Units: 1/sr

Format: Float_32

Valid range: 0.0000 2.0000

Dimensions: number of profiles × 1

Fill value: -9999

Flag values: -111.0 = column data quality degraded due to low laser energy

Description: The integral with respect to altitude of the 5 km horizontal average (15 shots) of the profiles of 532 nm total attenuated backscatter coefficients reported in the CALIOP level 1b product. The limits of integration are from the onset of the backscatter signal at ~40 km, down to the range bin immediately prior to the surface elevation specified by the digital elevation model (DEM). The column integrated attenuated backscatter provides a measure of atmospheric turbidity above the surface.

Column_IAB_Cumulative_Probability (APro and CPro)

Units: NoUnits

Format: Float_32

Valid range: 0.0000 1.0000

Dimensions: number of profiles \times 1

Fill value: -9999

Flag values: -111.0 = column data quality degraded due to low laser energy

Description: The cumulative probability of measuring a 532 nm total column integrated attenuated backscatter (γ'_{532}) value equal to the value computed for the current profile. For any profile, the limits of integration for γ'_{532} are from the first range in the profile, at ~40 km, down to one range bin above the surface altitude specific by the CALIPSO DEM. Values in this field range between 0 and 1. **Error! Reference source not found.** shows the cumulative probability distribution compiled using all CALIOP single shot γ'_{532} measurements acquired between 2008-07-01 thru 2008-07-15.

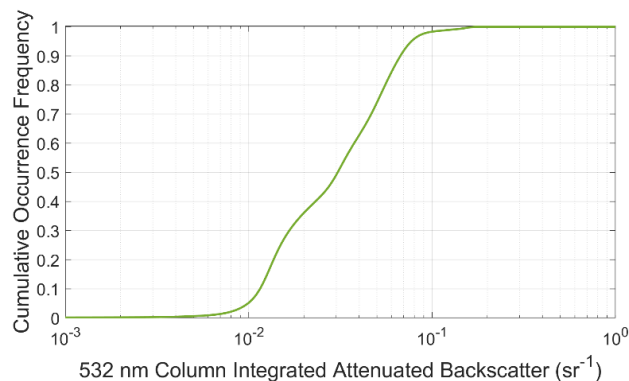


Figure 1: Cumulative distribution of 532 nm single shot total column integrated attenuated backscatter

Column_Optical_Depth_Cloud_532 (APro and CPro)

Units: NoUnits

Format: Float_32

Valid range: 0.0000 25.0000

Dimensions: number of profiles \times 1

Fill value: -9999

Flag values: -111.0 = column data quality degraded due to low laser energy

-333.0 = failed extinction retrieval within a column

-444.0 = suspicious/incomplete single-shot cloud clearing within a column

Description: Optical depth of all clouds detected within each 5 km vertical column, obtained by integrating the 532 nm cloud extinction profile reported in the CALIPSO 5 km Cloud Profile Products from the uppermost range bin to the lowest range bin.

Column_Optical_Depth_Cloud_Uncertainty_532 (APro and CPro)

Units: NoUnits

Format: Float_32

Dimensions: number of profiles \times 1

Fill value: -9999

Flag values: -111.0 = column data quality degraded due to low laser energy
-333.0 = failed extinction retrieval within a column
-444.0 = suspicious/incomplete single-shot cloud clearing within a column

Description: Estimated uncertainty in the Column Optical Depth Cloud 532 parameter calculated using

$$\Delta\tau_p = \sqrt{(\gamma_p \cdot \Delta\overline{S_p})^2 + (\Delta\gamma_p \cdot \overline{S_p})^2} . \quad (1)$$

$\Delta\tau_p$ is the uncertainty in the column optical depth and γ_p and $\Delta\gamma_p$ are, respectively, the column integrated particulate backscatter and its associated uncertainty. These quantities are computed using [trapezoid rule integration](#).

$$\gamma_p = \frac{1}{2} \sum_{n=TOA+1}^{surface} (z_{n-1} - z_n) (\beta_p(z_{n-1}) + \beta_p(z_n)) \quad (2)$$

$$\Delta\gamma_p = \sqrt{\frac{1}{4} \sum_{n=TOA+1}^{surface} (z_{n-1} - z_n)^2 \times (\Delta\beta_p(z_n)^2 + \Delta\beta_p(z_{n-1})^2)} \quad (3)$$

In those range bins for which $\beta(z_n)$ is a fill value (i.e., no feature detected), $\beta(z_n)$ is set to 0 prior to computing γ_p and $\Delta\gamma_p$.

$\overline{S_p}$ and $\Delta\overline{S_p}$ are, respectively, the backscatter-weighted column mean lidar ratio and its uncertainty, calculated for non-zero values of $\beta(z_n)$ as follows.

$$\overline{S_p} = \frac{\frac{1}{N} \sum_{n=TOA}^{surface} \beta(z_n) \times S_p(z_n)}{\frac{1}{N} \sum_{n=TOA}^{surface} \beta(z_n)} \quad (4)$$

The quantity N is initialized to 0, then incremented by 1 whenever $\beta(z_n) \neq 0$.

$$\Delta\overline{S_p} = \frac{\frac{1}{N} \sum_{n=TOA}^{surface} \beta(z_n) \times \Delta S_p(z_n)}{\frac{1}{N} \sum_{n=TOA}^{surface} \beta(z_n)} \quad (5)$$

Column_Optical_Depth_Tropospheric_Aerosols_532 (APro and CPro)

Column_Optical_Depth_Tropospheric_Aerosols_1064 (APro and CPro)

Units: NoUnits

Format: Float_32

Valid range: 0.0000 3.0000

Dimensions: number of profiles \times 1

Fill value: -9999

Flag values: -111.0 = column data quality degraded due to low laser energy
-333.0 = failed extinction retrieval within a column
-444.0 = suspicious/incomplete single-shot cloud clearing within a column

Description: Optical depth of all tropospheric aerosols detected within each 5 km vertical column, obtained by integrating, respectively, the 532 nm and 1064 nm tropospheric aerosol extinction coefficients reported in the CALIPSO 5 km Aerosol Profile Products from the uppermost range bin to the lowest range bin. At both

wavelengths, total column aerosol optical depth (AOD) is the sum of the tropospheric and stratospheric column AODs.

Column_Optical_Depth_Tropospheric_Aerosols_Uncertainty_532 (APro and CPro)

Column_Optical_Depth_Tropospheric_Aerosols_Uncertainty_1064 (APro and CPro)

Units: NoUnits

Format: Float_32

Dimensions: number of profiles × 1

Fill value: -9999

Flag values: -111.0 = column data quality degraded due to low laser energy
-333.0 = failed extinction retrieval within a column
-444.0 = suspicious/incomplete single-shot cloud clearing within a column

Description: Estimated uncertainty in, respectively the Column Optical Depth Tropospheric Aerosol 532 and Column Optical Depth Tropospheric Aerosol 1064 parameters, calculated according to equations 1 through 5 above.

Column_Optical_Depth_Stratospheric_Aerosols_532 (APro and CPro)

Column_Optical_Depth_Stratospheric_Aerosols_1064 (APro and CPro)

Units: NoUnits

Format: Float_32

Valid range: 0.0000 3.0000

Dimensions: number of profiles × 1

Fill value: -9999

Flag values: -111.0 = column data quality degraded due to low laser energy
-333.0 = failed extinction retrieval within a column
-444.0 = suspicious/incomplete single-shot cloud clearing within a column

Description: Optical depth of all stratospheric aerosols detected within each 5 km vertical column, obtained by integrating, respectively, the 532 nm and 1064 nm stratospheric aerosol extinction coefficients reported in the CALIPSO 5 km Aerosol Profile Products from the uppermost range bin to the lowest range bin. At both wavelengths, total column AOD is the sum of the tropospheric and stratospheric column AODs.

Column_Optical_Depth_Stratospheric_Aerosols_Uncertainty_532 (APro and CPro)

Column_Optical_Depth_Stratospheric_Aerosols_Uncertainty_1064 (APro and CPro)

Units: NoUnits

Format: Float_32

Dimensions: number of profiles × 1

Fill value: -9999

Flag values: -111.0 = column data quality degraded due to low laser energy
-333.0 = failed extinction retrieval within a column
-444.0 = suspicious/incomplete single-shot cloud clearing within a column

Description: Estimated uncertainty in, respectively the Column Optical Depth Stratospheric Aerosol 532 and Column Optical Depth Stratospheric Aerosol 1064 parameters, calculated according to equations 1 through 5 above.

Column_Feature_Fraction (APro and CPro)

Units: NoUnits

Format: Float_32

Valid range: 0.0000 1.0000

Dimensions: number of profiles × 1

Fill value: -9999

Flag values: -111.0 = column data quality degraded due to low laser energy

Description: The fraction of the 5-km horizontally averaged profile, between 30-km and the DEM surface elevation, which has been identified as containing an atmospheric feature (i.e., either a cloud, an aerosol, or a stratospheric layer) at any of the 5 km, 20 km, or 80 km horizontal averaging resolutions.

Some Notes on Evaluating CALIOP Column Optical Properties

Opacity: The CALIPSO lidar is only capable of penetrating to the surface in columns with total particulate optical depths less than ~5. (Note that this value considers the contribution of multiple scattering.) In opaque columns (i.e., when the column backscatter signal is totally attenuated before the Earth's surface can be detected), the reported "column" optical depths do not characterize the full vertical column, but instead report the integral of the particulate extinction coefficients from ~30 km down to the apparent base of the lowest feature observed. In the layer products, the opacity of any column can be determined by inspecting the opacity flag. Values of 1 indicate that the lowest detected layer in the column is classified as opaque.

Extinction QC: The extinction QC values in the column should be examined to determine if any of the cloud or aerosol extinction retrievals either failed or converged under suspicious circumstances. Low quality extinction retrievals in overlying layers can degrade the reliability of all extinction retrievals in the layers below (Young and Vaughan, 2009). For transparent layers, constrained retrievals (extinction QC = 1) yield the highest quality solutions. Solutions for which the final lidar ratio is unchanged from the initial estimate (extinction QC = 0) also generate physically plausible solutions. On the other hand, retrievals for which the initial lidar ratio must be reduced to achieve a solution can be problematic, as the retrieved optical depths in these cases tend to be biased high.

CAD Scores and Feature Subtypes: Irrespective of the extinction QC flag, extinction solutions for features with low magnitude CAD scores (e.g., $|CAD| \leq 20$) or "special" CAD scores should be regarded with caution. These features could not be confidently classified as either cloud or aerosol, and this lack of confidence extends to the choice of initial lidar ratio used in the extinction solution. Similarly, uncertain aerosol type classifications lead to increased uncertainties in the lidar ratios and hence lower confidence in the extinction retrievals.

Cloud phase: The extinction solutions in columns containing clouds predominately composed of horizontal oriented ice (HOI) crystals are likely to be highly unreliable. The anomalously high backscatter generated by HOI clouds, coupled with very low skill in selecting an appropriate lidar ratio for these clouds, frequently yields very large overestimates of cloud extinction coefficients and optical depths (e.g., [Mioche et al., 2010](#)).

Scientific Data Sets: Profiles of Optical Properties

Total_Backscatter_Coefficient_532 (APro and CPro)

Units: 1/(km * sr)

Format: Float_32

Valid range: 0.0000 0.0500 (aerosol)

Valid range: 0.0000 1.5000 (cloud)

Dimensions: number of profiles × 399

Fill value: -9999

Flag values: -111.0 = column data quality degraded due to low laser energy

-333.0 = failed extinction retrieval within a column

-444.0 = suspicious/incomplete single-shot cloud clearing within a column

Description: 532 nm total particulate backscatter coefficients, $\beta_{T,532}(z)$, reported for all range bins in which clouds (CPro) or aerosols (APro) were detected. Total particulate backscatter coefficients are the sum of the parallel and perpendicular channel particulate backscatter coefficients; i.e., $\beta_{T,532}(z) = \beta_{\parallel,532}(z) + \beta_{\perp,532}(z)$. A detailed description of the algorithms used to retrieve CALIOP backscatter and extinction coefficients is found in [Young et al., 2018](#).

Total_Backscatter_Coefficient_Uncertainty_532 (APro and CPro)

Units: 1/(km * sr)

Format: Float_32

Dimensions: number of profiles × 399

Fill value: -9999

Flag values: -111.0 = column data quality degraded due to low laser energy
 -333.0 = failed extinction retrieval within a column
 -444.0 = suspicious/incomplete single-shot cloud clearing within a column
 -29.0 = retrieval attempted on an opaque water cloud

Description: Absolute uncertainties for the 532 nm total particulate backscatter coefficients reported for all range bins in which clouds (CPro) or aerosols (APro) were detected. Backscatter and extinction retrievals in opaque water clouds are extremely uncertain, hence a special fill value of -29 is assigned for all range bins in these layers. A detailed description of the algorithms used to retrieve CALIOP backscatter and extinction coefficient uncertainties is found in the [supplemental material for Young et al., 2018](#). Figure 2 shows the cumulative distribution of relative uncertainties, $\Delta\beta_{532}(z) / \beta_{532}(z)$, for all transparent cirrus clouds detected at 5 km averaging resolution in all nighttime measurements acquired during February 2019.

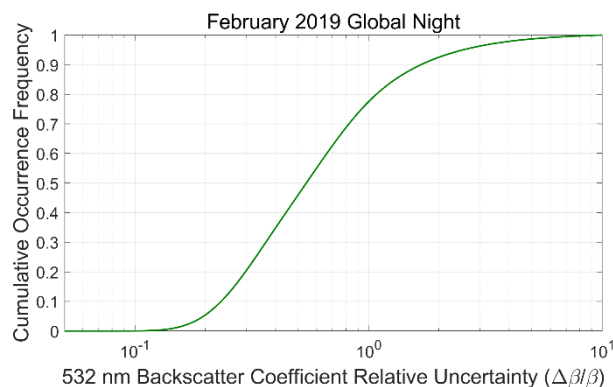


Figure 2. Relative uncertainty in the 532 nm backscatter coefficients retrieved within transparent cirrus detected at 5 km averaging resolution during global nighttime measurements acquired in February 2019.

Perpendicular_Backscatter_Coefficient_532 (APro and CPro)

Units: 1/(km * sr)

Format: Float_32

Valid range: 0.0000 0.0100 (aerosol)

Valid range: 0.0000 0.3500 (cloud)

Dimensions: number of profiles × 399

Fill value: -9999

Flag values: -111.0 = column data quality degraded due to low laser energy
 -333.0 = failed extinction retrieval within a column
 -444.0 = suspicious/incomplete single-shot cloud clearing within a column

Description: 532 nm perpendicular channel particulate backscatter coefficients ($\beta_{\perp,532}(z)$) reported for all range bins in which clouds (CPro) or aerosols (APro) were detected. Values are derived via equation (6) using the

retrieved particulate extinction profile ([Young & Vaughan, 2009](#)), from which we obtain the altitude resolved particulate two-way transmittance profile, $T_p^2(z)$; the molecular and ozone two-way transmittance profiles ($T_m^2(z)$ and $T_{O_3}^2(z)$, respectively) calculated from the [MERRA-2 meteorological data](#); the molecular backscatter coefficients, also from MERRA-2; and the measurements of attenuated backscatter coefficients made in the 532 nm perpendicular channel. The perpendicular component of the molecular backscatter coefficients is calculated using the depolarization ratio of Cabannes scattering, $D_c = 0.00366$ ([Powell et al., 2009](#)); i.e.,

$$\beta_{\perp,p}(z) = \frac{\beta'_{\perp}(z)}{T_p^2(z) \cdot T_m^2(z) \cdot T_{O_3}^2(z)} - \beta_{\perp,m}(z) \quad (6)$$

where $\beta_{\perp,m}(z) = D_c \times \beta_{T,m}(z)$ and $\beta_{T,m}(z)$ is the total molecular backscatter coefficient.

Perpendicular_Backscatter_Coefficient_Uncertainty_532 (APro and CPro)

Units: 1/(km * sr)

Format: Float_32

Dimensions: number of profiles × 399

Fill value: -9999

Flag values: -111.0 = column data quality degraded due to low laser energy
 -333.0 = failed extinction retrieval within a column
 -444.0 = suspicious/incomplete single-shot cloud clearing within a column
 -29.0 = retrieval attempted on an opaque water cloud

Description: Absolute uncertainties for the 532 nm perpendicular channel particulate backscatter coefficients reported for all range bins in which clouds (CPro) or aerosols (APro) were detected. Uncertainty estimates are obtained by applying a standard [propagation of errors](#) to equation (1).

Particulate_Depolarization_Ratio_Profile_532 (APro and CPro)

Units: NoUnits

Format: Float_32

Valid range: 0.0000 1.0000

Dimensions: number of profiles × 399

Fill value: -9999

Flag values: -111.0 = column data quality degraded due to low laser energy
 -333.0 = failed extinction retrieval within a column
 -444.0 = suspicious/incomplete single-shot cloud clearing within a column

Description: 532 nm particulate depolarization ratios, $\delta_p(z)$, are reported for all range bins in which either clouds (CPro) or aerosols (APro) were detected. Particulate depolarization ratios are computed by dividing the 532 nm perpendicular channel particulate backscatter coefficients by the 532 nm parallel channel particulate backscatter coefficients; i.e., $\delta_p(z) = \beta_{\perp,p}(z) / \beta_{\parallel,p}(z)$.

The quality of the $\delta_p(z)$ estimates is determined not only by the SNR of the backscatter measurements in parallel and perpendicular channels, but also the accuracy of the range-resolved two-way transmittance estimates within the layer. The two-way transmittances due to molecules and ozone are well characterized via the model data obtained from the [MERRA-2 meteorological data](#). The two-way transmittances due to particulates, however, are only as accurate as the CALIOP extinction retrieval. Retrievals near the apparent base within opaque layers can be particularly prone to errors in the particulate depolarization ratio, where very large attenuation corrections are applied to very weak, highly attenuated signals. On those occasions where one channel or the other becomes totally attenuated, this situation can generate very large, negative particulate depolarization ratio estimates. For layers that are not opaque, $\delta_p(z)$ is generally

reliable. However, in weakly scattering layers, the quality of the daytime estimate can be degraded by a factor of 2-4 due to the larger background noise compared with the nighttime estimate.

Particulate_Depolarization_Ratio_Uncertainty_532 (APro and CPro)

Units: NoUnits

Format: Float_32

Dimensions: number of profiles \times 399

Fill value: -9999

Flag values: -111.0 = column data quality degraded due to low laser energy
-333.0 = failed extinction retrieval within a column
-444.0 = suspicious/incomplete single-shot cloud clearing within a column
-29.0 = retrieval attempted on an opaque water cloud

Description: Absolute uncertainties for the 532 nm particulate depolarization ratios are calculated using standard [propagation of errors](#) and reported for all range bins in which clouds (CPro) or aerosols (APro) were detected.

Extinction_Coefficient_532 (APro and CPro)

Units: 1/km

Format: Float_32

Valid range: 0.0000 1.2500 (aerosol)

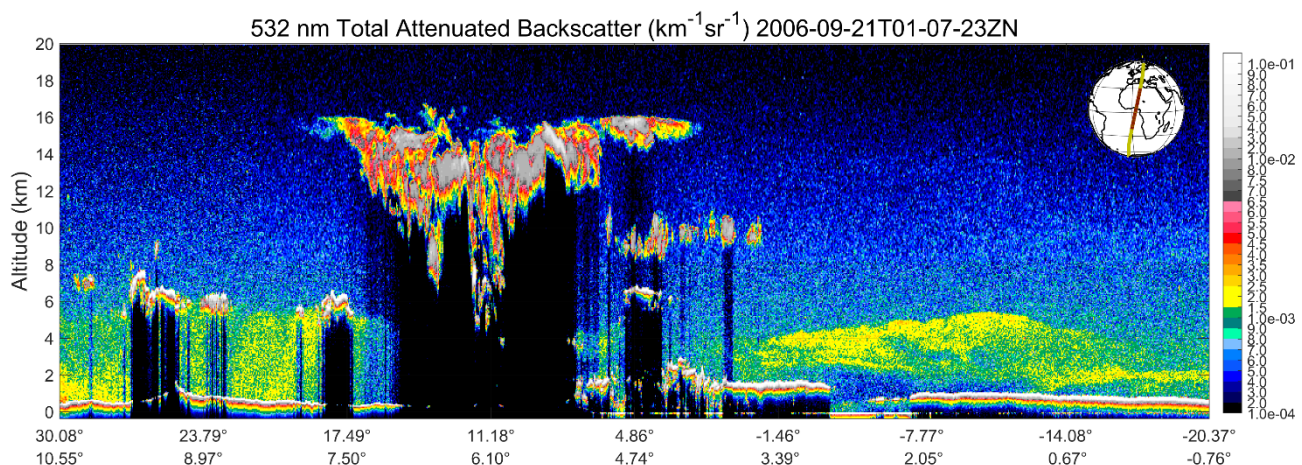
Valid range: 0.0000 12.0000 (cloud)

Dimensions: number of profiles \times 399

Fill value: -9999

Flag values: -111.0 = column data quality degraded due to low laser energy
-333.0 = failed extinction retrieval within a column
-444.0 = suspicious/incomplete single-shot cloud clearing within a column

Description: 532 nm particulate extinction coefficients reported for all range bins in which clouds (CPro) or aerosols (APro) were detected. A detailed description of the algorithms used to retrieve CALIOP backscatter and extinction coefficients is found in [Young et al., 2018](#). Cloud and aerosol extinction retrievals are illustrated in Figure 3.



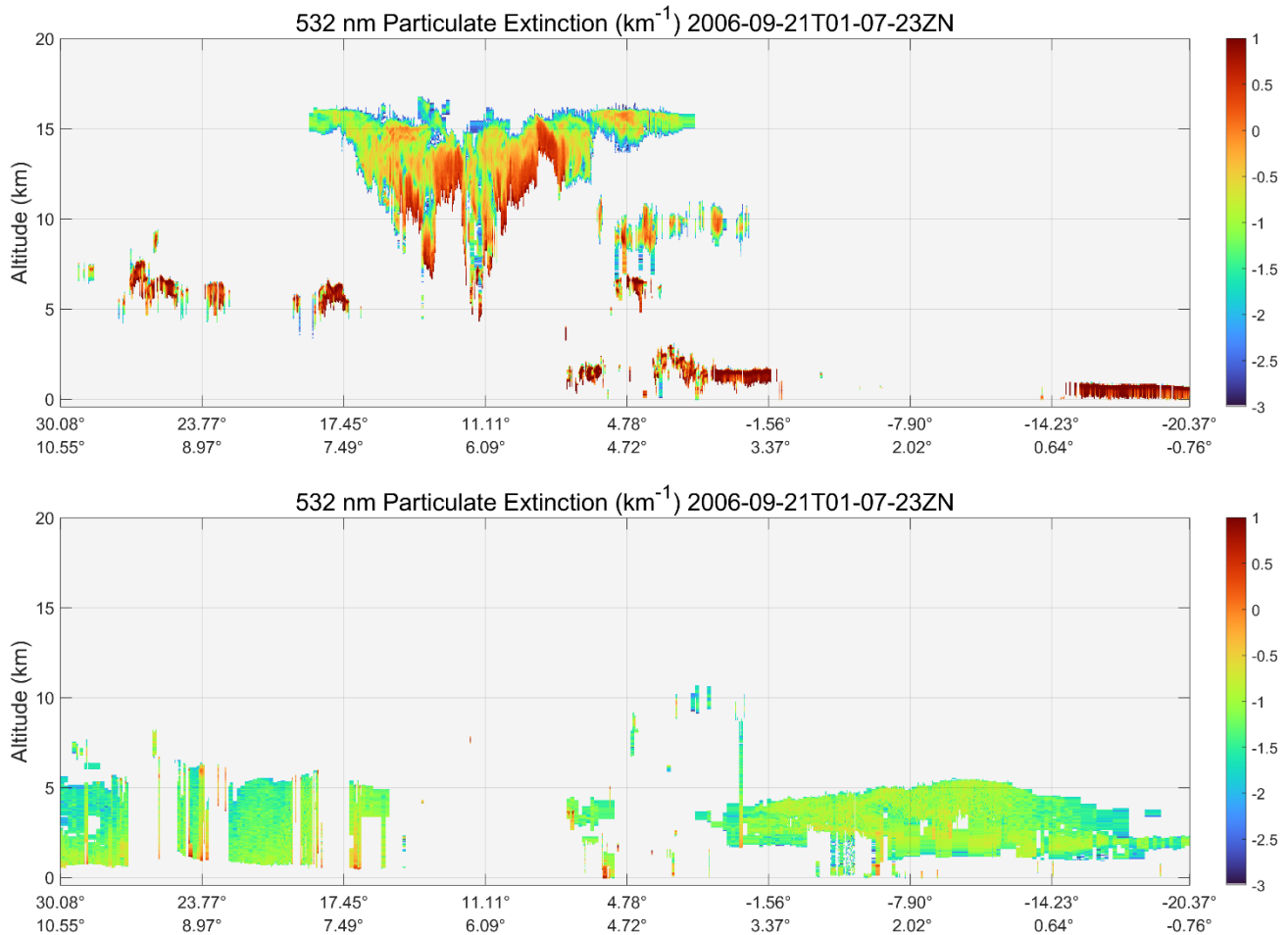


Figure 3: the upper panel shows the 532 nm attenuated backscatter coefficients measured 2006-09-21. Both clouds and aerosols are present in this scene. The middle panel shows cloud extinction coefficients using a log10 color bar. In general, water cloud extinction coefficients (darkest red) are substantially higher than ice cloud extinction coefficients (all colors). The lower panel shows aerosol extinction coefficients, also using a log10 color bar. Aerosols at latitudes above $\sim 3^\circ\text{N}$ are dust. Those below $\sim 3^\circ\text{N}$ are smoke. Low confidence feature detections ($|\text{CAD score}| < 20$) are excluded in the extinction images.

Extinction_Coefficient_Uncertainty_532 (APro and CPro)

Units: 1/km

Format: Float_32

Dimensions: number of profiles \times 399

Fill value: -9999

Flag values: -111.0 = column data quality degraded due to low laser energy
 -333.0 = failed extinction retrieval within a column
 -444.0 = suspicious/incomplete single-shot cloud clearing within a column
 -29.0 = retrieval attempted on an opaque water cloud

Description: Absolute uncertainties for the 532 nm particulate extinction coefficients reported for all range bins in which clouds (CPro) or aerosols (APro) were detected. A detailed description of the algorithms used to retrieve CALIOP backscatter and extinction coefficient uncertainties is found in the [supplemental material for Young et al., 2018](#). Extinction coefficients are the product of the backscatter coefficients and the lidar ratio used in the retrieval; i.e., $\alpha_p = S_p \times \beta_p$. The uncertainty in the particulate extinction coefficients, $\Delta\alpha_p$, is thus

$$\Delta\alpha_p(z) = \sqrt{(\beta_p(z) \cdot \Delta S_p(z))^2 + (\Delta\beta_p(z) \cdot S_p(z))^2} \quad (7)$$

where $\beta_p(z)$ and $S_p(z)$ are, respectively, the particulate backscatter coefficient and lidar ratio at altitude z and $\Delta\beta_p(z)$ and $\Delta S_p(z)$ are the associated uncertainties.

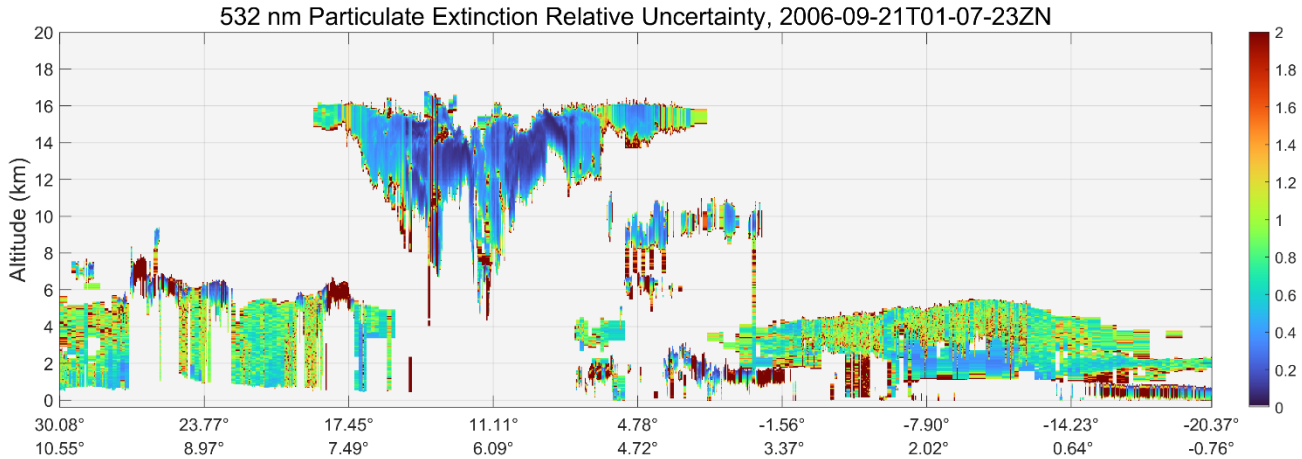


Figure 4: extinction coefficient relative uncertainties (i.e., $\text{abs}(\text{Extinction_Coefficient_Uncertainty}_{532}) / \text{Extinction_Coefficient}_{532}$) for both the cloud and aerosol extinction profiles shown in Figure 3. The lowest uncertainties in the scene are in the opaque ice clouds seen at $\sim 8^\circ\text{N}$ and ~ 14 km. Relative uncertainties are typically higher in aerosols than in ice clouds due to the much larger uncertainties ascribed to the aerosol lidar ratio, ΔS_p . The highest uncertainties are seen in opaque water clouds where the multiple scattering contributions to the total backscattered signals increase very rapidly as the signals penetrate deeper into the clouds. This effect causes a correspondingly rapid loss of accurate ranging information due to ‘pulse stretching’ (Miller and Stephens, 1999). In recognition of this phenomenon, the backscatter and extinction uncertainties reported for opaque water clouds set to a flag value of -29 , indicating zero confidence in the altitude-resolved retrievals (Young et al., 2018).

Backscatter_Coefficient_1064 (APro Only)

Units: $1/(\text{km} * \text{sr})$

Format: Float_32

Valid range: 0.0000 0.0300

Dimensions: number of profiles \times 399

Fill value: -9999

Flag values:
 -111.0 = column data quality degraded due to low laser energy
 -333.0 = failed extinction retrieval within a column
 -444.0 = suspicious/incomplete single-shot cloud clearing within a column

Description: 1064 nm particulate backscatter coefficients reported for all range bins in which aerosols were detected. The same algorithm used to retrieve 532 nm backscatter coefficients is also used for the 1064 nm retrievals. A detailed description of the algorithms used to retrieve CALIOP backscatter and extinction coefficients is found in Young et al., 2018.

Backscatter_Coefficient_Uncertainty_1064 (APro Only)

Units: $1/(\text{km} * \text{sr})$

Format: Float_32

Dimensions: number of profiles \times 399

Fill value: -9999

Flag values:
 -111.0 = column data quality degraded due to low laser energy
 -333.0 = failed extinction retrieval within a column

- 444.0 = suspicious/incomplete single-shot cloud clearing within a column
- 29.0 = retrieval attempted on an opaque water cloud

Description: Absolute uncertainties for the 1064 nm particulate backscatter coefficients reported for all range bins in which aerosols were detected. The same algorithm used to estimate 532 nm backscatter coefficient uncertainties is also used to derive the 1064 nm uncertainties. A detailed description of the algorithms used to retrieve CALIOP backscatter and extinction coefficient uncertainties is found in the [supplemental material for Young et al., 2018](#).

Extinction_Coefficient_1064 (APro Only)

Units: 1/km

Format: Float_32

Valid range: 0.0000 1.0000

Dimensions: number of profiles × 399

Fill value: -9999

Flag values: -111.0 = column data quality degraded due to low laser energy
 -333.0 = failed extinction retrieval within a column
 -444.0 = suspicious/incomplete single-shot cloud clearing within a column

Description: 1064 nm particulate extinction coefficients reported for all range bins in which aerosols were detected. The same algorithm used to retrieve 532 nm extinction coefficients is also used for the 1064 nm retrievals. A detailed description of the algorithms used to retrieve CALIOP backscatter and extinction coefficients is found in [Young et al., 2018](#).

Extinction_Coefficient_Uncertainty_1064 (APro Only)

Units: 1/km

Format: Float_32

Dimensions: number of profiles × 399

Fill value: -9999

Flag values: -111.0 = column data quality degraded due to low laser energy
 -333.0 = failed extinction retrieval within a column
 -444.0 = suspicious/incomplete single-shot cloud clearing within a column
 -29.0 = retrieval attempted on an opaque water cloud

Description: Absolute uncertainties reported for the 1064 nm particulate extinction coefficients reported for all range bins in which aerosols were detected. The same algorithm used to estimate 532 nm backscatter coefficient uncertainties is also used to derived the 1064 nm uncertainties. A detailed description of the algorithms used to retrieve CALIOP backscatter and extinction coefficient uncertainties is found in the [supplemental material for Young et al., 2018](#).

Ice_Water_Content_Profile (CPro Only)

Units: g/(m³)

Format: Float_32

Valid range: 0.0000 0.5400

Dimensions: number of profiles × 399

Fill value: -9999

Flag values: -111.0 = column data quality degraded due to low laser energy
 -333.0 = failed extinction retrieval within a column
 -444.0 = suspicious/incomplete single-shot cloud clearing within a column

Description: Ice water content (IWC) is calculated from ice cloud particulate 532 nm extinction coefficients using a temperature-dependent parameterization derived from in-situ measurements (see equation 9e in

[Heymsfield et al., 2014](#)). IWC is reported only for those range bins in which ice clouds were detected. An assessment of CALIOP IWC data quality and comparisons to IWC retrieved using different methods and different sensors is given in [Winker et al., 2024](#).

Ice_Water_Content_Profile_Uncertainty (CPro Only)

Units: $\text{g}/(\text{m}^3)$

Format: Float_32

Dimensions: number of profiles \times 399

Fill value: -9999

Flag values: -111.0 = column data quality degraded due to low laser energy
-333.0 = failed extinction retrieval within a column
-444.0 = suspicious/incomplete single-shot cloud clearing within a column

Description: Absolute uncertainties in ice water content calculated by applying standard [propagation of errors](#) to equation 9e in [Heymsfield et al., 2014](#), with Heymsfield's empirically determined α and β constants assumed to be error free for all temperature ranges.

Cloud_Multiple_Scattering_Profile_532 (CPro Only)

Units: NoUnits

Format: Float_32

Valid range: 0.0100 1.0000

Dimensions: number of profiles \times 399

Fill value: -9999

Flag values: -111.0 = column data quality degraded due to low laser energy

Description: 532 nm cloud multiple scattering factors are reported for all range bins in which clouds were detected, with values ranging between 0.01 and 1. Layers characterized by single scattering only have multiple scattering factors of 1. Smaller values indicate increasing contributions to the backscatter signal from multiple scattering.

Ice cloud multiple scattering factors are computed as a sigmoid function of cloud temperature, as shown in Figure 5. A full description of the development of this parameterization is given in [Garnier et al., 2015](#). Practical application of the ice cloud multiple scattering factors is discussed in [Young et al., 2018](#).

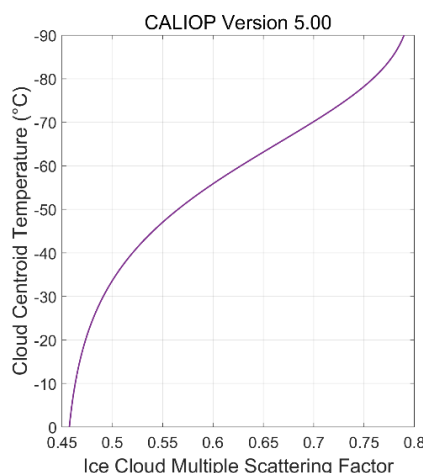


Figure 5. Multiple scattering factors as a function of the MERRA-2 temperature at the 532 nm attenuated backscatter centroids of ice clouds

Multiple scattering factors for opaque water clouds are calculated according to [Hu et al., 2007](#), and typically range between 0.193 and 0.887. Mean values are slightly higher at night (0.448 ± 0.105) than during the

day (0.436 ± 0.105). ([Young et al., 2018](#)). Transparent water clouds are assumed to have multiple scattering factors of 0.6. Based on Monte Carlo simulations, this value appears to be appropriate for clouds with optical depths less than ~ 1 . But at larger optical depths the multiple-scattering component of the signal becomes much larger than the single-scattering contributions and the true multiple scattering factors become dependent on both cloud extinction and range into the cloud. When this happens, the extinction retrieval becomes extraordinarily sensitive to errors in specifying the multiple scattering factor. And because these changes in multiple scattering are not accounted for in the current retrieval algorithm, the extinction retrieval results must be regarded as unreliable.

Aerosol_Multiple_Scattering_Profile_532 (APro Only)

Aerosol_Multiple_Scattering_Profile_1064 (APro Only)

Units: NoUnits

Format: Float_32

Valid range: 0.0000 1.0000

Dimensions: number of profiles \times 399

Fill value: -9999

Flag values: -111.0 = column data quality degraded due to low laser energy

Description: Aerosol multiple scattering factors at 532 nm and 1064 nm are reported for all range bins in which aerosols were detected, with values nominally ranging between 0.01 and 1. Layers for which multiple scattering does not contribute to the signal (i.e., single scattering only) have multiple scattering factors of 1. In V5.00, the aerosol multiple scattering factor set uniformly to 1 at both wavelengths for all aerosol subtypes.

Scientific Data Sets: Feature Type and Classification Confidence

Interpretation of 3-Dimensional SDSs

The onboard resolutions of the backscatter profiles downlinked from the CALIPSO satellite is given in Table 1. To create the CALIOP profile products, retrievals of cloud and aerosol optical properties are averaged or replicated to a uniform along-track resolution of 5 km ([Young and Vaughan, 2009](#)). The vertical resolution of the profile products above 20.2 km is 180 m, which exactly matches the vertical resolution of the downlinked data. Below 20.2 km, the vertical resolution of the profile products is 60 m, which exactly matches the downlinked data resolution in the upper troposphere (20.2 km to -0.5 km), but is a factor of two coarser in the lower troposphere (8.2 km to -0.5 km), where the native vertical resolution is 30 m. Internally, the CALIOP level 2 retrievals always operate at the highest possible vertical resolution, and hence generate 30 m vertical resolution results in the lower troposphere. To accommodate the coarser resolution reported by the profile products in this region, successive pairs of vertically adjacent 30 m optical property retrievals are averaged to create 60 m bins. As a result, some fraction of the lower troposphere optical properties reported in the profile products will be synthesized from a mixture of layer types; that is, layer type A is detected in the upper 30 m bin of the 60 m average and layer type B is detected in the lower 30 m bin.

Table 1. CALIOP's onboard data averaging scheme. Profile data are sampled onboard at 10 MHz (~ 15 m vertical resolution) then averaged to the spatial resolutions shown below prior to being downlinked. The number of bins given in the Vertical Resolution columns specifies the number of ~ 15 m bins averaged onboard to create a single vertical sample prior to downlink.

Region	Nominal Altitude Range (km)	Bin Numbers	Horizontal Resolution	532 nm Vertical Resolution	1064 nm Vertical Resolution
5	40.0 – 30.1	1 – 33	15 laser pulses (5 km)	20 bins (300 m)	N/A
4	30.1 – 20.2	34 – 88	5 laser pulses (5/3 km)	12 bins (180 m)	12 bins (180 m)
3	20.2 – 8.3	89 – 288	3 laser pulses (1 km)	4 bins (60 m)	4 bins (60 m)

Region	Nominal Altitude Range (km)	Bin Numbers	Horizontal Resolution	532 nm Vertical Resolution	1064 nm Vertical Resolution
2	8.3 – -0.5	289 – 578	1 laser pulse (1/3 km)	2 bins (30 m)	4 bins (60 m)
1	-0.5 – -2.0	578 – 583	1 laser pulse (1/3 km)	20 bins (300 m)	20 bins (300 m)

To allow users to identify potentially heterogenous range bins in the CALIOP profile products, the following profile product SDSs are stored as 3-dimensional arrays.

- ‘Atmospheric Volume Description’
- ‘CAD Score’
- ‘Extinction QC Flags’ at both wavelengths
- ‘Unique Layer ID’
- ‘Low Energy Mitigation Feature QC Flag’

The size of the first dimension equals the number of 5 km profiles reported in a granule, and hence can vary from one granule to another. The second dimension is the number of profile product altitude bins, and hence is a constant (399). The third and final dimension is two, so the entire array can be considered as an ordered pair of $N \times 399$ matrices. Values in the $[N \times 399 \times 1]$ matrix report properties of the upper 30 m bin used to create each 60 m averaged datum. Similarly, values in the $[N \times 399 \times 2]$ matrix report properties of the lower 30 m bin. This distinction between upper and lower bin values is only meaningful in the lower troposphere (i.e., below 8.2 km), where the downlinked vertical resolution is 30 m. At all higher altitudes, the values in the two $N \times 399$ matrices will be identical. Note that the optical properties data (e.g., particulate backscatter and extinction profiles) are reported as $N \times 399$ arrays, so that any array element in the lower troposphere can potentially represent the average of retrievals from two different layer types. However, these heterogenous bins will never be a mixture of cloud and aerosol because clouds and aerosols are reported separately.

Figure 6 offers an illustration of the mapping of 30 m retrieval information into the matrix elements of the ‘Atmospheric Volume Description’ (AVD) SDS. The multicolored 16 row \times 16 column segment on the left and center of the image represents feature detections for a hypothetical scene having a transparent low cloud lying above boundary layer aerosol. The numerical columns on the right show the array indexes of the three-dimensional AVD matrix and identify the feature from which the data in the upper and lower bins are obtained.

Users should also be aware that computing lidar ratios by dividing the extinction coefficients reported in these heterogenous bins by the corresponding backscatter coefficients can generate highly improbable values. Determining the lidar ratios used in the retrievals of the two different layers thus requires examining the lidar ratios in the range bins immediately above and immediately below any heterogeneous bin.

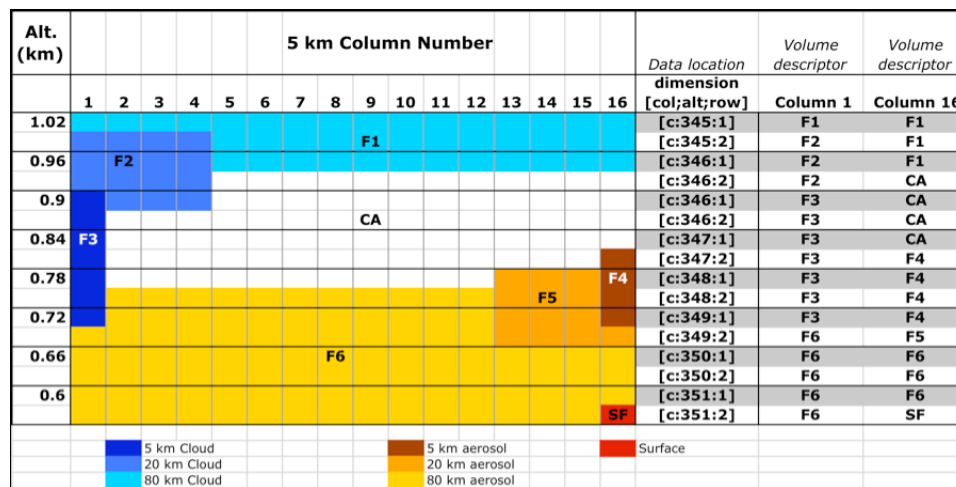


Figure 6. Wholly fictitious but heuristically useful schematic of layer detection results for a data segment in the lower troposphere extending 80-km horizontally and 480-m vertically. Six atmospheric features are depicted, labeled F1 through F6, with the yellow, orange, and brown colors indicating aerosol layers detected at horizontal

averaging resolutions of, respectively, 80 km, 20 km, and 5 km. Shades of blue likewise represent clouds at detected at 80 km, 20 km, and 5 km. Red represents the Earth's surface at 5 km, and the white regions indicate "clear air" where no features were found. The two rightmost columns list the feature numbers from which the upper and lower atmospheric volume descriptors are obtained for all 60 m bins in columns 1 and 16.

Atmospheric_Volume_Description (APro and CPro)

Units: NoUnits

Format: UInt_16

Valid range: 1 57338

Dimensions: number of profiles \times 399 \times 2

Description: The Atmospheric Volume Description (AVD) is a variant of the Feature Classification Flags (FCF) associated with each 5 km x 60 m (or 5 km x 180 m) range bin in the profile. Each AVD and FCF value is a bit-mapped 16-bit integer, where bit 0 is the least significant bit. The interpretations of bits 0–12 in the AVD, shown in Table 2, are identical to the FCF interpretations. However, because extinction solutions are only generated for features detected at 5 km, 20 km, and 80 km horizontal averaging resolutions, the interpretations of final three bits in the AVD, which define the averaging required for feature detection, are necessarily somewhat different from the interpretations that would be used for the feature classification flags. The AVD interpretations of bits 13–15 are shown in Table 3.

Table 2: interpretation of atmospheric volume description bits 0–12. The interpretation of the first 13 bits in the AVD is identical to the interpretation of the first 13 bits in the feature classification flags reported in the layer products and the vertical feature mask product.

Bits	Field Description	Bit Interpretation
0–2	Feature Type	0 = invalid (bad or missing data) 1 = "clear air" 2 = cloud 3 = tropospheric aerosol 4 = stratospheric aerosol 5 = surface 6 = subsurface 7 = no signal (totally attenuated)
3–4	Feature Type QA	0 = none 1 = low 2 = medium 3 = high
5–6	Ice/Water Phase	0 = unknown / not determined 1 = ice 2 = water 3 = oriented ice crystals
7–8	Ice/Water Phase QA	0 = none 1 = low 2 = medium 3 = high
9–11	Feature Sub-type	

Bits	Field Description	Bit Interpretation
	If feature type = tropospheric aerosol, bits 9–11 specify the tropospheric aerosol subtype	0 = not determined 1 = marine 2 = dust 3 = polluted continental/smoke 4 = clean continental 5 = polluted dust 6 = elevated smoke 7 = dusty marine
	If feature type = cloud, bits 9–11 specify the cloud subtype.	0 = low overcast, transparent 1 = low overcast, opaque 2 = transition stratocumulus 3 = low, broken cumulus 4 = altocumulus (transparent) 5 = altostratus (opaque) 6 = cirrus (transparent) 7 = deep convective (opaque)
	If feature type = stratospheric aerosol, bits 9–11 specify the stratospheric aerosol subtype.	0 = invalid 1 = polar stratospheric aerosol 2 = volcanic ash 3 = sulfate 4 = elevated smoke 5 = unclassified 6 = spare 7 = spare
	If feature type = clear-air, bits 9-11 will specify horizontal averages not searched for features due to low energy mitigation	0 = n/a 1 = not searched at 80 km 2 = not searched at 20 and 80 km
12	Feature Subtype QA	0 = not confident 1 = confident

Table 3: interpretations of bits 13–15 in the atmospheric volume description

Value	Atmospheric Volume Description	Feature Classification Flag
0	not applicable	not applicable
1	5 km	1/3 km
2	20 km	1 km
3	80 km	5 km
4	5 km w/ subgrid feature detected at 1/3 km	20 km
5	20 km w/ subgrid feature detected at 1/3 km	80 km
6	80 km w/ subgrid feature detected at 1/3 km	not used
7, 8	not used	not used

CAD_Score (APro and CPro)

Units: NoUnits

Format: Int_8

Valid range: -101 110

Dimensions: number of profiles × 399 × 2

Fill value: -127

Flag values: see Table 4

Description: The cloud-aerosol discrimination (CAD) score provides a numerical confidence level for the classification of layers by the CALIOP cloud-aerosol discrimination algorithm ([Liu et al., 2019](#)). The standard CAD scores reported in the CALIPSO layer products range between –100 and 100. The sign of the CAD score indicates the feature type, with positive values signifying clouds and negative values signifying aerosols. The absolute value of the CAD score provides the confidence level for any classification. The larger the magnitude of the CAD score, the higher the confidence that the classification is correct. A value of 0 indicates that a feature has an equal likelihood of being a cloud and an aerosol. Additional special CAD scores have been defined to alert users to possibly off-nominal classification. These special CAD scores are listed in Table 4 and are derived from additional information that is not normally considered in the standard CAD algorithm. All atmospheric layers detected by CALIOP are assigned a CAD score, irrespective of altitude (i.e., stratosphere vs. troposphere) or the amount of along-track averaging required for detection.

Table 4: listing of special CAD scores outside the normal range of –100 to 100

Value	Interpretation
-111	Data quality degraded due to low laser energy
-101	Negative mean attenuated backscatter encountered
101	Not used after the V3.x release
102	Not used after the V3.x release
103	Layer integrated attenuated backscatter at 532 nm is suspiciously high
104	Boundary layer clouds that were found to be opaque at the initial 5 km horizontal averaging resolution used by the layer detection algorithm
105	Layer detected at one of the coarser averaging resolutions (20 km or 80 km) for which the initial estimates of measured properties have been negatively impacted
106	A cirrus cloud ‘fringe’ that was initially classified as an aerosol by the CAD algorithm and subsequently reclassified via spatial proximity analysis as a randomly oriented ice cloud (see Liu et al., 2019)
107	Classification made by the single-shot cloud-clearing algorithm; layer detected at 5 km resolution is irrevocably classified as a high confidence cloud prior to any attenuation corrections for overlying layers (see Tackett et al., 2022)
108	Classification made by the single-shot cloud-clearing algorithm; layer detected at 5 km is irrevocably classified as an aerosol prior to any attenuation corrections for overlying layers
109	Classification made by the single-shot cloud-clearing algorithm; single shot cloud is reclassified as an aerosol
110	Classification made by the single-shot cloud-clearing algorithm; indeterminate layer reclassified as a cloud

Aerosol_Layer_Fraction (APro and CPro)

Units: NoUnits

Format: Int_8

Dimensions: number of profiles × 399

Valid range: 0, 30

Scale range: 0.0...1.0

Scale factor: 30.0

Scale equation: data/scale_factor

Flag values: -111 = column data quality degraded due to low laser energy

Description: Reports the fraction (by area) of each vertical range bin that is identified as aerosol by the [CALIOP CAD algorithm](#). The values reported by Aerosol_Layer_Fraction range between 0 and 30 because up to 30 single-shot resolution attenuated backscatter samples can contribute to a 60 m vertical x 5 km horizontal resolution range bin in the level 2 profile product. The fractional contribution of single-shot resolution

aerosol samples is computed by dividing the value reported in the SDS by the scale factor 30.0, yielding a scaled range of 0.0 to 1.0. For example, a reported value of 11 would indicate an aerosol fraction of $11/30 = 0.367$. Range bins in which no aerosols were detected have values of 0.

Known Issue: the LEM algorithm will reject single-shot profiles affected by low energy laser pulses within any 5 km horizontal segment. In these situations, the total number of single shots contributing to the average will be something less than 30. The single-shot resolution Low Energy Mitigation Column QC Flag can be used to determine the number of single-shot samples excluded.

Cloud_Layer_Fraction (APro and CPro)

Units: NoUnits

Format: Int_8

Valid range: 0, 30

Dimensions: number of profiles \times 399

Scale range: 0.0...1.0

Scale factor: 30.0

Scale equation: data/scale_factor

Flag values: -111 = column data quality degraded due to low laser energy

Description: Reports the fraction (by area) of each vertical range bin that is identified as cloud by the [CALIOP CAD algorithm](#). The values reported by Cloud_Layer_Fraction range between 0 and 30 because up to 30 single-shot resolution attenuated backscatter samples can contribute to a 60 m vertical \times 5 km horizontal resolution range bin in the level 2 profile product. The fractional contribution of single-shot resolution aerosol samples is computed by dividing the value reported in the SDS by the scale factor 30, yielding a scaled range of 0.0 to 1.0. For example, a reported value of 11 would indicate a cloud layer fraction of $11/30 = 0.367$. Range bins in which no clouds were detected have values of 0. **Known issue:** the LEM algorithm can reject single-shot profiles affected by low energy laser pulses within a 5 km horizontal segment. In these situations, the total number of single shots contributing to the average will not be 30. The single-shot resolution Low Energy Mitigation Column QC Flag can be used to determine the number of single-shot samples excluded.

Scientific Data Sets: Quality Assurance

Extinction_QC_Flag_532 (APro and CPro)

Extinction_QC_Flag_1064 (APro only)

Units: NoUnits

Format: UInt_16

Valid range: 0 32768

Dimensions: number of profiles \times 399 \times 2

Fill value: 32768

Description: The 532 nm and 1064 nm Extinction Quality Control (QC) Flags are bit-mapped 16-bit integers, reported for each range bin in which an extinction retrieval was attempted. Flag values are decoded as shown in Table 5. Bit 0 is the least significant bit. The bit assignments are additive, so that (for example) an extinction QC value of 66 represents an unconstrained retrieval for which the lidar ratio was reduced to achieve a physically plausible solution (bit 2 is set; QC value = 2) in a layer containing a negative signal anomaly (bit 7 is set; QC value = 2 + 64 = 66). Complete information about the conditions under which each extinction QC bit is toggled can be found in [Young et al., 2018](#). Bit 13 does not necessarily indicate an anomalous condition. Instead, it flags those range bins in the lower troposphere (8.2 km to -0.5 km) in which the 60 m averaged optical properties were created from higher resolution (30 m) retrievals of two different layer types (i.e., either two different aerosol types or two different cloud types).

Table 5: interpretation of the bits in the 532 nm and 1064 nm extinction QC flags

Bit	Value	Interpretation
0	0	unconstrained retrieval; initial lidar ratio unchanged during solution process
0	1	constrained retrieval; initial lidar ratio optimized to match measured layer optical depth
1	2	Initial lidar ratio reduced to achieve successful solution
2	4	Suspicious retrieval due to the 532 nm integrated attenuated backscatter being too high either within or above the layer or due to excessively large lidar ratio reductions
3	8	Lidar ratio has been reduced and has converged, but a physically realistic backscatter uncertainty solution does not exist
4	16	Layer being analyzed has been identified by the feature finder as being opaque (i.e., totally attenuating)
5	32	Estimated optical depth error exceeds the maximum allowable value
6	64	Negative signal anomaly detected
7	128	Retrieval terminated at maximum iterations for a constrained retrieval
8	256	No solution possible within allowable lidar ratio bounds
9	512	Two-way particulate transmittance has converged but constrained retrieval still not achieved
10	1024	Backscatter coefficients not converging and maximum lidar ratio correction iterations reached
11	2048	Uncertainties not converging and maximum lidar ratio correction iterations achieved
12	4096	Lidar ratio converged but retrieval still not converging
13	8192	60 m range bin contains two different feature types that likely have different lidar ratios
14	16384	Complex retrieval failure (see Young et al., 2009)
15	32768	Fill value; no solution attempted

Minimum_Laser_Energy_532 (APro and CPro)

Units: J

Format: Float_32

Typical range: 0.003...0.135

Dimensions: number of profiles × 1

Description: Minimum single shot laser energy at 532 nm, measured Joules, within each 80 km along-track data segment (80 km = 240 consecutive laser pulses). The 80 km distance matches the largest horizontal extent considered in CALIOP's standard level 2 data analyses. Since layers can be detected at horizontal resolutions as large as 80 km, anomalously low laser energies in coarse resolution upper layers can potentially introduce biases in the spatial and optical property retrievals of underlying layers detected at finer spatial resolutions. The Minimum_Laser_Energy_532 SDS enables ready identification of these problematic situations.

Low_Energy_Mitigation_Column_QC_Flag (APro and CPro)

Units: NoUnits

Format: UInt_16

Valid range: 0 63

Dimensions: number of profiles × 1

Description: In mid-2016, the CALIOP laser began intermittently emitting low energy laser pulses, and the occurrence frequency of these pulses slowly increased as the mission progressed. For the version 5.00 data release, CALIOP's low energy mitigation algorithm (LEM; [Tackett et al., 2025](#)) was enhanced for use in the level 2 data processing. The LEM algorithm identifies level 1 backscatter data resulting from low energy

pulses and, when appropriate, excludes it from the level 2 analyses. The low energy mitigation column quality control (QC) flags are $N \times 1$ arrays of bit-mapped 16-bit integers that summarize the operation of the LEM algorithm within each 5 km vertical column (i.e., each frame) in the CALIOP profile products. Bit interpretation is given in Table 6.

Table 6: interpretation of the bits in the LEM column QC flags; bit 0 is the least significant bit.

bit	interpretation
0	Column contains LEM affected data (data has been rejected or contains low energy shots that LEM accepts)
1	Column belongs to a 5 km resolution frame that has been rejected due to too many unusable profiles
2	Column belongs to a 5 km resolution frame that has been rejected due to too many rejected subregions in altitude region 3
3	Column belongs to a 5 km resolution frame that has been rejected due to too many rejected subregions in altitude region 4
4	Feature detection at 20 km resolution not performed in this column due to an insufficient fraction of usable 5 km resolution frames
5	Feature detection at 80 km resolution not performed in this column due to an insufficient fraction of usable 5 km resolution frames
6–15	unused

Low_Energy_Mitigation_Feature_QC_Flag (APro and CPro)

Units: NoUnits

Format: Int_8

Valid range: 0 1

Fill value: -127

Dimensions: number of profiles \times 399 \times 2

Description: The low energy mitigation (LEM) feature quality control flags are a matrix of 8-bit integers that report LEM results within each range bin in which a was feature detected. Features wholly unaffected by low energy shots are assigned a value of 0. Values of 1 are assigned where features contain one or more low energy shots and/or the data rejected entirely by the LEM algorithm. Range bins in which no feature was detected have fill values of -127.

Unique_Layer_ID (APro and CPro)

Units: NoUnits

Format: Int_32

Valid range: 1 83475

Dimensions: number of profiles \times 399 \times 2

Fill value: -9999

Flag values: -111 = column data quality degraded due to low laser energy

Description: Unique integer value assigned to each layer detected at 5 km, 20 km, and 80 km (i.e., all resolutions for which optical properties are retrieved). In the profile products, unique layer IDs are reported for all range bins and all profiles in which a feature was detected. Unique layer IDs are also reported in the CALIOP layer products, thus allowing direct two-way mapping between the altitude-resolved data reported in the profile products and the integrated feature statistics reported in the layer products.

Scientific Data Sets: Ancillary Meteorological Data

Molecular_Number_Density (APro and CPro)

Units: $1/(m^3)$

Format: Float_32

Valid range: 8.0×10^{22} 5.0×10^{25}

Dimensions: number of profiles \times 399

Fill value: -9999

Description: 5 km horizontal mean molecular number densities interpolated from [MERRA-2](#) reanalysis data and reported for the midpoint of each range bin in the profile.

Ozone_Number_Density (APro and CPro)

Units: $1/(m^3)$

Format: Float_32

Valid range: 9.0×10^{16} 1.0×10^{19}

Dimensions: number of profiles \times 399

Fill value: -9999

Description: 5 km horizontal mean ozone number densities interpolated from [MERRA-2](#) reanalysis data and reported for the midpoint of each range bin in the profile.

Temperature (APro and CPro)

Units: degC

Format: Float_32

Valid range: -120.0000 60.0000

Dimensions: number of profiles \times 399

Fill value: -9999

Description: 5 km horizontal mean temperatures interpolated from [MERRA-2](#) reanalysis data and reported for the midpoint of each range bin in the profile.

Pressure (APro and CPro)

Units: hPa

Format: Float_32

Valid range: 1.0000 1086.0000

Dimensions: number of profiles \times 399

Fill value: -9999

Description: 5 km horizontal mean atmospheric pressures interpolated from [MERRA-2](#) reanalysis data and reported for the midpoint of each range bin in the profile.

Relative_Humidity (APro and CPro)

Units: NoUnits

Format: Float_32

Valid range: 0.0000 1.5000

Dimensions: number of profiles \times 399

Fill value: -9999

Description: 5 km horizontal mean relative humidities interpolated from [MERRA-2](#) reanalysis data and reported for the midpoint of each range bin in the profile.

Surface_Wind_Speeds_02m (APro and CPro)

Units: m/s

Format: Float_32

Valid range: -80.0000 80.0000

Dimensions: number of profiles × 1

Fill value: -9999

Description: Mean zonal and meridional components of the surface wind speed 2 meters above the surface, interpolated from the [MERRA-2](#) data products, and computed over the 5 km horizontal distance spanned by each profile product record. The first array dimension reports the zonal (eastward, u) component. The second array dimension reports the meridional (northward, v) component.

Tropopause_Height (APro and CPro)

Units: km

Format: Float_32

Valid range: 4.0000 22.0000

Dimensions: number of profiles × 1

Fill value: -9999

Description: Tropopause heights for each 5 km profile, interpolated from the [MERRA-2](#) data products.

Tropopause_Temperature (APro and CPro)

Units: degC

Format: Float_32

Valid range: -95.0000 -20.0000

Dimensions: number of profiles × 1

Fill value: -9999

Description: Tropopause temperatures for each 5 km profile, interpolated from the [MERRA-2](#) data products.

Scientific Data Sets: Surface Information

DEM_Surface_Elevation (APro and CPro)

Units: km

Format: Float_32

Valid range: -1.0000 9.0000

Dimensions: number of profiles × 1

Fill value: -9999

Description: Reports the minimum, maximum, mean, and standard deviation of the surface elevation at the laser footprint, computed for all 15 laser pulses in a 5 km along-track averages. Surface elevations are expressed as “above local mean sea level” (AMSL) and are obtained from the CloudSat science team digital elevation model (DEM).

IGBP_Surface_Type (APro and CPro)

Units: NoUnits

Format: Int_8

Valid range: 1 18

Dimensions: number of profiles × 1

Fill value: -9

Description: International Geosphere–Biosphere Programme (IGBP) surface type at the laser footprint, provided by the [CERES IGBP land classification map](#), with values as shown in Table 7:

Table 7: interpretation of the IGBP surface type values

Value	Surface Type	Value	Surface Type
1	Evergreen-Needleleaf-Forest	10	Grassland
2	Evergreen-Broadleaf-Forest	11	Wetland
3	Deciduous-Needleleaf-Forest	12	Cropland
4	Deciduous-Broadleaf-Forest	13	Urban
5	Mixed-Forest	14	Crop-Mosaic
6	Closed-Shrubland	15	Permanent-Snow
7	Open-Shrubland (Desert)	16	Barren/Desert
8	Woody-Savanna	17	Water
9	Savanna	18	Tundra

Vgroup : Lidar_Surface_Detection

This Vgroup reports the results of CALIPSO’s dedicated search for backscatter signals from the Earth’s surface. These “surface returns” have both a top altitude, indicating the onset of the surface signal, and a base altitude, indicating when the signal has been completely attenuated. Both altitudes are reported in kilometers above local mean sea level (AMSL). The apparent depth of the surface return is due to [low-pass Bessel filters in the CALIOP receiver](#) and, at 532 nm, the [non-ideal response of the photomultipliers](#). The surface top and base altitudes can be different at the two wavelengths, since the 532 nm signals are downlinked at 30 m vertical resolution whereas the 1064 nm signals are downlinked at 60 m resolution. All surface data reported in the cloud and aerosol profile products are derived from attenuated backscatter profiles averaged to 5 km (15 laser pulses) along track resolution. When no surface is detected for a given wavelength, all surface detection data fields report fill values.

Surface_Top_Altitude_532

Surface_Top_Altitude_1064

Units: km

Format: Float_32

Valid range: -0.5000 8.2000

Flag values: -111.0 = column data quality degraded due to low laser energy

Description: Top altitude of the surface return at the lidar footprint detected at, respectively, 532 nm and 1064 nm.

Surface_Base_Altitude_532

Surface_Base_Altitude_1064

Units: km

Format: Float_32

Valid range: -0.5000 8.2000

Flag values: -111.0 = column data quality degraded due to low laser energy

Description: Apparent “base” altitude of the surface return nm at the lidar footprint detected at, respectively, 532 nm and 1064 nm.

Surface_Integrated_Attenuated_Backscatter_532

Surface_Integrated_Attenuated_Backscatter_1064

Units: 1/sr

Format: Float_32

Valid range: 0.0000 2.0000

Flag values: -111.0 = column data quality degraded due to low laser energy

Description: Vertically integrated total attenuated backscatter of the surface return detected at either 532 nm or 1064 nm. Limits of integration are the wavelength-specific surface top and base altitudes. The integrated attenuated backscatter measurements quantify the relative strengths of the surface returns.

Surface_532_Integrated_Depolarization_Ratio

Surface_1064_Integrated_Depolarization_Ratio

Units: NoUnits

Format: Float_32

Valid range: 0.0000 1.0000

Flag values: -111.0 = column data quality degraded due to low laser energy

Description: The depolarization ratio of surface return at 532 nm, computed as the ratio of the vertically integrated 532 nm perpendicular channel attenuated backscatter to the vertically integrated 532 nm parallel channel attenuated backscatter. Integration limits for the 532 nm integrated depolarization ratio are from the 532 nm surface top altitude to the 532 nm surface base altitude. For the 1064 nm integrated depolarization ratio, integration limits are from the 1064 nm surface top altitude to the 1064 nm surface base altitude. Surface depolarization ratios provide some insight into surface type, with liquid water surfaces having very low depolarization ratios, snow and ice having very high depolarization ratios, and land surfaces typically having midrange values that depend on vegetation and soil conditions (see [Lu et al., 2017](#)).

Surface_532_Integrated_Attenuated_Color_Ratio

Surface_1064_Integrated_Attenuated_Color_Ratio

Units: NoUnits

Format: Float_32

Valid range: 0.0000 2.0000

Flag values: -111.0 = column data quality degraded due to low laser energy

Description: Total attenuated backscatter color ratio of the surface return, computed by dividing the vertically integrated 1064 nm attenuated backscatter coefficients by the vertically integrated 532 nm total attenuated backscatter coefficients. Integration limits for the 532 nm integrated attenuated color ratio are from the 532 nm surface top altitude to the 532 nm surface base altitude. For the 1064 nm integrated attenuated color ratio, integration limits are from the 1064 nm surface top altitude to the 1064 nm surface base altitude.

Surface_Detection_Flags_532

Surface_Detection_Flags_1064

Units: NoUnits

Format: UInt_16

Valid range: 0 8192

Description: Surface detection quality assurance flags that describe the wavelength-specific outcomes of the respective surface searches. Surface detection flags are stored as 16-bit integers with bit 0 being the least significant bit. Bit interpretations are given in Table 8: Bit interpretations for the surface detection flags reported for each wavelength for all 532 nm and 1064 nm surface detection attempts..

Table 8: Bit interpretations for the surface detection flags reported for each wavelength for all 532 nm and 1064 nm surface detection attempts.

Bit(s)	Interpretation
0	Surface detected? 0 = no 1 = yes
1-2	Surface detection method 0 = derivative test 1 = multi-shot averaged data test 2 = single shot surface detection fraction test 3 = unused
3	532 nm parallel channel saturated
4	532 nm perpendicular channel saturated
5	1064 nm channel saturated
6	532 nm parallel channel negative signal anomaly
7	532 nm perpendicular channel negative signal anomaly
8	1064 nm channel negative signal anomaly
9	Derivative method failure: $Z(\text{min gradient}) < Z(\text{max gradient})$
10	Derivative method failure: vertical extent exceeds limit
11	Derivative method failure: peak signal below threshold
12	Failure: vertical separation between 532 and 1064 surface top altitudes exceeds allowable limit
13	Failure: surface detected at 1064 nm only, but overlying atmospheric total attenuated backscatter color ratio is below a threshold value. This test is disabled in the V5.00 release.
14-15	Unused

Surface_Overlying_Integrated_Attenuated_Backscatter_532

Surface_Overlying_Integrated_Attenuated_Backscatter_1064

Units: 1/sr

Format: Float_32

Valid range: 0.0000 2.0000

Flag values: -111.0 = column data quality degraded due to low laser energy

Description: Wavelength-specific vertically integrated total attenuated *atmospheric* backscatter from the top of the profile measurement (40 km at 532 nm, 30 km at 1064 nm) to one range bin above the detected surface top altitude.

Surface_Scaled_RMS_Background_532

Surface_Scaled_RMS_Background_1064

Units: 1/(km * sr)

Format: Float_32

Valid range: 0.0000 0.0500

Flag values: -111.0 = column data quality degraded due to low laser energy

Description: Background noise estimate computed from RMS baseline noise measurements between 65 and 80 km above mean sea level, rescaled to create pseudo-attenuated backscatter coefficients at, respectively, 532 nm and 1064 nm. These pseudo-attenuated backscatter coefficients are used to determine surface detection thresholds ([Vaughan et al., 2016](#)).

Surface_Peak_Signal_532**Surface_Peak_Signal_1064**

Units: 1/(km * sr)

Format: Float_32

Valid range: 0.0000 3.5000

Flag values: -111.0 = column data quality degraded due to low laser energy

Description: Maximum attenuated backscatter coefficient in the surface signals detected at, respectively, 532 nm and 1064 nm.

Surface_Detections_333m_532**Surface_Detections_333m_1064**

Units: NoUnits

Format: Int_16

Valid range: 0 15

Flag values: -111 = column data quality degraded due to low laser energy

Description: These fields report the number of single shot surface detections within each 5 km resolution profile. Detection results are reported separately for the 532 nm and 1064 nm channels.

Surface_Detections_1km_532**Surface_Detections_1km_1064**

Units: NoUnits

Format: Int_16

Valid range: 0 5

Flag values: -111 = column data quality degraded due to low laser energy

Description: These fields report the number of 1 km resolution surface detections within each 5 km resolution profile. Detection results are reported separately for the 532 nm and 1064 nm channels.

Vgroup : Ocean_Derived_Column_Optical_Depth**ODCOD_Effective_Optical_Depth_532**

Units: NoUnits

Format: Float_32

Valid range: 0.0000 25.0000

Flag values: -111.0 = column data quality degraded due to low laser energy

Description: Estimates of total column apparent particulate optical depth derived from the magnitude of the integrated ocean surface backscatter measured at 532 nm ([Ryan et al., 2024](#)). These are apparent optical depths rather than true optical depths because no corrections are made for multiple scattering effects from cloud and aerosol layers that may be present within any column.

ODCOD_Effective_Optical_Depth_532_Uncertainty

Units: NoUnits

Format: Float_32

Flag values: -111.0 = column data quality degraded due to low laser energy

Description: Estimated absolute uncertainties in the ODCOD Effective Optical Depths at 532 nm ([Ryan et al., 2024](#)).

ODCOD_QC_Flag_532

Units: NoUnits

Format: UInt_32

Valid range: 0 4294967295

Description: Ocean Derived Column Optical Depth (ODCOD) quality control flags describing retrievals at 532 nm

Table 9: Interpretation of the bits in the ODCOD quality control flags; least significant bit = bit 0

Bit(s)	Interpretation
0	The fundamental time delay was shifted from the first point
1	Lidar surface data too many data points for a valid surface spike
2	Range bin above recorded lidar surface data added
3	Range bin below recorded lidar surface data added
4	The surface point ratio indicated that the first point of the surface spike is missing
5	To find the time delay# the surface spike index range had to be shifted down
6	The retrieval inputs fall outside of confidence ranges indicating a confident retrieval
7-9	Unused
10	No Lidar surface was found
11	The surface is not ocean
12	The surface is ice
13	The wind speed is outside the valid range (0.025 to 43 m/s)
14	The fundamental time delay found was too low; insufficient data samples to conduct a second search
15	Too few data points to solve
16	The low pass filter impulse response model curve area was too large
17	The low pass filter impulse response model curve scale factor could not be found
18	Lidar surface saturated
19	Lidar surface has negative signal anomaly
20	Lidar surface data is not valid
21	Flags bad input/ancillary data
22	No Lidar surface was detected via derivative method at greater than single shot resolutions
23-31	Unused

ODCOD_Surface_Wind_Speeds_10m

Units: m/s

Format: Float_32

Valid range: -43.0000 43.0000

Description: Mean zonal and meridional components of the wind speeds 10 meters above the Earth's surface reported in the lidar level 1b file. Lidar L1b wind speeds are interpolated from the [MERRA-2](#) ancillary meteorological data and reported for each laser pulse as $N \times 2$ arrays, where the first column gives the magnitude of the eastward, zonal, u component and the second column reports the northward, meridional, v component.

ODCOD_Surface_Wind_Speed_Correction

Units: m/s

Format: Float_32

Valid range: -43.0000 43.0000

Description: An additive correction derived from global analysis of AMSR wind speeds and applied during the ODCOD retrievals to the MERRA-2 wind speed magnitudes.

Metadata Parameter Descriptions

Product_ID (APro and CPro)

A character string (80-byte maximum) specifying the data product name. For all CALIPSO Level 2 lidar data products, the value of this string will be "L2_Lidar".

Date_Time_at_Granule_Start (APro and CPro)

A 27-byte character string that specifies the granule UTC start date and time. The format is yyyy-mm-ddThh:nn:ss.ffffffZ, where yyyy is the year, mm is the month, dd is the day, hh is the hour, nn is the minute, ss is the second, and fffffff is the fractional second. Date and time are separated by the character 'T'. The 'Z' indicates that time is given in UTC.

Date_Time_at_Granule_End (APro and CPro)

A 27-byte character string that specifies the granule UTC end date and time. The format is yyyy-mm-ddThh:nn:ss.ffffffZ, where yyyy is the year, mm is the month, dd is the day, hh is the hour, nn is the minute, ss is the second, and fffffff is the fractional second. Date and time are separated by the character 'T'. The 'Z' indicates that time is given in UTC.

Date_Time_of_Production (APro and CPro)

A 27-byte character string that specifies the UTC start date and time at which the data was generated. The format is yyyy-mm-ddThh:nn:ss.ffffffZ, where yyyy is the year, mm is the month, dd is the day, hh is the hour, nn is the minute, ss is the second, and fffffff is the fractional second. Date and time are separated by the character 'T'. The 'Z' indicates that time is given in UTC.

Number_of_Bad_Profiles (APro and CPro)

A 32-bit integer specifying the number of bad attenuated backscatter profiles contained the level 1b file used to generate the level 2 analyses. Profiles are considered bad if (a) any of the three measurement channels are missing (see bits 0, 1, and 2 in the QC Flags SDS); (b) the measurement data could not be geolocated (see bit 3 in the QC flags SDS); or (c) the energy in either the 532 nm or 1064 nm channel falls below the low energy threshold (see bits 5 and 6 in the QC Flags SDS).

Number_of_Good_Profiles (APro and CPro)

A 32-bit integer specifying the number of good (i.e., not identified as being bad) attenuated backscatter profiles contained in the level 1b file used to generate the level 2 analyses.

Initial_Subsatellite_Latitude (APro and CPro)

This field reports the first subsatellite latitude contained in the granule.

Initial_Subsatellite_Longitude (APro and CPro)

This field reports the first subsatellite longitude contained in the granule.

Final_Subsatellite_Latitude (APro and CPro)

This field reports the last subsatellite latitude contained in the granule.

Final_Subsatellite_Longitude (APro and CPro)

This field reports the last subsatellite longitude contained in the granule.

Orbit_Number_at_Granule_Start (APro and CPro)**Orbit_Number_at_Granule_End (APro and CPro)****Orbit_Number_Change_Time (APro and CPro)**

Orbit Number consists of three fields that define the number of revolutions by the CALIPSO spacecraft around the Earth. This number is incremented each time the spacecraft passes the equator on the ascending node. To maintain consistency between the CALIPSO and CloudSat orbit parameters, the Orbit Number is keyed to the CloudSat orbit 2121 at 23:00:47 on 2006/09/20. Because the CALIPSO data granules are organized according to satellite lighting conditions, based on fixed Sun-Earth-Satellite angles, day/night boundaries do not coincide with transition points for defining orbit number. As such, three parameters are needed to describe the orbit number for each granule as:

- **Orbit Number at Granule Start:** orbit number at the granule start time
- **Orbit Number at Granule End:** orbit number at the granule stop time
- **Orbit Number Change Time:** time at which the orbit number changes in the granule

Path_Number_at_Granule_Start (APro and CPro)**Path_Number_at_Granule_End (APro and CPro)****Path_Number_Change_Time (APro and CPro)**

Path Number consists of three fields that define an index ranging from 1-233 that references orbits to the Worldwide Reference System (WRS). This global grid system was developed to support scene identification for Landsat imagery. Since the A-Train is maintained to the WRS grid within ± 10 km, the Path Number provides a convenient index to support data searches, instead of having to define complex latitude and longitude regions along the orbit track. The Path Number is incremented after the maximum latitude in the orbit is realized and changes by a value of 16 between successive orbits. Because the CALIPSO data granules are organized according to satellite lighting conditions, day/night boundaries do not coincide with transition points for defining path number. As such, three parameters are needed to describe the path number for each granule as:

- **Path Number at Granule Start:** path number at the granule start time
- **Path Number at Granule End:** path number at the granule stop time
- **Path Number Change Time:** time at which the path number changes in the granule

While CALIPSO was formation flying in the A-Train all path numbers are exact. Beginning in September 2018, when CALIPSO lowered its orbit into the C-Train, path numbers are no longer exact, but instead indicate the closest WRS reference orbit.

Rayleigh_Extinction_Cross-section_532 (APro and CPro)

Rayleigh extinction cross-section = $5.1670\text{e-}31 \text{ m}^2$ used to convert molecular number densities into 532 nm molecular extinction coefficients.

Rayleigh_Extinction_Cross-section_1064 (APro and CPro)

Rayleigh extinction cross-section = $3.1270\text{e-}32 \text{ m}^2$ used to convert molecular number densities into 1064 nm molecular extinction coefficients.

Rayleigh_Backscatter_Cross-section_532 (APro and CPro)

Rayleigh backscatter cross-section = $5.9300\text{e-}32 \text{ m}^2 \text{ sr}$ used to convert molecular number densities into 532 nm molecular backscatter coefficients.

Rayleigh_Backscatter_Cross-section_1064 (APro and CPro)

Rayleigh backscatter cross-section = $3.5920\text{e-}33 \text{ m}^2 \text{ sr}$ used to convert molecular number densities into 1064 nm molecular backscatter coefficients.

Ozone_Absorption_Cross-section_532 (APro and CPro)

Ozone absorption cross-section = $2.7285 \times 10^{-25} \text{ m}^2$ used to convert ozone number densities into 532 nm ozone extinction coefficients.

Ozone_Absorption_Cross-section_1064 (APro and CPro)

Because ozone absorption is negligible at 1064 nm, the ozone absorption cross-section for this wavelength is set to 0.

Lidar_Level_1_Production_Date_Time (APro and CPro)

For each CALIOP Lidar Level 2 data product, the Lidar Level 1 Production Date Time field reports the file creation time and date for the CALIOP Level 1 Lidar data file that provided the source data used in the Level 2 analyses.

Ocean_Fresnel_Reflection_Coefficient_532 (APro and CPro)

Estimated reflectance coefficient of the 532 nm signal by seawater. The value of this parameter is 0.0213, based on work documented in [Vaughan et al., 2019](#).

MERRA-2_Wind_Uncertainty (APro and CPro)

Estimated global relative uncertainty of the 10 m wind speed reported in the MERRA-2 meteorological model data product. The value of this parameter is 0.1506, based on work documented in [Ryan et al., 2024](#).

AMSR_Wind_Correction_Uncertainty (APro and CPro)

Estimated global correction uncertainty between the AMSR and MERRA-2 winds. As documented in [Ryan et al., 2024](#), the value of this parameter is 0.2537.

Lidar_Data_Altitude (APro and CPro)

Altitudes (above mean sea level) that specify the vertical midpoints of the 583 range bins in the profile measurements downlinked from the CALIPSO satellite. The values in this field are identical to those in the Lidar_Data_Altitudes SDS and are retained in V5.00 for backward compatibility with existing software.

Initial_Lidar_Ratio_Clouds_532 (CPro only)

Characteristic lidar ratios used to initiate extinction solutions for water clouds and ice clouds when no additional information is available to suggest more accurate values. Water cloud lidar ratios are 17.7 sr for daytime measurements and 18.8 sr for nighttime measurements. For ice clouds, the characteristic value is 28.3 sr both daytime and nighttime. See [Young et al., 2018](#) for additional detail.

Initial_Lidar_Ratio_Tropospheric_Aerosols_532 (APro only)

Initial_Lidar_Ratio_Stratospheric_Aerosols_1064 (APro only)

Characteristic lidar ratios used to initiate extinction solutions for tropospheric aerosol layers when no additional information is available to suggest a more accurate value. See [Kim et al., 2018](#) for additional detail.

At 532 nm only, these fields no longer accurately report the lidar ratios used for the marine and dusty marine types. Instead, the initial values used for these types are interpolated from lookup tables and varying both spatially and seasonally. Details are provided in [Toth et al., 2025](#).

Table 10: Characteristic lidar ratios for CALIPSO tropospheric aerosol types reported in the file metadata.

Tropospheric Aerosol Type	532 nm	1064 nm
Marine	23 sr	23 sr
Dust	44 sr	44 sr
Polluted Continental/Smoke	70 sr	30 sr
Clean Continental	53 sr	45 sr

Tropospheric Aerosol Type	532 nm	1064 nm
Polluted Dust	55 sr	48 sr
Elevated Smoke	70 sr	30 sr
Dusty Marine	37 sr	37 sr

Initial_Lidar_Ratio_Stratospheric_Aerosols_532 (APro only)

Initial_Lidar_Ratio_Tropospheric_Aerosols_1064 (APro only)

Characteristic lidar ratios used to initiate extinction solutions for stratospheric aerosol layers when no additional information is available to suggest a more accurate value. See [Tackett et al., 2023](#) for additional detail.

Table 11: Characteristic lidar ratios for CALIPSO tropospheric aerosol types

Stratospheric Aerosol Type	532 nm	1064 nm
Undetermined	50 sr	50 sr
Polar Stratospheric Aerosol	50 sr	25 sr
Volcanic Ash	61 sr	44 sr
Sulfate	50 sr	30 sr
Smoke	70 sr	30 sr
Unclassified	50 sr	30 sr

GEOS_Version (APro and CPro)

Specifies the version of the meteorological data used in the level 2 analyses. For the version 5.0 data release, this field is always “MERRA2”

GMAO_Files_Used (APro and CPro)

Lists the four MERRA-2 meteorological data files used to create the level 2 data files for this granule.

Classifier_Coefficients_Version_Number (APro and CPro)

Version number of the classifier coefficients file that stores the five-dimensional probability distribution functions used by the [cloud-aerosol discrimination \(CAD\) algorithm](#).

Classifier_Coefficients_Version_Date (APro and CPro)

Creation date of the classifier coefficients file that stores the five-dimensional probability distribution functions used by the [cloud-aerosol discrimination \(CAD\) algorithm](#).

Production_Script (APro and CPro)

Provides the configuration information and command sequences that were executed during the processing of the CALIOP Lidar Level 2 data products. Documentation for many of the control constants found within this field is contained in the CALIPSO Lidar Level 2 Algorithm Theoretical Basis Documents.

CALIPSO Data Quality Information

Data Release Information

At the conclusion of the mission, the CALIPSO project had released five major versions of the lidar level 2 data products, as well as several minor version updates. Table 12 lists all major and minor releases.

Table 12: release date, version number, data date range, and production strategy for all CALIPSO lidar level 2 data products

Lidar Level 2: Half orbits (Night and Day)			
Release Date	Version	Data Date Range	Production Strategy
October 2025	5.00	June 13, 2006 to June 30, 2023	Standard
June 2023	4.51	June 13, 2006 to June 30, 2023	Standard
October 2020	4.21	July 01, 2020 to January 19, 2022	Standard
October 2018	4.20	June 13, 2006 to June 20, 2020	Standard
November 2016	4.10	June 13, 2006 to September 30, 2020	Standard
October 2020	3.41	October 1, 2020 to June 30, 2023	Validated Stage 1
December 2016	3.40	December 1, 2016 to September 31, 2020	Validated Stage 1
April 2013	3.30	March 1, 2013 to November 30, 2016	Validated Stage 1
December 2011	3.02	November 1, 2011 to February 28, 2013	Validated Stage 1
May 2010	3.01	June 13, 2006 to October 31, 2011	Validated Stage 1
October 2008	2.02	September 14, 2008 to October 29, 2009	Provisional
January 2008	2.01	June 13, 2006 to September 13, 2008	Provisional
December 2006	1.10	June 13, 2006 to November 11, 2007	Provisional / Beta

CALIPSO Data Quality Information

Relevant External Documentation

This section lists CALIPSO Algorithm Theoretical Basis Documents (ATBDs) and peer-reviewed journal articles that provide detailed descriptions of the algorithms used to calibrate the lidar and retrieve the CALIOP level 2 science data products.

ATBDs and Project Documentation

- CALIPSO Data Management Team: CALIPSO Data Products Catalog, PC-SCI-503, Release 5.00.
- Vaughan, M. A., D. M. Winker, and K. A. Powell, 2005: CALIOP Algorithm Theoretical Basis Document, Part 2: Feature Detection and Layer Properties Algorithm, PC-SCI-202.02, <https://ntrs.nasa.gov/citations/20250006627>.
- Liu, Z., A. H. Omar, Y. Hu, M. A. Vaughan, and D.M. Winker, 2005: CALIOP Algorithm Theoretical Basis Document, Part 3: Scene Classification Algorithms, PC-SCI-202.03, <https://ntrs.nasa.gov/citations/20250006628>.
- Winker, D. M., C. A. Hostetler, M. A. Vaughan, and A. H. Omar, 2006: CALIOP Algorithm Theoretical Basis Document, Part 1: CALIOP Instrument and Algorithms Overview, PC-SCI-202.01, <https://ntrs.nasa.gov/citations/20250006626>.

Peer-Reviewed Journal Papers

- Liu, Z., M. J. McGill, Y. Hu, C. A. Hostetler, M. Vaughan, and D. Winker, 2004: "Validating lidar depolarization calibration using solar radiation scattered by ice clouds", *IEEE Geosci. Remote Sens. Lett.*, **1**, 157–161, <https://doi.org/10.1109/LGRS.2004.829613>.
- Liu, Z., M. Vaughan, D. Winker, C. A. Hostetler, L. R. Poole, D. L. Hlavka, W. D. Hart, and M. J. McGill, 2004: Use of probability distribution functions for discriminating between cloud and aerosol in lidar backscatter data, *J. Geophys. Res.*, **109**, D15202, <https://doi.org/10.1029/2004JD004732>.

- Liu, Z., W. Hunt, M. Vaughan, C. Hostetler, M. McGill, K. Powell, D. Winker, and Y. Hu, 2006: Estimating Random Errors Due to Shot Noise in Backscatter Lidar Observations, *Appl. Opt.*, **45**, 4437–4447, <https://doi.org/10.1364/AO.45.004437>.
- Hu, Y., M. Vaughan, Z. Liu, K. Powell, and S. Rodier, 2007: Retrieving Optical Depths and Lidar Ratios for Transparent Layers Above Opaque Water Clouds From CALIPSO Lidar Measurements, *IEEE Geosci. Remote Sens. Lett.*, **4**, 523–526, <https://doi.org/10.1109/LGRS.2007.901085>.
- Hu, Y., D. Winker, M. Vaughan, B. Lin, A. Omar, C. Trepte, D. Flittner, P. Yang, W. Sun, Z. Liu, Z. Wang, S. Young, K. Stamnes, J. Huang, R. Kuehn, B. Baum, and R. Holz, 2009: CALIPSO/CALIOP Cloud Phase Discrimination Algorithm, *J. Atmos. Oceanic Technol.*, **26**, 2293–2309, <https://doi.org/10.1175/2009JTECHA1280.1>.
- Hunt, W. H., D. M. Winker, M. A. Vaughan, K. A. Powell, P. L. Lucker, and C. Weimer, 2009: CALIPSO Lidar Description and Performance Assessment, *J. Atmos. Oceanic Technol.*, **26**, 1214–1228, <https://doi.org/10.1175/2009JTECHA1223.1>.
- Liu, Z., M. A. Vaughan, D. M. Winker, C. Kittaka, R. E. Kuehn, B. J. Getzewich, C. R. Trepte, and C. A. Hostetler, 2009: The CALIPSO Lidar Cloud and Aerosol Discrimination: Version 2 Algorithm and Initial Assessment of Performance, *J. Atmos. Oceanic Technol.*, **26**, 1198–1213, <https://doi.org/10.1175/2009JTECHA1229.1>.
- Omar, A., D. Winker, C. Kittaka, M. Vaughan, Z. Liu, Y. Hu, C. Trepte, R. Rogers, R. Ferrare, R. Kuehn, and C. Hostetler, 2009: The CALIPSO Automated Aerosol Classification and Lidar Ratio Selection Algorithm, *J. Atmos. Oceanic Technol.*, **26**, 1994–2014, <https://doi.org/10.1175/2009JTECHA1231.1>.
- Powell, K. A., C. A. Hostetler, Z. Liu, M. A. Vaughan, R. E. Kuehn, W. H. Hunt, K. Lee, C. R. Trepte, R. R. Rogers, S. A. Young, and D. M. Winker, 2009: CALIPSO Lidar Calibration Algorithms: Part I - Nighttime 532 nm Parallel Channel and 532 nm Perpendicular Channel, *J. Atmos. Oceanic Technol.*, **26**, 2015–2033, <https://doi.org/10.1175/2009JTECHA1242.1>.
- Vaughan, M., K. Powell, R. Kuehn, S. Young, D. Winker, C. Hostetler, W. Hunt, Z. Liu, M. McGill, and B. Getzewich, 2009: Fully Automated Detection of Cloud and Aerosol Layers in the CALIPSO Lidar Measurements, *J. Atmos. Oceanic Technol.*, **26**, 2034–2050, <https://doi.org/10.1175/2009JTECHA1228.1>.
- Winker, D. M., M. A. Vaughan, A. H. Omar, Y. Hu, K. A. Powell, Z. Liu, W. H. Hunt, and S. A. Young, 2009: Overview of the CALIPSO Mission and CALIOP Data Processing Algorithms, *J. Atmos. Oceanic Technol.*, **26**, 2310–2323, <https://doi.org/10.1175/2009JTECHA1281.1>.
- Young, S. A. and M. A. Vaughan, 2009: The retrieval of profiles of particulate extinction from Cloud Aerosol Lidar Infrared Pathfinder Satellite Observations (CALIPSO) data: Algorithm description, *J. Atmos. Oceanic Technol.*, **26**, 1105–1119, <https://doi.org/10.1175/2008JTECHA1221.1>.
- Garnier, A., J. Pelon, M. A. Vaughan, D. M. Winker, C. R. Trepte, and P. Dubuisson, 2015: Lidar multiple scattering factors inferred from CALIPSO lidar and IIR retrievals of semi-transparent cirrus cloud optical depths over oceans, *Atmos. Meas. Tech.*, **8**, 2759–2774, <https://doi.org/10.5194/amt-8-2759-2015>.
- Getzewich, B. J., M. A. Vaughan, W. H. Hunt, M. A. Avery, K. A. Powell, J. L. Tackett, D. M. Winker, J. Kar, K.-P. Lee, and T. Toth, 2018: CALIPSO Lidar Calibration at 532-nm: Version 4 Daytime Algorithm, *Atmos. Meas. Tech.*, **11**, 6309–6326, <https://doi.org/10.5194/amt-11-6309-2018>.
- Kar, J., M. A. Vaughan, K. P. Lee, J. Tackett, M. Avery, A. Garnier, B. Getzewich, W. Hunt, D. Josset, Z. Liu, P. Lucker, B. Magill, A. Omar, J. Pelon, R. Rogers, T. D. Toth, C. Trepte, J.-P. Vernier, D. Winker, and S. Young, 2018: CALIPSO Lidar Calibration at 532 nm: Version 4 Nighttime Algorithm, *Atmos. Meas. Tech.*, **11**, 1459–1479, <https://doi.org/10.5194/amt-11-1459-2018>.
- Kim, M.-H., A. H. Omar, J. L. Tackett, M. A. Vaughan, D. M. Winker, C. R. Trepte, Y. Hu, Z. Liu, L. R. Poole, M. C. Pitts, J. Kar, and B. E. Magill, 2018: The CALIPSO Version 4 Automated Aerosol Classification and Lidar Ratio Selection Algorithm, *Atmos. Meas. Tech.*, **11**, 6107–6135, <https://doi.org/10.5194/amt-11-6107-2018>.
- Lu, X., Y. Hu, Y. Yang, M. Vaughan, Z. Liu, S. Rodier, W. Hunt, K. Powell, P. Lucker, and C. Trepte, 2018: Laser pulse bidirectional reflectance from CALIPSO mission, *Atmos. Meas. Tech.*, **11**, 3281–3296, <https://doi.org/10.5194/amt-11-3281-2018>.

- Young, S. A., M. A. Vaughan, J. L. Tackett, A. Garnier, J. B. Lambeth, and K. A. Powell, 2018: Extinction and Optical Depth Retrievals for CALIPSO's Version 4 Data Release, *Atmos. Meas. Tech.*, **11**, 5701–5727, <https://doi.org/10.5194/amt-11-5701-2018>.
Supplement: <https://doi.org/10.5194/amt-11-5701-2018-supplement>
- Liu, Z., J. Kar, S. Zeng, J. Tackett, M. Vaughan, M. Avery, J. Pelon, B. Getzewich, K.-P. Lee, B. Magill, A. Omar, P. Lucker, C. Trepte, and D. Winker, 2019: Discriminating Between Clouds and Aerosols in the CALIOP Version 4.1 Data Products, *Atmos. Meas. Tech.*, **12**, 703–734, <https://doi.org/10.5194/amt-12-703-2019>.
- Vaughan, M., A. Garnier, D. Josset, M. Avery, K.-P. Lee, Z. Liu, W. Hunt, J. Pelon, Y. Hu, S. Burton, J. Hair, J. Tackett, B. Getzewich, J. Kar, and S. Rodier, 2019: CALIPSO Lidar Calibration at 1064 nm: Version 4 Algorithm, *Atmos. Meas. Tech.*, **12**, 51–82, <https://doi.org/10.5194/amt-12-51-2019>.
- Avery, M. A., R. A. Ryan, B. J. Getzewich, M. A. Vaughan, D. M. Winker, Y. Hu, A. Garnier, J. Pelon, and C. A. Verhappen, 2020: “CALIOP V4 Cloud Thermodynamic Phase Assignment and the Impact of Near-Nadir Viewing Angles”, *Atmos. Meas. Tech.*, **13**, 4539–4563, <https://doi.org/10.5194/amt-13-4539-2020>.
- Ryan, R. A., M. A. Vaughan, S. D. Rodier, J. L. Tackett, J. A. Reagan, R. A. Ferrare, J. W. Hair, and B. J. Getzewich, 2024: “Total Column Optical Depths Retrieved from CALIPSO Lidar Ocean Surface Backscatter”, *Atmos. Meas. Tech.*, **17**, 6517–6545, <https://doi.org/10.5194/amt-17-6517-2024>.
- Tackett, J. L., J. Kar, M. A. Vaughan, B. Getzewich, M.-H. Kim, J.-P. Vernier, A. H. Omar, B. Magill, M. C. Pitts, and D. Winker, 2023: “The CALIPSO version 4.5 stratospheric aerosol subtyping algorithm”, *Atmos. Meas. Tech.*, **16**, 745–768, <https://doi.org/10.5194/amt-16-745-2023>.
- Tackett, J. L., R. A. Ryan, A. E. Garnier, J. Kar, B. Getzewich, X. Cai, M. A. Vaughan, C. R. Trepte, R. Verhappen, D. M. Winker and K.-P. A. Lee, 2025: Mitigating Impacts of Low Energy Laser Pulses on CALIOP Data Products, *EGUsphere* [preprint], <https://doi.org/10.5194/egusphere-2025-2376>.
- Toth, T. D., G. Schuster, M. Clayton, Z. Li, D. Painemal, S. Rodier, J. Kar, T. Thorsen, R. Ferrare, M. Vaughan, J. Tackett, H. Bian, M. Chin, A. Garnier, E. Welton, R. Ryan, C. Trepte and D. Winker, 2025: “Mapping CALIPSO Marine and Dusty Marine Aerosol Lidar Ratios using MODIS AOD Constrained Retrievals and GOCART Model Simulations” *EGUsphere* [AMTD], <https://doi.org/10.5194/egusphere-2025-2832>.

Data Release Information

At the conclusion of the mission, the CALIPSO project had released five major versions of the lidar level 2 data products, as well as several minor version updates. Table 12 lists all major and minor releases.

Table 13: release date, version number, data date range, and production strategy for all CALIPSO lidar level 2 data products

Lidar Level 2: Half orbits (Night and Day)			
Release Date	Version	Data Date Range	Production Strategy
October 2025	5.00	June 13, 2006 to June 30, 2023	Standard
June 2023	4.51	June 13, 2006 to June 30, 2023	Standard
October 2020	4.21	July 01, 2020 to January 19, 2022	Standard
October 2018	4.20	June 13, 2006 to June 20, 2020	Standard
November 2016	4.10	June 13, 2006 to September 30, 2020	Standard
October 2020	3.41	October 1, 2020 to June 30, 2023	Validated Stage 1
December 2016	3.40	December 1, 2016 to September 31, 2020	Validated Stage 1
April 2013	3.30	March 1, 2013 to November 30, 2016	Validated Stage 1
December 2011	3.02	November 1, 2011 to February 28, 2013	Validated Stage 1
May 2010	3.01	June 13, 2006 to October 31, 2011	Validated Stage 1

Lidar Level 2: Half orbits (Night and Day)			
Release Date	Version	Data Date Range	Production Strategy
October 2008	2.02	September 14, 2008 to October 29, 2009	Provisional
January 2008	2.01	June 13, 2006 to September 13, 2008	Provisional
December 2006	1.10	June 13, 2006 to November 11, 2007	Provisional / Beta

Data Quality Summaries

Data Quality Statement for CALIPSO's Version 5.00 Lidar Level 2 Data Product Release

Data Version: 5.00
Data Release Date: 1 October 2025
Data Date Range: June 13, 2006 to June 30, 2023

The sections below highlight the most significant changes made in the CALIOP version 5.00 (V5.00) level 2 data products. The magnitude and effects of these changes are frequently illustrated with comparisons to the previous release of the version 4.51 (V4.51) data products.

Modifications for Low Energy Mitigation (LEM)

During final seven years of the CALIPSO mission, a slow leak in the laser canister ([Hunt et al., 2009](#)) reduced the internal pressure below the voltage breakdown limit described by [Pachen's law](#). Once this occurred, intermittent coronal arcing across the Q switch caused the CALIOP laser to begin emitting an increasing number of low-to-no energy laser pulses. As seen in Figure 7, early on this behavior was confined almost exclusively to the South Atlantic Anomaly (SAA; [Rodriguez et al., 2022](#)) but toward the end of the mission the phenomenon occurred worldwide.

Because CALIOP profiles are time-averaged onboard the satellite prior to downlink ([Hunt et al., 2009](#)), the deleterious effects of individual low energy pulses are not localized, but instead cause a degradation in signal quality across multiple consecutive shots. To minimize these effects, the CALIPSO lidar science working group (LSWG) developed a family of low energy mitigation (LEM) algorithms ([Tackett et al., 2025](#)) that identify compromised level 1b data segments on small, targeted scales. Using a highly optimized data filtering scheme, these segments are subsequently excluded from all level 2 data analyses. The level 1 LEM algorithm corrects a pervasive low daytime calibration bias (3% to 4%) and reduces daytime calibration uncertainties by 20% to 40% in the SAA latitude band. In addition, the V5.00 level 1 energy normalization process now correctly compensates for the inclusion of no energy laser pulses in data averaged onboard the satellite. As demonstrated by Figure 8, this level 1 modification, in combination with the level 2 LEM algorithms, yields a substantial reduction in the number of false positive feature detections.

Note that averaged profiles containing one or more low energy pulses are not automatically excluded in the level 2 analyses. Horizontally averaged data segments that are "LEM-affected" (i.e., some low energy shots are present, but the filtered profile is still deemed acceptable for science retrievals) experience a signal-to-noise ratio reduction of 6–9 % which slightly increases the probability of false detections relative to unaffected data. However, as illustrated by Figure 9, the median measured optical properties of the LEM-affected layers typically differ from the properties of unaffected layers by ~1.0% or less.

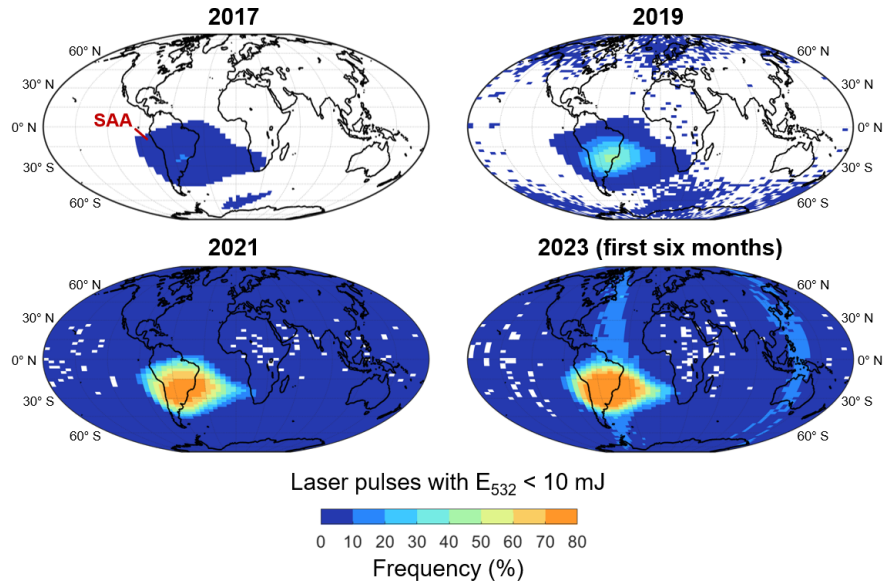


Figure 7: Global frequencies of laser pulses having 532 nm energies less than 10 mJ during 2017, 2019, 2021, and the first six months of 2023. The vertical bands of high frequencies seen in 2023 are caused by daytime granules having nearly continuous low energy pulses during May and June; e.g., see 2023-06-12T05-54-23ZD. (Figure from [Tackett et al., 2025](#))

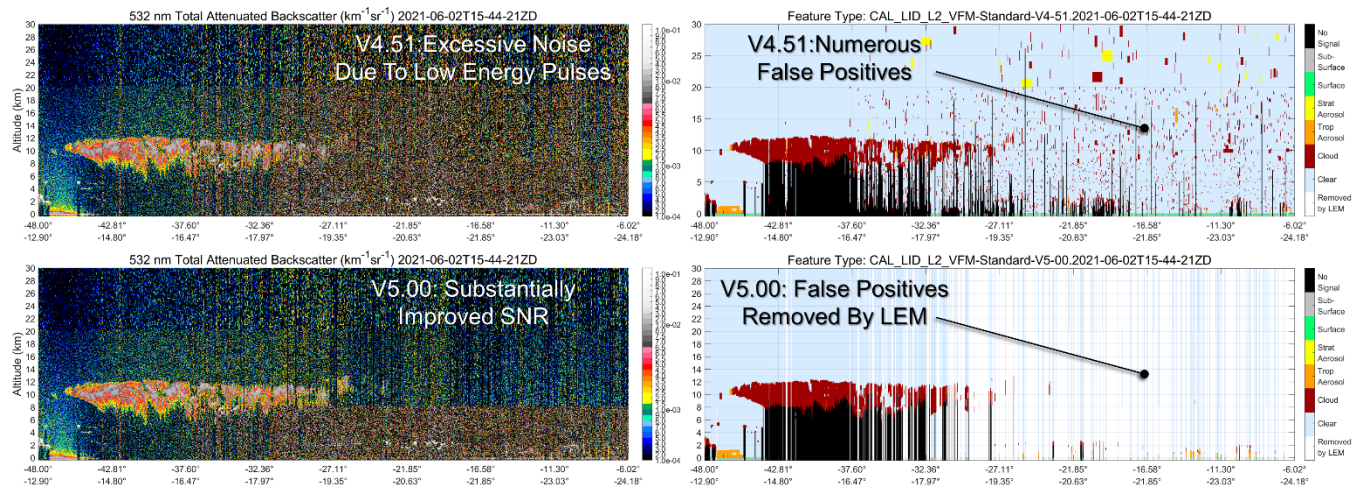


Figure 8: Top row shows the level 1 532 nm total attenuated backscatter ($\beta'(z)$, left) and the corresponding level 2 vertical feature mask (VFM, right) from the V4.51 release for a granule strongly affected by low energy pulses on 02 June 2021 at 16Z. Similarly, the bottom row shows the same quantities for the V5.00 release. Relative to V4.51, the SNR above 8.2 km is noticeably higher in the LEM-filtered V5.00 532 nm $\beta'(z)$ example. Similarly, the V5.00 VFM arguably eliminates all of the false positive feature detections seen in V4.51. (Figure adapted from [Tackett et al., 2025](#).)

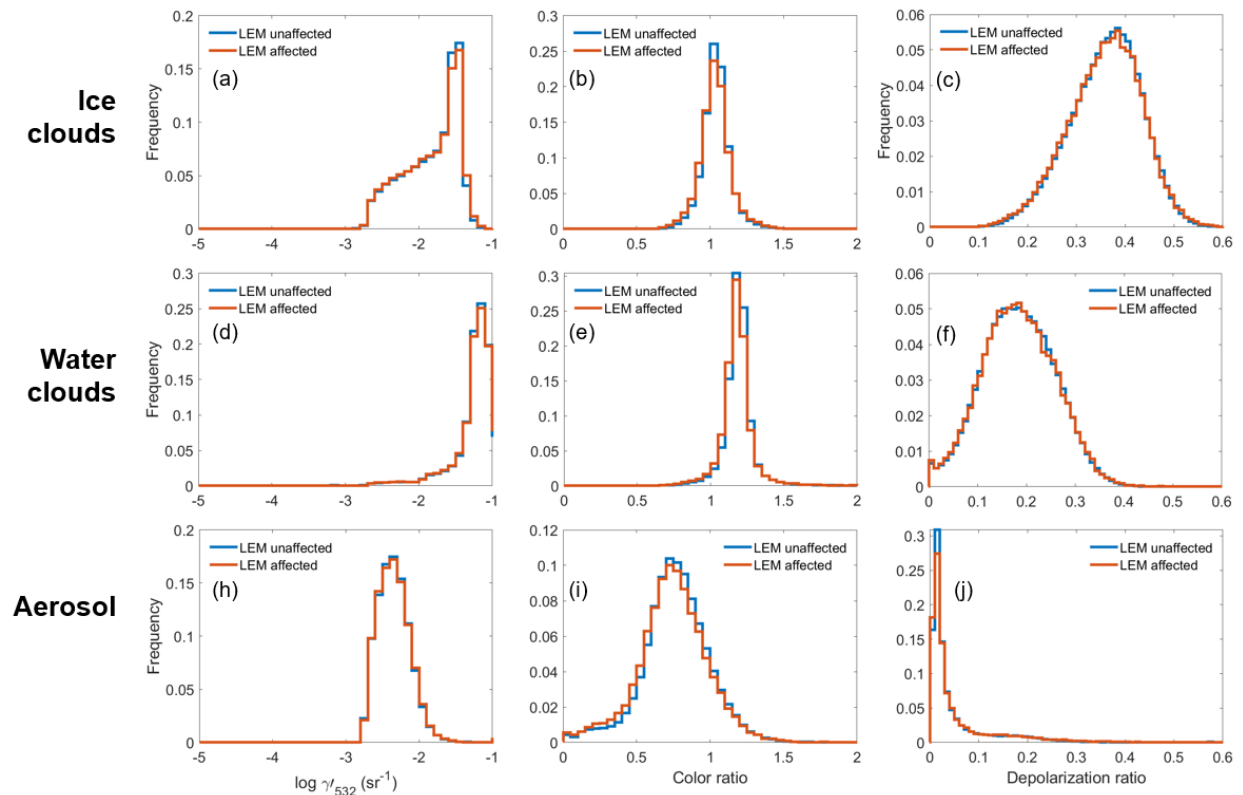


Figure 9: Frequency distributions of layer-integrated 532 nm attenuated backscatter (γ'_{532}), layer-mean attenuated backscatter color ratio ($\bar{\beta}'_{1064}/\bar{\beta}'_{532}$), and layer-integrated volume depolarization ratio for ice clouds (panels a-c), water clouds (panels d-f), and aerosol layers (panels h-j). Distributions from layers wholly unaffected by low energy pulses are shown in aqua. Distributions for LEM-affected layers are shown in orange. Statistics are computed from layers detected in nighttime measurements at 5 km horizontal resolution between 50°S-50°N, excluding the SAA, during all of 2021. (Figure from [Tackett et al., 2025](#).)

To enable users to easily identify LEM-affected features and profiles that have been wholly excluded by the LEM algorithm, the CALIOP level 2 layer products and profile products now report a ‘Low Energy Column QC Flag’ for each atmospheric column in the respective data sets. These flags are bit-mapped 16-bit integers that indicate which columns contain low energy laser pulses, which columns have been wholly rejected as unusable, why rejected columns have been excluded, and which of CALIOP’s altitude-dependent averaging regions contain LEM-rejected data. The interpretations of individual bits are given in Table 14. With the exception of the 333 m merged layer products, all layer products and profile products also report a Boolean ‘Low Energy Mitigation Feature QC Flag’. When this flag is true, the corresponding feature (layer products) or range bin (profile products) contains either LEM-affected data, in which some low energy pulses were included in the data averaged onboard the satellite prior to downlink, or LEM-rejected data that have been wholly excluded from the level 2 analyses. The layer descriptions (e.g., top and base altitudes, integrated attenuated backscatter, etc.) in LEM-rejected columns are identified with a LEM flag value of -111.

LEM information is reported in the vertical feature mask (VFM) product via the new ‘VFM Feature Detection Quality Flag’. Like the ‘Feature Classification Flags’, which have always been reported in the VFM files, the ‘VFM Feature Detection Quality Flag’ is an array of bit-mapped 16-bit integers, with one value reported for each element in the downlinked data stream. As shown in Table 15, these bits inform data users which range bins contain low energy shots, which have been rejected by LEM, and which feature finder averaging resolution was required for the feature to be detected.

Table 14: Interpretation of the individual bits in the Low Energy Column QC Flag; note that “a frame” consists of 15 consecutive laser pulses that have been averaged onboard the satellite to the vertical and horizontal spatial resolutions given in ([Hunt et al., 2009](#)). Bit 0 is the least significant bit.

Bit	Interpretation
0	Column contains LEM-affected data (data has been rejected or contains low energy pulses that LEM accepts)
1	Column belongs to a 5 km frame that has been rejected due to too many unusable profiles
2	Column belongs to a 5 km frame that has been rejected due to too many rejected subregions in altitude region 3
3	Column belongs to a 5 km frame that has been rejected due to too many rejected subregions in altitude region 4
4	Feature detection not performed at 20 km resolution in this column due to too many rejected frames
5	Feature detection not performed at 80 km resolution in this column due to too many rejected frames
6	Unused
7	Column has data rejected in altitude regions 1 and 2 (only reported at single-shot resolution)
8	Column has data rejected in altitude region 3 (only reported at single-shot resolution)
9	Column has data rejected in altitude region 4 (only reported at single-shot resolution)
10	Column does not have low energy, but data is rejected in regions 1 & 2 due to rejected data in altitude region 3 (only reported at single-shot resolution)
11–15	Unused

Table 15: bit interpretations for the ‘VFM Feature Detection Quality Flag’; bit 0 is the least significant bit.

Bit	Interpretation
0	First single-shot profile has low energy
1	Second single-shot profile has low energy
2	Third single-shot profile has low energy
3	Fourth single-shot profile has low energy
4	Fifth single-shot profile has low energy
5	Bin in first single-shot profile is rejected by LEM
6	Bin in second single-shot profile is rejected by LEM
7	Bin in third single-shot profile is rejected by LEM
8	Bin in fourth single-shot profile is rejected by LEM
9	Bin in fifth single-shot profile is rejected by LEM
10	Contributed to feature detection at 1/3 km resolution
11	Contributed to feature detection at 1 km resolution
12	Contributed to feature detection at 5 km resolution
13	Contributed to feature detection at 20 km resolution
14	Contributed to feature detection at 80 km resolution
15	Unused

The effects of the low energy mitigation filtering are pervasive throughout the CALIPSO level 2 data products, particularly in the final years of the mission. To optimize the functioning of the LEM algorithms required several LEM-related changes to the lidar level 2 analyses.

- The feature classification flags (in the layer products and VFM) and the atmospheric volume descriptions (in the profile products) no longer include an “invalid” feature category. Previously, invalid features could be readily identified whenever the three least significant bits were all set to zero. Invalid features occurred extremely rarely – e.g., 872 of the 41,194,051 (~0.002%) of the unique atmospheric features detected during

all of 2012 we designated as invalid. These features were also assigned special cloud-aerosol discrimination (CAD) scores ([Liu et al., 2019](#)) to give users some insight into the failure mechanism that cause the layer to be identified as invalid. In V5.0, having the three least significant bits of a feature classification flag evaluate to zero no longer represents an ‘invalid’ classification of a detected layer, but instead indicates that data in the column has been rejected by the level 2 LEM filter. The spatial and optical properties within these columns (e.g., top and base altitudes, CAD scores, and optical depths) are all set to a special LEM flag value (-111). Features that were previously classified as invalid are now identified as zero-confidence clouds and they retain any of the special CAD scores that were assigned in previous data releases.

- Substantial modifications were required to add “LEM awareness” to the CALIOP boundary layer cloud clearing (BLCC) algorithm. The function of this procedure is to separate boundary layer clouds from the surrounding aerosols at single shot resolution so that the signal-to-noise ratios (SNR) of the aerosol data could be improved by large scale averaging, thus greatly reducing uncertainties in the aerosol extinction retrievals. Problems arose, however, when dense aerosols lay immediately above stratus decks. In these cases, the combined aerosol and cloud signals were often detected as a single, heterogenous feature in CALIOP’s initial 5 km (15 shot) resolution profile scan ([Vaughan et al., 2009](#)). The clouds in these multi-type features were subsequently identified at single shot resolution. However, when 15 horizontally adjacent clouds were detected at single shot resolution within a single 5 km segment, a logic flaw in the BLCC scheme failed to separate these clouds from the overlying aerosol. This, in turn, introduced significant errors into the affected aerosol extinction retrievals. While this flaw was largely eliminated in the V4.51 data release ([Tackett et al., 2022](#)), some residual errors remained. When checking for the presence of 15 horizontally adjacent clouds detected at single shot resolution, the V4.51 BLCC did not account for contamination by low energy laser pulses. Since no clouds would be detected in these single shot low energy pulses, the count of horizontally adjacent clouds within the 5 km segment would fall below 15. As a consequence, these clouds were not properly separated from the overlying aerosol prior to calculating an extinction solution. Not surprisingly, the extinction solutions retrieved for these unintentionally heterogenous layers were completely unreliable. This situation is ameliorated in V5.00 by excluding low energy pulses when calculating the fraction of laser shots in which clouds are detected at single shot resolution.
- In concert with the above change to the BLCC, the calculation of the ‘Single Shot Cloud Cleared Fraction’ parameter reported in all 5 km averaged products was updated to correctly account for LEM-rejected profiles. As an example, if 5 clouds are detected at single shot resolution within a 5 km along-track segment that also included 5 low energy laser pulses, the single shot cloud cleared fraction in the V5.00 data products will be $5/10 = 0.5$ versus $5/15 = 0.333$ in the V4.51 products.
- To improve the accuracy of the surface detection algorithm and prevent spurious detections, the surface detection algorithm was modified to recognize and exclude LEM-rejected data.
- To accommodate the addition of the special LEM flag value (-111), the data types of the ‘Cloud Layer Fraction’, ‘Aerosol Layer Fraction’, and ‘High Resolution Layers Cleared’ scientific data sets (SDSs) were changed from unsigned integers to signed integers.

Changes to Aerosol Lidar Ratios

The [Models, In situ, and Remote sensing of Aerosols \(MIRA\)](#) working group was formed by an international team of aerosol research scientists shortly after the successful conclusion of the [CALIPSO Version 5 Aerosol Lidar Ratio Workshop](#) in March 2021. One of the primary goals initially identified by the MIRA group was to develop a solid empirical basis for creating a global set of spatially and seasonally varying [Maps of Aerosol lidar ratios for CALIPSO \(MAC\)](#). Based on in-depth analyses by MAC researchers, CALIPSO’s V5.00 data release makes extensive changes to the default lidar ratios used to initiate extinction solutions for the marine and dusty marine aerosol types.

In all previous data releases, the CALIOP aerosol subtypes were characterized by a single, type specific, globally applicable lidar ratio, together with an associated uncertainty estimate that defined the lidar ratio’s expected natural variability ([Kim et al., 2018](#)). For example, the lidar ratios for marine and dusty marine types were,

respectively, 23 ± 5 sr and 37 ± 15 sr. In preparation for the V5.00 release, the MAC team constructed tropospheric aerosol optical depth (AOD) estimates by subtracting the stratospheric AODs reported in CALIPSO's level 3 stratospheric aerosol product ([Kar et al., 2019](#)) from the full column AODs reported by [MODIS](#). These tropospheric AODs were then paired with collocated CALIOP 532 nm attenuated backscatter profiles to retrieve aerosol lidar ratio estimates from constrained solutions of the lidar equation ([Toth et al., 2025](#)). Retrievals were limited to cloud-free scenes over oceans in which CALIPSO identified only a single aerosol type (i.e., either marine or dusty marine) within a 5 km averaged column. Solutions were calculated for all qualifying measurements obtained while CALIPSO flew in the [A-Train](#) with MODIS-Aqua, from June 2006 through August 2018. The retrieved lidar ratios for each of the two aerosol types were then aggregated into four seasonal maps (winter, spring, summer, and fall) having a spatial resolution of 2° latitude \times 4.8° longitude. Grid cells having fewer than 50 samples – e.g., in polar winters, when the MODIS orbit does not allow for the daytime measurements necessary to retrieve AOD – are excluded from these maps. These excluded values are replaced with an approximation derived from the relationship between the constrained lidar ratios and the sea salt volume fraction (SSVF) computed using parameters reported by the [Goddard Chemistry Aerosol Radiation and Transport \(GOCART\)](#) model ([Toth et al., 2025](#)). For any V5.00 CALIOP footprint, the locally appropriate lidar ratio and its associated uncertainty are interpolated in both time and space from the map data.

Figure 10 shows the seasonal maps developed for marine aerosols. Seasonal and regional variations in marine lidar ratios are plainly visible and often show a marked difference from the 23 ± 5 sr value used globally in previous data releases. These differences highlight an important conceptual difference between the V5.00 marine lidar ratios and the marine lidar ratios in previous data releases. Previously, the marine lidar ratio represented our best approximation of “clean marine” conditions (e.g., see [Kim et al., 2018](#)). In V5.00, marine lidar ratios are assigned to aerosols detected over oceans that are dominated by marine constituents but that can also be mixed with other, mostly anthropogenic components. As seen in Figure 10, genuinely pristine marine aerosols are largely confined to the remote southern oceans. Coastal regions frequently exhibit a pronounced influence from other aerosol sources that elevates the lidar ratios to values significantly higher than those seen in the southern oceans.

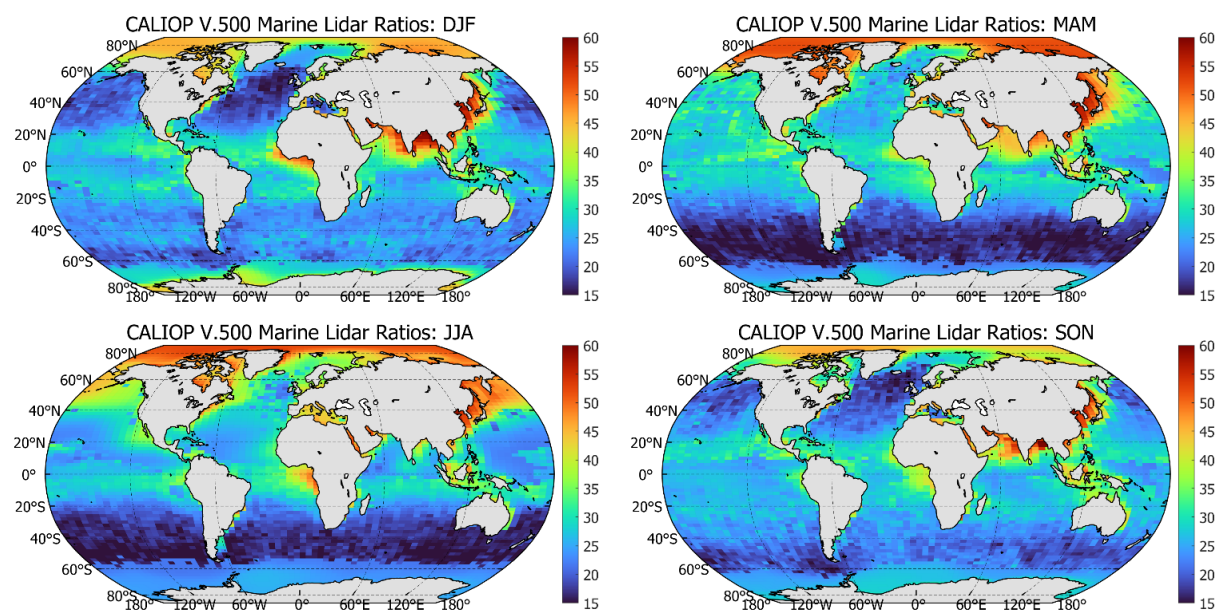


Figure 10: CALIOP initial marine lidar ratios (units = sr) derived from CALIOP 532 nm attenuated backscatter profiles constrained by collocated MODIS aerosol optical depths. The top left shows median values for the winter months (December, January, and February); the top right shows median values for the spring (March, April, and May); the bottom left shows median values for the summer (June, July, and August); and the bottom right shows median values for the fall (September, October, and November).

Our approach for constructing dusty marine maps was, with two notable exceptions, essentially identical to the method we used for marine aerosols. The first exception is that for the dusty marine maps we also included lidar

ratio solutions constrained by CALIOP's ocean-derived column optical depth (ODCOD; [Ryan et al., 2024](#)) retrievals. For the marine lidar ratios, ODCOD retrievals were excluded so that they could later be used to validate the MODIS constrained retrievals. However, for the dusty marine type, sun glint contaminating the collocated MODIS measurements precluded their use as an AOD constraint in important dust transport corridors (e.g., during boreal summers in the Caribbean and central western Atlantic). Consequently, we chose to include ODCOD constrained solutions in developing the dusty marine maps. The second exception is that, unlike the marine lidar ratio maps, the seasonal variability in the dusty marine maps is limited to the green shaded region shown in Figure 11. While other parts of the hydrosphere showed little, if any, seasonal variation (perhaps due to temporal changes in dust concentrations), significant seasonal variations in dusty marine lidar ratios were observed over the Mediterranean Sea, the Persian Gulf, the Arabian Sea, and the Bay of Bengal. Furthermore, the seasonal sample counts in these regions were large enough in each season to retrieve confident lidar ratio estimates. Neither of these conditions were met simultaneously in any other extended regions of the globe.

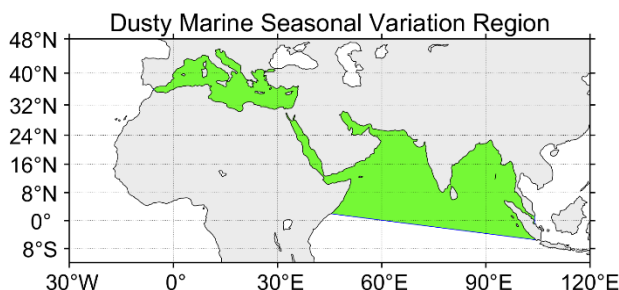


Figure 11: the green shaded area of the map indicates those regions where CALIOP's dusty marine lidar ratios are observed to vary seasonally.

The V5.00 dusty marine maps are shown in Figure 12. As expected, the dusty marine lidar ratios are uniformly larger than the marine lidar ratios. The spatial patterns of the two types are generally similar, simply because anthropogenic aerosol transport patterns are essentially identical for both types and the inclusion of anthropogenic aerosols elevates both sets of values.

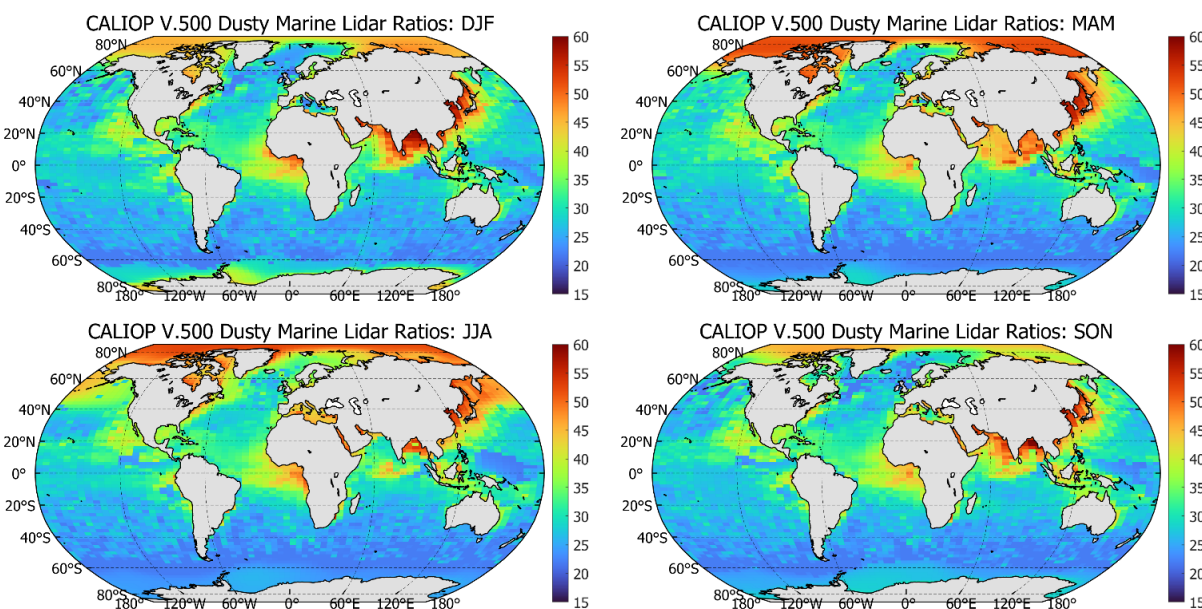


Figure 12: CALIOP initial dusty marine lidar ratios (units = sr) derived from CALIOP 532 nm attenuated backscatter profiles constrained by collocated aerosol optical depth measurements from MODIS and ODCOD. The top left shows median values for the winter months (December, January, and February); the top right shows median values

for the spring (March, April, and May); the bottom left shows median values for the summer (June, July, and August); and the bottom right shows median values for the fall (September, October, and November).

A second change to the CALIOP aerosol lidar ratios is the selection of a new value of 45 ± 24 sr for 1064 nm retrievals of clean continental aerosol. This change is based on field measurements of continental aerosol made by [Haarig et al., 2025](#) using a 1064 nm rotational Raman lidar. The 532 nm lidar ratio for the clean continental type remains unchanged at 53 ± 24 sr.

Changes to Aerosol Type Identification

In addition to the MAC lidar ratio work, the V5.00 data set contains a second fairly substantial (albeit localized) change. CALIOP's V4.51 aerosol subtyping algorithm classified planetary boundary layer (PBL) aerosols located over ocean surfaces as marine, with ocean surfaces being identified using the CALIPSO land-water mask. In Arctic winter however, most of the "ocean surfaces" reported by the land-water mask are actually extended over-ocean ice sheets, and the aerosol above is not marine but instead some species of anthropogenic aerosol arriving in the polar regions via long range transport. In these cases, assigning a marine aerosol lidar ratio to the aerosol layer both misrepresents the true aerosol type and leads to sometimes substantial underestimates of aerosol optical depth. By expanding the surface type identification scheme to also include snow and ice data reported in the CALIOP level 1b files and by making small modifications to the aerosol subtyping flowchart (see Figure 13), the V5.00 CALIOP data product now more correctly classifies a large fraction of these "over frozen ocean" aerosols.

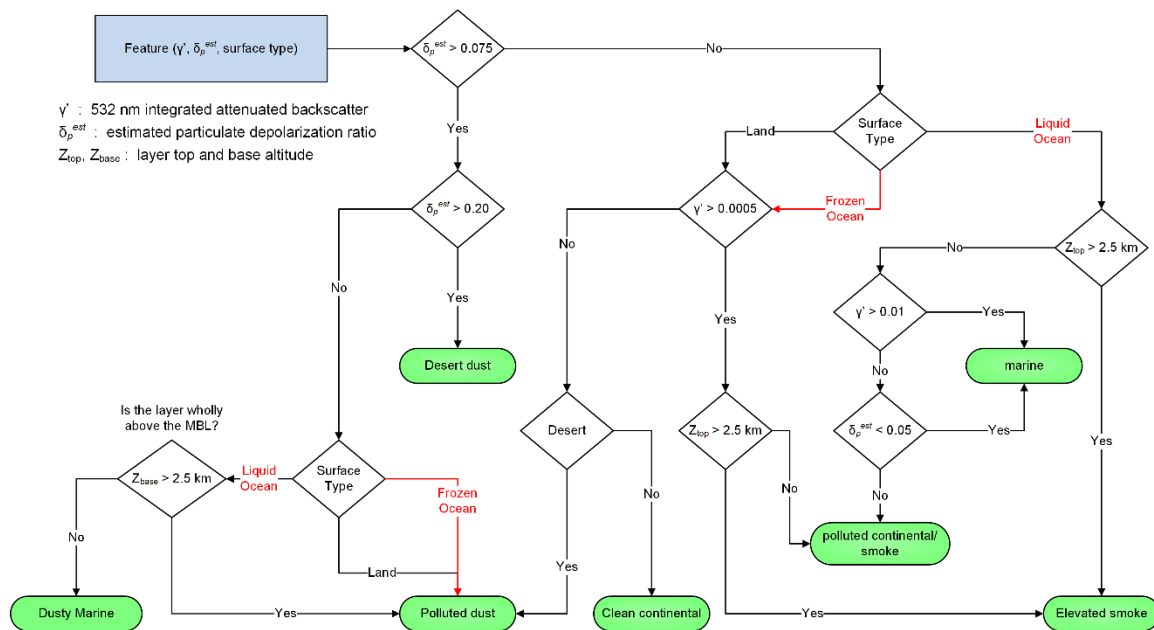


Figure 13: revised tropospheric aerosol subtyping flowchart; paths and labels in red were added for the V5.00 release.

New ODCOD Retrieval Confidence Flag

In response to data user requests, a new confidence flag has been added to the existing 'ODCOD QC Flag' SDS reported in the 'Ocean Derived Column Optical Depth' Vgroup included in all layer products and profile products. Table 17 describes how to interpret all of the bits used in the 'ODCOD QC Flag'. The new confidence flag (shown in orange) is reported in bit 6. In this new configuration, all valid ODCOD retrievals will have an 'ODCOD QC Flag' of 127 or less. All high confidence ODCOD retrievals will have an 'ODCOD QC Flag' value of 63 or less. Any of the following conditions will cause bit 6 to be toggled on, indicating a low confidence solution.

- Wind speed out of range; the AMSR corrected MERRA-2 wind speed is less than 3 m/s or greater than 15 m/s
- Surface integrated depolarization ratio is greater than 0.05, suggesting that the surface is not pure sea water

- c) Surface integrated attenuated backscatter exceeds the upper bound specified in Table 16.

Table 16: maximum values of surface integrated attenuated backscatter for confident retrievals; higher values may include undetected surface saturation.

	Daytime	Nighttime
532 nm	0.0413 sr ⁻¹	0.0353 sr ⁻¹
1064 nm	0.0384 sr ⁻¹	0.0325 sr ⁻¹

- d) The number of range bins shifted by the altitude registration algorithm ([Powell et al., 2009](#)) is not constant over all profiles used to create the averaged surface return. This is only a concern for averaged profiles where having multiple “bins shifted” will distort the shape of the spatially averaged surface return and degrade the quality of the fit to the CALIOP response model (CRM; [Ryan et al., 2024](#)). To aid in diagnosing the presence of non-constant bin shifts, a new SDS (‘ssNumber Bins Shift’) was added to the ‘Single Shot Detection’ Vgroup reported in the 5 km layer products.

Table 17: interpretation of the individual bits in the ODCOD QC flags (adapted from [Ryan et al., 2024](#)); bit 0 is the least significant bit.

Bit	Interpretation
0	Of the measurements provided to the ODCOD algorithm by the surface detection algorithm, ODCOD adjusted the CRM such that the first data point of the surface detection data was not the first point on the CRM
1	The surface detection algorithm provided surface measurements covering a range greater than 120 m
2	The ODCOD algorithm used range bins above the top of the detected surface altitude
3	The ODCOD algorithm used range bins below the base of the detected surface altitude
4	When solving for the alignment of the CRM, the first measurement that should fall on the CRM curve was not originally provided by the surface detection algorithm
5	ODCOD had to adjust the CRM such that the first measurement provided by the surface detection algorithm was not the first point on the CRM
6	ODCOD retrieval confidence flag; a value of 1 indicates a confident retrieval whereas 0 signals low confidence
7-9	Unused
10	The surface detection algorithm did not find a surface
11	The International Geosphere–Biosphere Programme (IGBP) surface type is not 17 for ocean
12	The depolarization ratio of the surface is greater than 0.15
13	The corrected MERRA-2 wind speed is outside of the inclusive range 0.025 m s ⁻¹ to 43 m s ⁻¹
14	ODCOD has failed to find the time delay of the CRM from the surface measurements provided by the surface detection algorithm
15	The vertical extent of the detected surface contains too few samples to derive a time delay solution
16	When solving for the CRM area, the solution grew unrealistically large
17	A failure occurred while attempting to solve for the scale factor
18	Surface saturation was detected in the surface return
19	Negative signal anomaly was detected in the surface return
20	The detected surface contains negative or invalid backscatter measurements
21	Necessary input data is either fill or invalid
22	The surface detection algorithm had to resort to an alternative method of finding the surface when the surface return was averaged to coarser resolutions that may not be reliable for ODCOD

Bit	Interpretation
23–31	Unused

Wrong profile starts for a new chunk after missing data gap

The CALIOP level 2 processing ingests level 1 data in 80 km “chunks”, equivalent to the largest horizontal averaging resolution used in the search for features. Each chunk contains 240 consecutive single-shot profiles distributed uniformly across 16 consecutive 5-km (15 shot) frames. If there are any missing data within these 240 consecutive profiles, the candidate chunk is discarded, and the level 2 processing resumes beginning with the first single shot profile in the first frame available after the data gap. However, the V4.51 and earlier level 2 code contained an “off by one” error that caused this processing restart to begin with the second profile in the frame instead of the first. As a consequence of eliminating this error, in granules containing data gaps – e.g., for planned activities such as boresight alignments and polarization gain ratio calibrations or for unplanned events such as the repeated ground station downlink anomalies that occurred between 21:20:46 UTC on 2020-12-12 and 00:12:12 UTC on 2020-12-13 – the level 2 chunks built following those data gaps will use a somewhat different collection of single shot profiles in V5.00 relative to all previous versions. Figure 14 shows an example of the kinds of changes that can occur due to this change in profiles averaged. The upper panel shows daytime data acquired in the southern Pacific Ocean on 2020-12-12 at ~22:27 UTC. On this day, data downlink from the satellite was intermittently interrupted by ground station errors. The white vertical strips in the upper panel show where individual frames were missing or irretrievably corrupt in the downlink data stream. The lower panel is a “red-green-black” diagram comparing feature detections in V4.51 to those in V5.00. The green areas represent features detected in both data processing versions, while the red areas show features that were detected in V4.51 but not V5.00 and the black areas show the opposite; i.e., features that were detected in V5.00 but not V4.51. Regions where no features were detected in either analysis are shown in white. The vertical gray bars show where chunks have been rejected by the level 2 processing due to the presence of missing data. In some cases – e.g., following the first to data gaps beginning at ~41.5°S and ~37.2°S – there are no layer detection changes. On the other hand, the region following the final data gap shows substantial changes, though not all of them can be attributed to the change in the selection of pseudo-single shot profiles to average. The red range bins not detected in V5.00 were eliminated by the LEM algorithm described above. In this and other segments, the intermittent detection changes in individual range bins adjacent to the Earth’s surface occur due to V5.00 changes in VFM altitude registration, as described below in the Revised VFM Layer Detection Altitudes section. The additional aerosol detections highlighted by the black areas in this data segment are a fortuitous result of the combination of a shift in profiles averaged combined with LEM filtering. We note, however, that additional feature detections are not a guaranteed outcome of this code change.

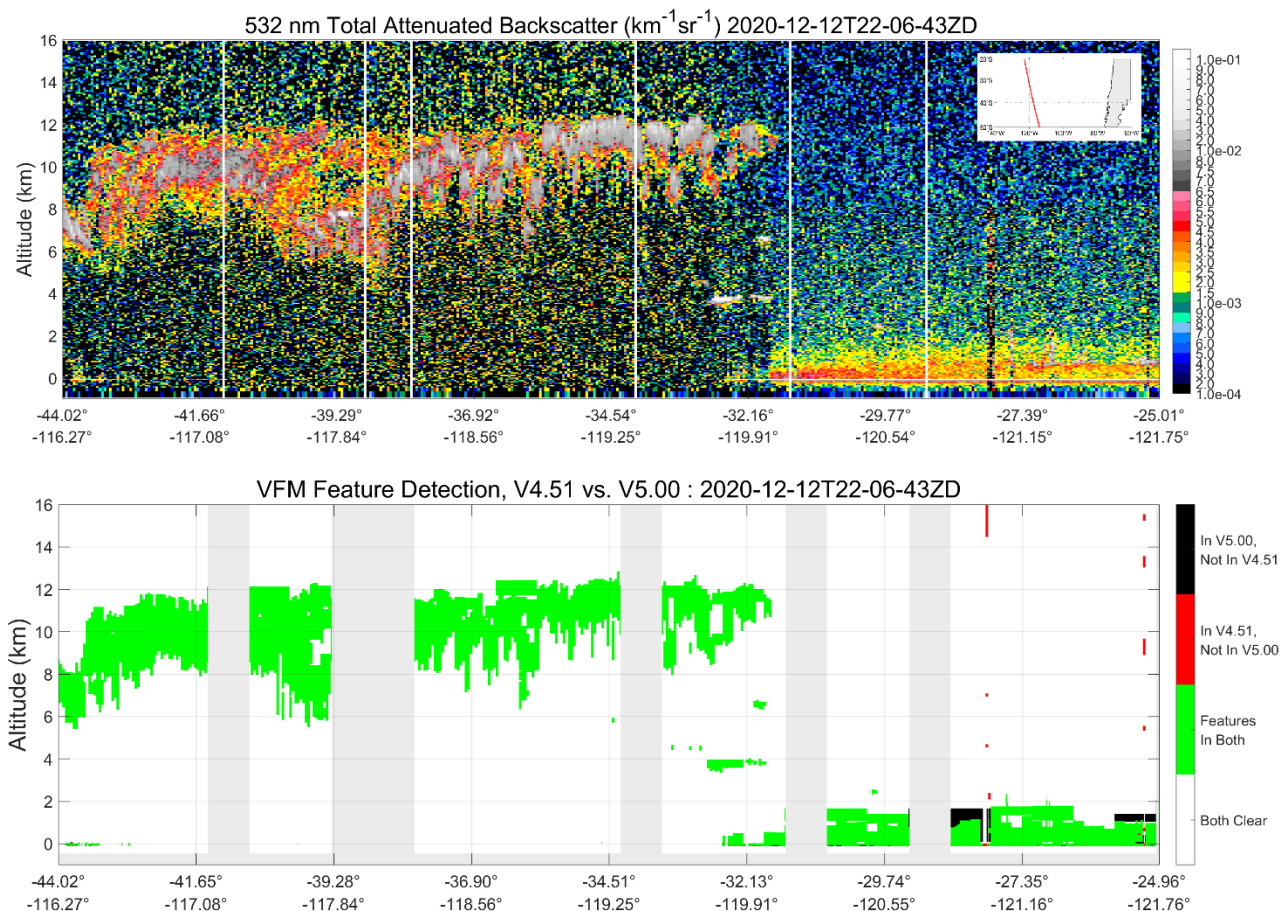


Figure 14: The upper panel shows 532 nm total attenuated backscatter coefficients measured in the southern Pacific Ocean on 2020-12-12 at ~22:27 UTC. The white vertical stripes in the image represent frames (i.e., 15 consecutive shots) containing missing data. The lower panel compares V4.51 and V5.00 VFM feature detections for the scene shown in the upper panel. The gray vertical stripes show where chunks (i.e., 240 consecutive shots) were rejected by the level 2 processing algorithms due to missing data in one or more included frames.

HDF File Changes

The V5.00 CALIPSO data products are distributed as Hierarchical Data Format Version 4 (HDF4) files, consistent with the EOS requirement in effect when CALIPSO launched in 2006. Since launch, there have been substantial technological advances in data discoverability and access to resources. To make CALIPSO data more readily accessible to the scientific community beyond the life of the mission and take advantage of newer data access capabilities, several modifications were made to the format and content of the CALIOP HDF files. These include:

- Updating all units to conform to [NetCDF Climate and Forecast \(CF\)](#) metadata conventions.
- Ensuring that all dimensions are named, to allow HDF to NCDF conversions using commercial off the shelf (COTS) tools that currently exist.
- Creating/expanding SDS attributes and comments to make the data products more self-documenting.

New Data Product: CAL_LID_L2_MLay_Diagnostic-Beta-V5-00*.hdf

The newly released CAL_LID_L2_MLay_Diagnostic-Beta-V5-00*.hdf data products are augmented versions of the standard CAL_LID_L2_05kmMLay_Standard-V5-00*.hdf products. The production strategy for these products is 'Beta', indicating that some of the included parameters have not been fully validated. In particular, these 'not fully validated' parameters include the cloud values reported in the 1064 nm derived optical properties SDSs (e.g.,

‘Feature Optical Depth 1064’). While the Diagnostic Beta products contain all the information reported in the Standard products, they also contain the five SDSs listed below that are not reported in the Standard products.

1. Low Energy Mitigation Internal Column QC Flag – a 16-bit unsigned integer that offers extra insight into the internal workings of the LEM algorithm. Bit interpretations are given in Table 18.
2. Initial Integrated Attenuated Backscatter 532 – The standard ‘Integrated Attenuated Backscatter 532’ (γ'_{std}) values reported in all CALIOP lidar level 2 layer files are calculated assuming that the feature attenuated backscatter coefficients have been corrected for signal attenuation due to all layers detected above. The ‘Initial Integrated Attenuated Backscatter 532’ (γ'_{init}) values are recorded immediately after feature detection during the initial 5 km search for features. At this point in the processing, no single shot cloud clearing has been done nor have the layers been classified by the CAD algorithm. Assuming perfect detection and classification and perfect knowledge of layer lidar ratios and multiple scattering factors, $\gamma'_{init} = T^2_{above} \times \gamma'_{std}$, where T^2_{above} is the two-way transmittance of all overlying particulate layers. In special cases, when particulate layers lie above opaque water clouds, measurements of γ'_{init} can be used to derive estimates of T^2_{above} and hence obtain estimates of the overlying particulate optical depths ([Hu et al., 2007](#)). These measurements of γ'_{init} are an essential input required for calculating the ‘Column Particulate Optical Depth Above Opaque Water Cloud 532’ values reported in all layer products.
3. Initial Integrated Attenuated Backscatter Uncertainty 532 – uncertainty estimates for the ‘Initial Integrated Attenuated Backscatter 532’ which are subsequently used to calculate the ‘Column Particulate Optical Depth Above Opaque Water Cloud Uncertainty 532’ values.
4. Initial Integrated Attenuated Backscatter 1064 – this is the 1064 nm analog of the ‘Initial Integrated Attenuated Backscatter 532’. Because CALIOP does not make depolarization ratio measurements at 1064 nm, this parameter is unused in the V5.00 analyses. In any (currently unforeseen) future version of the CALIOP data products, the ‘Initial Integrated Attenuated Backscatter 1064’ values could potentially be used in the algorithm proposed by [Chand et al., 2008](#) to derive column Ångström exponents for particulates above opaque water clouds.
5. Initial Integrated Attenuated Backscatter Uncertainty 1064 – this is the 1064 nm analog of the ‘Initial Integrated Attenuated Backscatter Uncertainty 532’. Because CALIOP does not make depolarization ratio measurements at 1064 nm, this parameter is unused in the V5.00 analyses.

Table 18: internal low energy mitigation (LEM) quality control flags set during LEM algorithm operations; bit 0 us the least significant bit

Bit	Interpretation
0	Single shot columns have data rejected in regions 1 and 2 but the 5 km resolution column was NOT rejected by LEM
1	Column has data rejected in altitude region 3 but the 5 km resolution column was not rejected by LEM
2	Column has data rejected in altitude region 4 but the 5 km resolution column was not rejected by LEM
3	Full column is rejected by LEM
4	Column rejected due to altitude region 3
5	Frame rejected due to too many low energy shots
6	Frame rejected due to too many rejected subregions in altitude region 3
7	Frame rejected due to too many rejected subregions in altitude region 4
8	Feature detection was not attempted at 20 km resolution due to too many LEM-rejected columns
9	Feature detection was not attempted at 80 km resolution due to too many LEM-rejected columns
10	Feature detection was not attempted at resolution 6 due to too many LEM-rejected columns
11	Column contains LEM affected data in altitude region 3
12	Column contains LEM affected data in altitude region 4
13-15	Unused

In addition to the new SDSs, the Diagnostic Beta products also contain an extra Vgroup. The ‘01 km Detection’ Vgroup replicates the majority of the SDSs reported in the CAL_LID_L2_01kmCLay_Standard-V5-00*.hdf products. Information in the excluded SDSs is either (a) replicated in the 5 km SDS of the same name (e.g., ‘Day Night Flag’ and ‘IGBP Surface Type’) or (b) easily derived from the SDS of the same name reported in the ‘Single Shot Detection’ Vgroup (e.g., ‘Solar Zenith Angle’, ‘Solar Azimuth Angle’, and ‘Troposphere Height’).

Finally, the ‘Ocean Derived Column Optical Depth’ (ODCOD) Vgroup in the Diagnostic Beta products augments the information contained in the Standard products by reporting column particulate optical depth retrievals at 1064 nm. In addition, ODCOD Vgroup in the Diagnostic Beta products contains a wealth of diagnostic information and intermediate calculations for the ODCOD retrievals at both wavelengths. Comments in the HDF attributes for each SDS in this Vgroup describe the function of each parameter in the ODCOD calculation chain. Researchers considering using this information should first very thoroughly review the ODCOD retrieval technique described in [Ryan et al., 2024](#).

Unique Layer IDs for Features Detected at 5 km, 20 km, and 80 km Resolutions

Within each granule, unique layer IDs are now assigned for all layers detected at 5 km, 20 km, and 80 km averaging resolutions. Unique layer IDs are unsigned 16-bit integers that enable unambiguous mapping between the integrated optical properties for the individual layers reported in the 5 km layer products and the corresponding profiles of vertically resolved optical properties reported in the 5 km profile products. Because extinction retrievals are not attempted for layers detected at single shot and 1 km resolutions, unique layer IDs are not assigned for the features reported in the 333 merged layer files and the 1 km cloud layer files.

In the 5 km aerosol, cloud, and merged layer files, unique layer IDs are reported in the same manner as layer optical properties. Recall that layer properties are reported at a uniform 5 km along-track resolution, and that for layers detected at 20 km and 80 km resolution, these properties are replicated over four 5 km columns for 20 km detections and sixteen 5 km columns for 80 km detections. Consequently, while a unique layer ID may appear as many as sixteen times in a single data file, these sixteen instances all reference the same layer, and the layer properties reported for all instances – e.g., top and base heights, integrated attenuated backscatters, and optical depths – will also be replicated across all sixteen 5 km columns. In the 5 km profile products, unique layer IDs are reported at the same latitude, longitude, and time coordinates as in the layer products. But, instead of appearing once in each 5 km column, layer IDs are replicated over the full vertical extent of a layer. For example, for a 480 m thick aerosol layer detected at 80 km horizontal averaging in a rectangular region would extend over eight 60 m altitude bins and sixteen 5 km profile segments.

New ‘Scene Flag’ SDS Added to All Layer Products

To enable rapid identification of all columns containing specific feature types, the CALIPSO layer products now include a ‘Scene Flag’ SDS. The Scene Flag is implemented as a 32-bit integer with individual bit interpretations as defined in Table 19. Fill values (-9999) are used to identify columns that do not pass the LEM quality checks. Users are therefore warned to check the sign of the Scene Flags and discard/ignore any negative values before querying the flags to determine column feature types.

Table 19: Bit interpretations for positive values of the new ‘Scene Flag’ SDS. Bit 0 is the least significant bit.

Bit	Interpretation
0	column contains tropospheric aerosol, marine subtype
1	column contains tropospheric aerosol, dust subtype
2	column contains tropospheric aerosol, polluted continental/smoke subtype
3	column contains tropospheric aerosol, clean continental subtype
4	column contains tropospheric aerosol, polluted dust subtype
5	column contains tropospheric aerosol, elevated smoke subtype
6	column contains tropospheric aerosol, dusty marine subtype

Bit	Interpretation
7	column contains stratospheric aerosol, polar stratospheric aerosol subtype
8	column contains stratospheric aerosol, volcanic ash subtype
9	column contains stratospheric aerosol, sulfate subtype
10	column contains stratospheric aerosol, elevated smoke subtype
11	column contains stratospheric aerosol unclassified
12	column contains ice clouds composed of randomly oriented crystals
13	column contains ice clouds composed of horizontally oriented crystals
14	column contains water clouds
15	column contains clouds with unknown ice-water phase
16–31	Unused

More Readily Accessible Altitude Information

To make CALIOP altitude information easier to access, new ‘Lidar Data Altitudes’ SDSs have been added to all level 2 data products. The ‘Lidar Data Altitudes’ array reports the altitudes, relative to mean sea level, that specify the vertical midpoints of all range bins in the profile measurements downlinked from the CALIPSO satellite. In all previous versions of the CALIPSO lidar data products, the 583-element ‘Lidar Data Altitudes’ array was stored only in the file metadata. To ensure backward compatibility with existing software, the metadata copy of the ‘Lidar Data Altitudes’ is retained in all files.

In the V5.00 vertical feature mask (VFM) product, the altitude array now contains 545 elements instead of the 583 elements reported in all other products. Because the VFM product does not report layer detections in the highest (~30 km to ~40 km) or lowest (~-0.5 km to ~-2.0 km) CALIOP onboard averaging regions, the superfluous altitude bins were eliminated. Making this change now matches the VFM altitude array size to the vertical dimension of the (unpacked) ‘Feature Classification Flags’ SDS.

Revised VFM Layer Detection Altitudes

Some changes were made to the altitude registration of layer tops and bases in the VFM product to more accurately reflect the top and base altitudes reported in the CALIOP layer products. Differences between the V4.51 and V5.00 VFM files are small, confined to the high resolution (i.e., single shot) data regime between -0.5 km and 8.2 km, and typically no more than ± 1 range bin. The images below show a particularly egregious example of altitude mismatches between V4.51 and V5.00. Approximately 1% of all range bins reporting feature detection in either V4.51 or V5.00 were detected only in V4.51. Similarly, approximately 0.4% were detected only in V5.00. This apparent altitude registration anomaly is, fortunately, confined solely to the VFM files. When comparing V4.51 data products versus V5.00, the layer top and base altitudes reported in the 333 m merged layer files, the 1 km cloud layer files, and the 5 km merged layer files are identical for all layers detected in this granule.

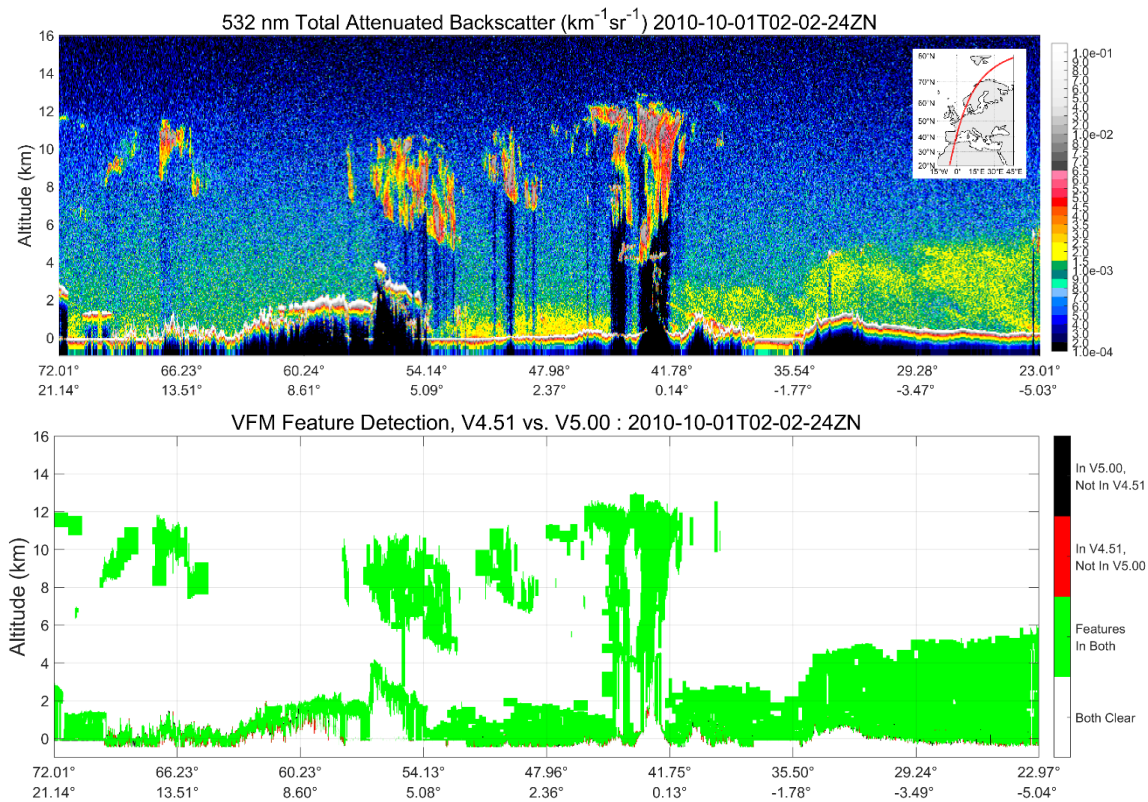


Figure 15: CALIOP nighttime observations of clouds and aerosols over Scandinavia, western Europe, and into northern Africa. These measurements were acquired on 2010-10-01 beginning at 02:02:42 UTC. The top panel shows attenuated backscatter coefficients measured at 532 nm. The bottom panel shows the VFM differences between V4.51 and V5.00. In the majority of the cases, V5.00 extends one range bin below the layer base altitude reported in the V4.51 analyses.

Summary of Newly Added and Removed SDSs

The tables below contain a comprehensive listing of all SDSs that were either added or removed. Included in the listing are SDSs that were renamed in the transition from V4.51 to V5.00.

Table 20: new scientific data sets reported in the CALIOP V5.00 lidar level 2 data products; horizontal resolution suffixes are A = aerosol, C = cloud, and M = merged layers (i.e., both aerosol and cloud).

SDS name	VFM	Layer					Profile	
		1/3kmM	1kmC	5kmA	5kmC	5kmM	5kmA	5kmC
Lidar_Data_Altitudes		✓	✓	✓	✓	✓	✓	✓
Low_Energy_Mitigation_Column_QC_Flag		✓	✓	✓	✓	✓	✓	✓
Low_Energy_Mitigation_Feature_QC_Flag			✓	✓	✓	✓	✓	✓
Scene_Flag		✓	✓	✓	✓	✓		
DEM_Surface_Elevation							✓	✓
Unique_Layer_ID				✓	✓	✓	✓	✓
VFM_Feature_Detection_Quality_Flag	✓							
Number_Bins_Shift		✓						
Extinction_QC_Flag_532				✓	✓	✓		
Extinction_QC_Flag_1064				✓	✓	✓		
Single_Shot_Detection::ssLow_Energy_Mitigation_Column_QC_Flag			✓	✓	✓	✓	✓	✓
Single_Shot_Detection::ssScene_Flag			✓	✓	✓	✓	✓	✓

	VFM	Layer					Profile	
SDS name		1/3kmM	1kmC	5kmA	5kmC	5kmM	5kmA	5kmC
Single_Shot_Detection::ssNumber_ Bins_Shift			✓	✓	✓	✓	✓	✓

Table 21: scientific data sets removed from the CALIOP V5.00 lidar level 2 data products; horizontal resolution suffixes are A = aerosol, C = cloud, and M = merged layers (i.e., both aerosol and cloud).

	VFM	Layer					Profile	
SDS name		1/3kmM	1kmC	5kmA	5kmC	5kmM	5kmA	5kmC
Samples_Averaged							✗	✗
Surface_Elevation_Statistics							✗	✗
ExtinctionQC_532				✗	✗	✗		
ExtinctionQC_1064				✗	✗	✗		

Data Quality Statement for CALIPSO's Version 4.51 Lidar Level 2 Data Product Release

Data Version: 4.51
Data Release Date: June 1, 2023
Data Date Range: June 13, 2006 to June 30, 2023

The new version 4.51 (V4.51) of the CALIPSO lidar (CALIOP) Level 2 (L2) data products contains a number of improvements and additions over the previous version (V4.2) that was released in October 2018. A summary of the major changes addressed in this release is detailed below, as well as a section highlighting known issues.

Improved Smoke Layer Accuracy above Clouds

The CALIOP L2 feature detection algorithm employs an iterative thresholding technique applied to profiles of 532nm attenuated scattering over differing horizontal resolutions to identify and vertically resolve layers ([Vaughan et al., 2009](#)). [Rajapakshe et al., 2017](#) identified instances when CALIPSO was under-reporting the vertical extent of dense smoke layers above low-level clouds when compared with coincident observations made by the Cloud-Aerosol Transport System (CATS) lidar instrument. Figure 1 (a, c) shows one of those specific over-flights, in which the 532nm total attenuated backscatter (a) and vertical feature mask (c) show a clear delineation on the order of 1 km between the base of the upper-level smoke layer and the top of a marine cloud layer below. Further examination of this scene showed that this smoke layer was dense enough to rapidly attenuate the 532nm signal to such a degree that the CALIOP feature detection algorithm artificially elevated the layer base. This is confirmed by seeing that the rapid attenuation is not seen in the 1064 nm signal response (Figure 1b), where the aerosol extinction is not as great as that seen in the 532nm signal. The 1064 nm response, which appears to close the clear-air gap between the smoke and cloud layer, is also why CATS was able to fully identify the smoke layer as that instrument uses 1064 nm for feature detection. The inability of CALIPSO to fully detect these layers can have the consequence of underestimating global aerosol optical depths, critically important for the derivation and understanding of radiative forcings ([Lu et al., 2018](#)).

In the version 3 (V3) release of the CALIOP L2 data a technique was developed for the feature finder algorithm to extend the base of near-surface aerosol layers down to the surface. A variant of this same approach was applied for these overlying dense smoke layer cases. Several criteria need to be met before the layer could be extended, a summary of which are detailed in the V4.51 CALIOP layer level 2 data product description.

Figure 1d shows the application of this new technique, in which the clear-air gap has been closed. The mean 532nm optical depth of these extended smoke layers has also increased, from 0.94 to 0.122, an increase of nearly 30%. A global representation of all extended layers for the month of August 2016, seen in figure 2a, show a concentration in the south-eastern Atlantic during the African burn season, the same region noted in the CALIPSO/CATS comparisons previously documented. Figure 2b shows the impact on the 532nm optical depth for those extended smoke layers, where in a majority of those cases in which the layer was extended the optical depths increase. The

few outliers that exist have been traced to instances when the negative values of the 532nm extinction are included, which could happen during rapid attenuation of the signal.

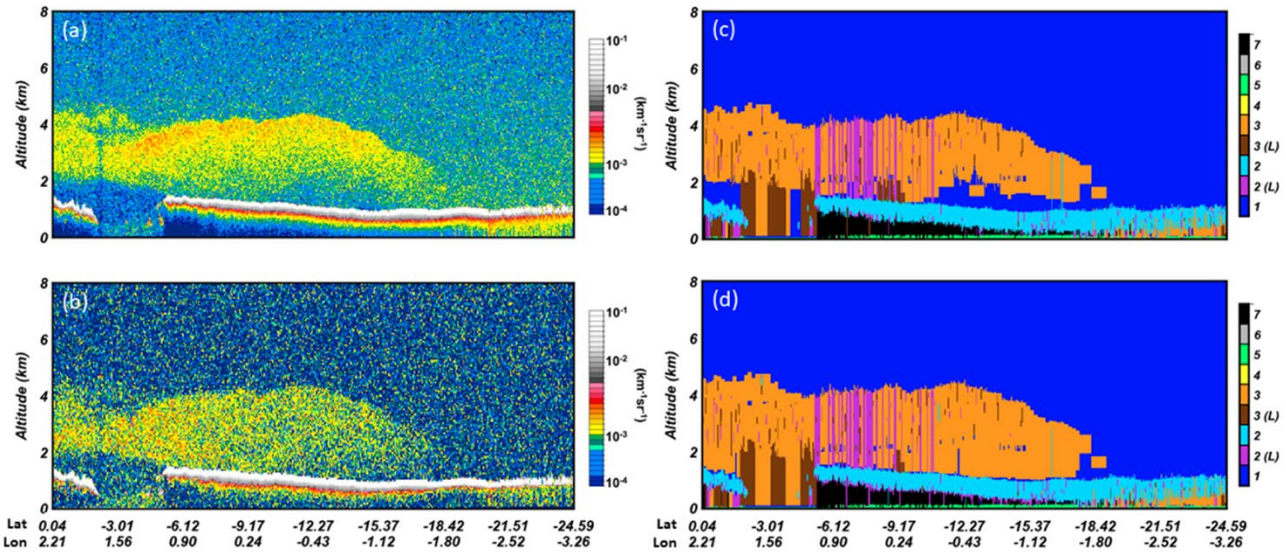


Figure 1: (a) 532 nm total attenuated backscatter from the V4.51 CALIOP Level 1B, (b) 1064 nm attenuated backscatter from the V4.51 CALIOP Level 1B, (c) feature type from the V4.21 CALIOP Level 2 Vertical Feature Mask (VFM), and (d) feature type from the V4.51 CALIOP Level 2 VFM between 1:35:03 and 1:41:44 on August 6th, 2016.

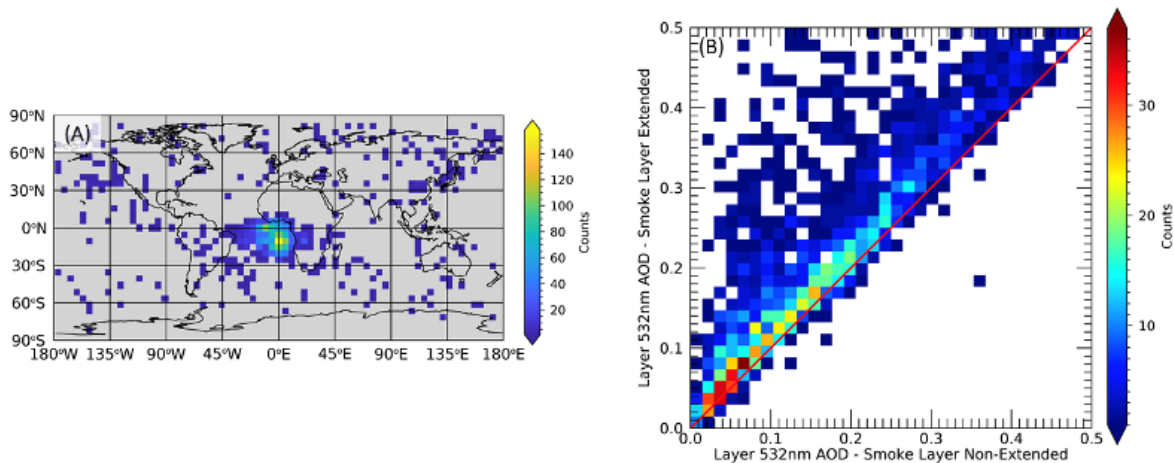


Figure 2: (a) Global distribution of all (day and night) extended smoke layers for August 2016 and (b) 532nm aerosol optical depth changes between extended (y-axis) and non-extended (x-axis) smoke layers. Data used to generate both plots were pulled from the V4.51 Lidar Level 2 5km Merged layer files. Non-extended smoke layers were created by running the V4.51 Lidar Level 2 algorithm but with the smoke extension turned off.

Improved Classifications for Stratospheric Aerosols

The stratospheric aerosol subtyping algorithm has been updated in V4.51 to improve the ability to discriminate between volcanic ash and depolarizing smoke from pyrocumulonimbus (pyroCb) injections, improve the fidelity of the sulfate classification, and to update the 532 nm volcanic ash lidar ratio to the current state of knowledge. The stratospheric aerosol subtypes are now: volcanic ash, sulfate, smoke, polar stratospheric aerosol, and unclassified. A full description of changes with the V4.51 algorithm are documented in [Tackett et al., 2023a](#).

Summary of changes:

- The stratospheric aerosol subtyping algorithm now relies solely on depolarization and integrated attenuated backscatter (γ') to discriminate between volcanic ash, sulfate, and smoke. Removing the reliance on layer

color ratio that was included in the V4.2 subtyping algorithm allows more accurate identification of sulfate and less misclassification of sulfate as smoke.

- The estimated particulate depolarization ratio threshold used to discriminate between smoke from pyroCb injections and volcanic ash has been increased from 0.15 to 0.25 based on empirical analysis of recent major pyroCb events.
- The V4.2 “sulfate/other” stratospheric aerosol subtype has been separated into two subtypes in V4.51 - sulfate, and unclassified. Previously, the sulfate/other type included both aerosol layers likely to be sulfate and layers with low values of γ' , representing the “other” component of the combined class. In V4.51, layers with low γ' are now reported separately as “unclassified”.
- The 532 nm lidar ratio for volcanic ash has been increased to 61 ± 17 sr based on CALIOP-constrained retrievals of volcanic ash plumes.

Figure 3 demonstrates the improvements in stratospheric aerosol subtyping between V4.2 and V4.51. Panels in each row show the frequency of classification of each stratospheric aerosol subtype for manually identified layers associated with a dominant aerosol type. In V4.51, there are fewer misclassifications of volcanic ash as sulfate, more accurate classifications sulfate from true sulfate events, and fewer misclassifications of true smoke as volcanic ash. There remain some misclassifications of sulfate as smoke due to the difficulty of separating these types with CALIOP observables.

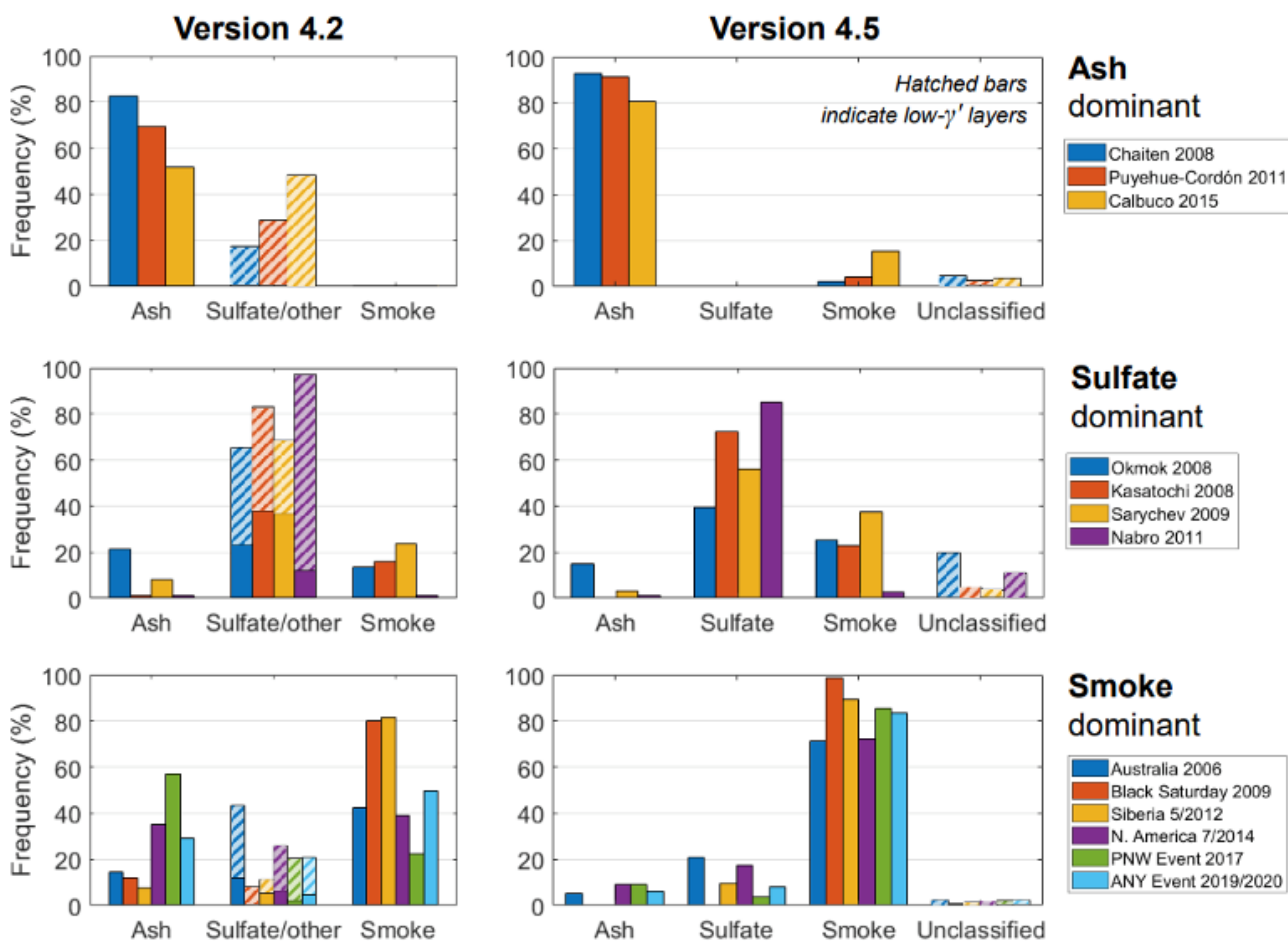


Figure 3: Stratospheric aerosol subtype classification frequency for events dominated by volcanic ash (top row), sulfate (middle row), and smoke (bottom row). V4.2 and V4.51 classifications are in the left and right columns, respectively. Taken from [Tackett et al., 2023a](#).

[Hu et al., 2007](#) developed an approach to estimate 532nm total particulate optical depth above opaque water clouds. The 532nm layer integrated attenuated backscatter (γ') for an opaque water cloud, assuming clear air-above, could be estimated as a function of the lidar ratio of the water cloud (S_0) and the multiple scattering factor. If there are features above, then γ' will be reduced based on the overlaying two-way transmittance, which is a function of the optical depth (τ_{above}). Using this information an estimate of the above cloud optical depth can be inferred directly from current CALIPSO measurements, as seen in equation 1. The multiple scattering is a ratio of the layer integrated 532 nm volume depolarization ratio (δ_v), which along with γ' are parameters that are already computed in the CALIOP L2 data products. An estimate of S_0 for opaque water clouds is assumed to be 19 sr.

$$\tau_{\text{above}} = -\frac{1}{2} \ln \left(2 \left(\frac{1 - \delta_v}{1 + \delta_v} \right)^2 S_0 \gamma' \right) \quad (1)$$

This new column particulate optical depth and uncertainty are detailed further in the V4.51 CALIOP Layer Level 2 data product description. These two new parameters are denoted as ‘particulate’, and do not differentiate between feature typing as seen in other column optical depth parameters in the CALIOP level 2 data product.

A comparison between this new approach and data collected from NASA Langley’s High Spectral Resolution Lidar (HSRL-2) during a leg of the ORACLES-2 field campaign ([Redemann et al., 2020](#)) can be seen in Figure 4. This particularly scene, taken from September 18th, 2016, of a CALIPSO transit from 13:33:50 to 13:36: 52 UTC and coincident with the ER-2 over-flight, is in the south-eastern Atlantic Ocean off the coast of Africa and is characterized by an elevated smoke layer from seasonal biomass burning over a dense marine stratiform cloud layer. The 532nm aerosol optical depth derived from HSRL-2 (black triangles) compares favorably with the new depolarization ratio approach (blue circles) at 5km resolution. The particulate optical depth is also reported at 1km and 333m (single shot) resolution. Profiles of 532nm extinction reported in the Lidar Level 2 5km aerosol profile products were used to compute aerosol optical depths for this scene, using both the V4.51 (red) and V4.20 (green, previous version) data. These two optical depths do not track the depolarization approach as well, given that the profiles of extinction are for aerosol only, as determined by the level 2 typing algorithm, while the depolarization method uses the entire column. The differences between V4.20 and V4.51 aerosol optical depths, in which V4.51 is always greater than/equal to V4.21, is due to the increase in depth of layer associated with smoke base extension.

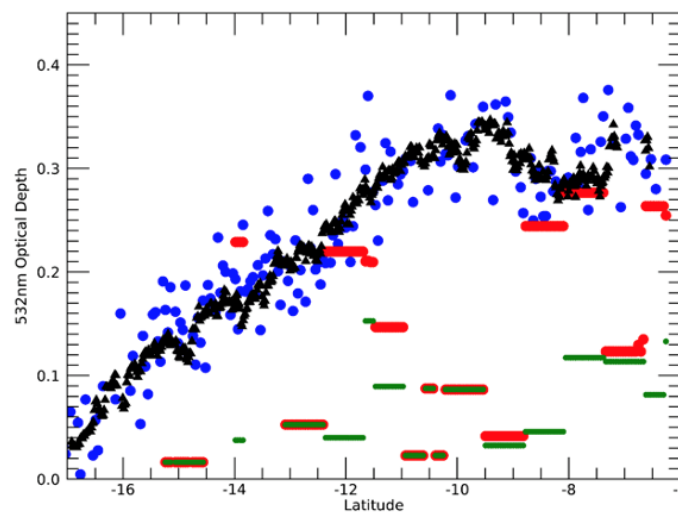


Figure 4: 532nm aerosol optical thickness above clouds from the HSRL-2 (black triangles), 532nm particulate optical depth above opaque water clouds at 5km resolution using the V4.51 Lidar Level 2 depolarization ratio technique (blue circles), and 532nm aerosol optical depth (V4.51 red circles, V4.20 green circles) computed by integration of aerosol profile extinction above opaque water clouds during CALIPSO over-flight of HSRL-2 track on September 18th, 2016, from 13:33:50 to 13:36:52 UTC in the south-east Atlantic Basin during the ORACLES-2 field campaign.

Total Column Particulate Optical Depths from Ocean Surface Returns

The Ocean Derived Column Optical Depth (ODCOD) product is an estimate of total column effective optical depth. ODCOD relates the measured magnitude of the lidar ocean surface return and the two-way transmittance overhead to a modelled ocean returned by the equation 2 below ([Venkata and Reagan 2016](#)).

$$T_p^2(z_s) = \frac{c A T_m^2(z_s)}{2 R_\lambda} \quad (2)$$

In the relationship, $T^2(z_s)$ is the two-way transmittance at range z_s from the spacecraft where molecular/ozone and particulate components are denoted by the subscripts 'm' or 'p', respectively. Variable c is the speed of light, A is the area of the ocean surface return, and R_λ is the modelled backscatter reflectance from the ocean surface. The retrieval is for the total column, from the CALIOP top of the atmosphere calibration region to the lidar detected ocean surface. The estimate is an *effective* optical depth because no attempt is made to separate multiple scattering and single scattering from the cloud and aerosol particulates in the column ([Ryan et al., 2024](#)).

The V4.51 Lidar Level 2 algorithms only estimate 532 nm optical depths in regions of the column where clouds and aerosol are directly detected. The regions where no layers are detected are assumed to be particulate free. This assumption is known to yield an underestimate total column particulate optical depth by on the order of 0.03–0.05 ([Toth et al., 2018](#)). ODCOD compliments the CALIPSO data record by providing estimates of optical depth for the entire column including regions CALIOP does not detect particulate.

Figure 5 shows cloud screened seasonal difference of medians (ODCOD - MODIS) of the 5km ODCOD daytime retrieval to MODIS derived Effective Optical Depth Average Ocean interpolated to 532 nm and to the CALIOP 5km footprint midpoint. Generally, ODCOD shows good agreement in each season and over most of the globe with global median differences of 0.019 in December, January, and February; 0.025 in March, April, and May, 0.015 in June July and August; and 0.017 in September, October, November. Regionally, some parts of the globe see larger differences possibly due to uncertainties in wind speed and the surface reflectance model used.

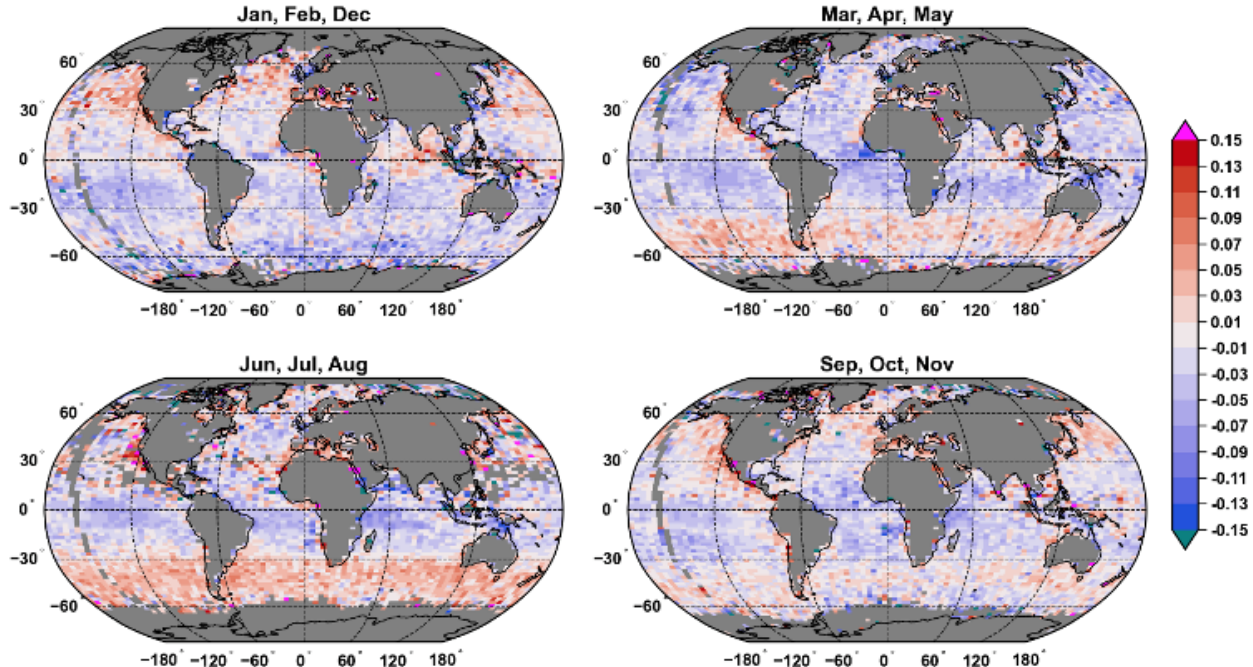


Figure 5: The four panels show cloud screened seasonal difference of medians (ODCOD - MODIS) comparisons of the 5km ODCOD daytime retrieval to MODIS derived Effective Optical Depth Average Ocean interpolated to 532 nm and to the CALIOP 5km footprint midpoint. ODCOD higher than MODIS is shown in red and ODCOD lower is shown in blue. Taken from [Ryan et al., 2024](#).

Corrections to Single-Shot Cloud Clearing

An anomalous condition was identified in the CALIOP Level 2 Selective Iterated Boundary Layer (SIBYL) algorithm, in which 333m single shot clouds identified and retained in the boundary layer could inadvertently be reclassified as an aerosol. The V4.51 layer product description details the error and new approach used, in which a boundary layer scene could be broken apart and these newly defined layers reclassified based on a number of criteria.

Figure 6 illustrates this error and the resultant amelioration. In this scene a dense water cloud underlies a dust plume (Figure 6a). For a majority of this scene the V4.2 algorithm retains the 333m single shot water cloud layer, which occurs when the single shot clouds are detected throughout the entirety of each 5km block of data. The Cloud-Aerosol Discrimination (CAD; [Liu et al, 2019](#)) doesn't know that the clouds haven't been removed and reclassifies those bins as having aerosols, as seen in Figure 6b. The consequence of this error can be seen in Figure 6c, as the 532nm 'aerosol' extinction for that layer are clearly biased when compared with the overlying aerosol. When applying the corrected algorithm, the single shot layer remains as a cloud (Figure 6d) and the 532nm aerosol extinction bias has been eliminated (Figure 6e). [Tackett et al, 2022](#) also detailed the consequence of this error, in which nearly 3% of all 5km resolution layers for June-August 2007, 2013, and 2014, clustered around regions of continental aerosol outflow (smoke or desert dust), were impacted.

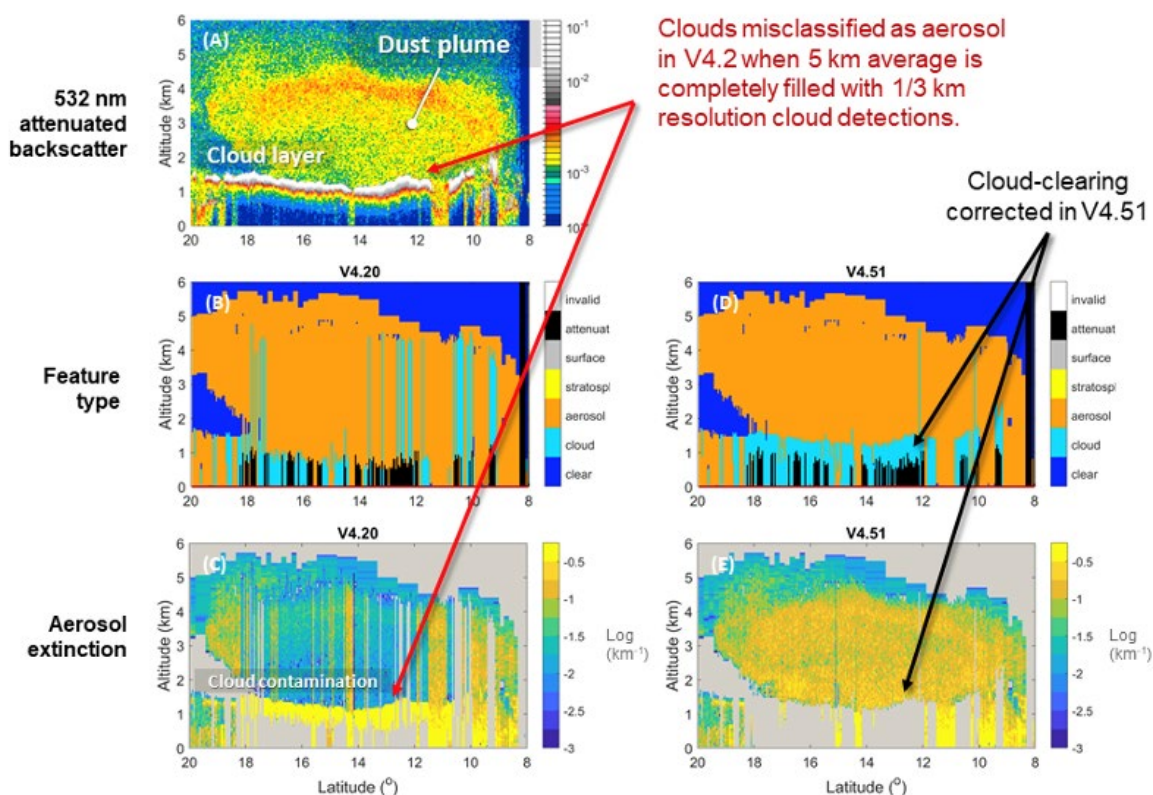


Figure 6: June 15th, 2013, scene in the eastern Atlantic Ocean between CALIOP V4.21 Level 1 and Level 2 data (a-c) and the V4.51 Level 2 data (d-e). The left most column shows the prescience of the low-level water cloud and the implications on extinction of the cloud layer being recast as an aerosol by the Cloud-Aerosol Discrimination algorithm. The right most column shows that the updated V4.51 algorithm now properly accounts for the cloud and the 532nm extinction bias has been eliminated. Taken from [Tackett, 2023](#).

Table 1: new scientific data sets reported in the CALIOP V4.51 L2 data products

	VFM	Layer					Profile	
SDS name		1/3kmM	1kmC	5kmA	5kmC	5kmM	5kmA	5kmC
Surface_Wind_Speeds_02m				✓		✓	✓	✓

Data Quality Statement for CALIPSO's Version 4.21 Lidar Level 2 Data Product Release

Version: 4.21
Data Release Date: October 02, 2020
Data Date Range: October 01, 2020 to present

A minor version bump (+0.01) has been applied to all CALIPSO data products due to a required upgrade to the operating system on the CALIPSO production cluster. All program executables were re-compiled to process in this new environment with no changes made to the underlying science algorithms or inputs.

Data Quality Statement for CALIPSO's Version 4.20 Lidar Level 2 Data Product Release

Data Version: 4.20
Data Release Date: October 10, 2018
Data Date Range: June 13, 2006 to September 30, 2020

The Version 4.20 (V4) CALIOP Level 2 data product is identical to the V4.10 data product with the addition of several HDF science data sets (SDS) that provide information to the user for filtering out low laser energy shots. The technical advisory of this phenomena, shown below, was posted on the CALIPSO website in June of 2018.

Table 2: new scientific data sets reported in the CALIOP V4.20 L2 data products

	VFM	Layer				Profile	
SDS name		1/3kmM	1kmC	5kmA	5kmC	5kmA	5kmC
Minimum_Laser_Energy_532	✓	✓	✓	✓	✓	✓	✓

Data Release: June 12, 2018

CALIOP Instrument Anomaly Advisory: Low Energy Laser Shots

Dates Affected: September 01, 2016 – present

Applies to: CALIOP Level 1B and Level 2 Data Products, V4.10 and earlier

CALIOP (CALIPSO's LIDAR instrument) is experiencing an elevated frequency of low energy laser shots within the South Atlantic Anomaly (SAA) region due to decreased pressure inside the laser canister. The low energy laser shots began in September 2016 and have increased in frequency, particularly since the second half of 2017 (Fig. 1). Science quality of affected profiles within the SAA is degraded and these profiles should be excluded from scientific analyses. The document below provides guidance on how to identify affected profiles in CALIOP level 1B and level 2 products. Science quality of profiles with nominal laser energies is unaffected by this issue. The IIR (Imaging Infrared Radiometer) and the WFC (Wide Field Camera) instruments are also unaffected.

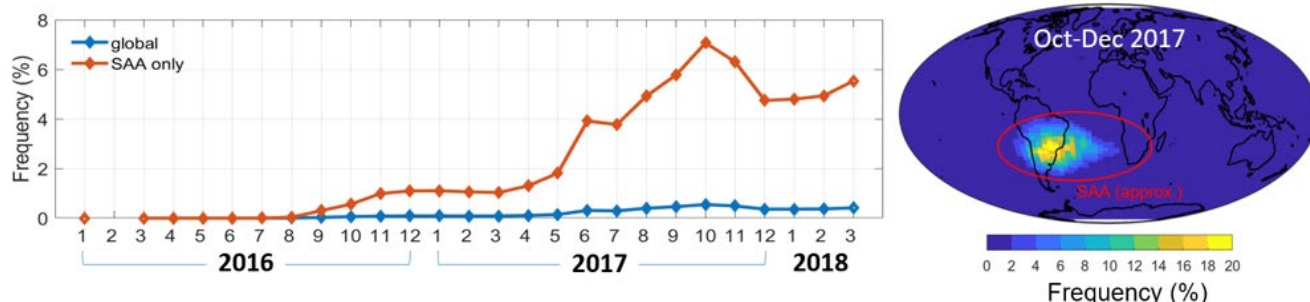


Figure 1 Monthly frequency of low energy laser shots ($E_{532} < 80$ mJ) from January 2016 to March 2018, globally and in the SAA region (left). Spatial distribution of low energy shot frequency from October to December 2017 (right).

Data Quality Statement for CALIPSO's Version 4.10 Lidar Level 2 Data Product Release

Data Version: 4.10
Data Release Date: November 8, 2016
Data Date Range: June 13, 2006 to May 31, 2018

Version 4.10 (V4) is the first wholly new release of the CALIPSO lidar level 2 data products since the initial release of the Version 3 (V3) series of products in May 2010. As expected, V4.10 provides a substantial advance over V3 and earlier releases; known retrieval artifacts have been eliminated and numerous enhancements have been incorporated to increase the accuracy of the science data while simultaneously reducing uncertainties. The most significant code, algorithm, and data product changes include

- a stand-alone surface detection algorithm
- revised probability density functions (PDFs) for the cloud aerosol discrimination (CAD) algorithm
- application of the CAD algorithm to layers detected at single shot resolution and to layers detected in the stratosphere
- a major overhaul of the aerosol subtyping algorithms in which separate algorithms are now used to classify tropospheric and stratospheric aerosols
- improved cloud subtyping and ice-water phase determination
- temperature-dependent determination of multiple scattering factors for ice clouds
- multiple scattering factors for opaque water clouds derived from measured depolarization ratios
- updated extinction retrievals for opaque layers; improved uncertainty estimates and more in-depth quality assurance reporting for all extinction retrievals
- a new algorithm for deriving ice-water content from CALIOP extinction retrievals
- introduction of a new 5-km merged layer product that reports the spatial and optical properties of all cloud and aerosol layers detected in a single file
- new browse image showing cloud subtypes identified within each granule
- the addition of several new parameters in the data products files

Each of these is discussed in some detail in the sections below.

Lidar Surface Detection

In previous versions of the CALIOP level 2 (L2) data products, the altitude of the Earth's surface was determined using a [general purpose layer detection scheme](#) that scans lidar profiles from the top of the atmosphere downward, looking for significant positive excursions rising above an expected molecular backscatter signal. In general, this approach works well. However, in multi-layer scenes and/or highly turbid atmospheres the effectiveness of the top-down technique can be degraded by signal attenuation from intervening atmospheric layers that limit its ability to reliably detect surface returns. In the V4.10 data products, detection of the Earth's surface is accomplished using a dedicated, newly developed search routine that scans upward from the bottom of the profile using a derivative-based peak finding algorithm. This new technique [demonstrates significant improvement](#) over the V3 method in turbid atmospheres, while maintaining equal or better performance in clear skies. As a result of this improved detection scheme, there are fewer opaque layers identified in the V4.10 data than there were in V3, especially at night. Because regions below layers previously classified as opaque are now scanned for the presence of atmospheric features, there is also a slight increase in the number of cloud and aerosol layers reported. Signal strengths in these 'not previously scanned' regions tend to be quite low, and thus many of these newly detect layers will have low CAD scores.

The V4.10 data products report substantially more surface detection information than was available in V3. The Lidar_Surface_Elevation and Surface_Elevation_Detection_Frequency parameters reported in the V3 data products have been discontinued in V4.10. Instead, surface detection information is recorded in a multi-parameter Lidar_Surface_Detection Vgroup. In addition to the surface detection status (i.e., detected or not detected) and

surface altitude information provided in V3, this new Vgroup reports the following parameters at both 532 nm and 1064 nm.

- surface top and base altitudes
- integrated attenuated backscatter
- integrated volume depolarization ratio
- integrated attenuated backscatter color ratio
- where applicable, surface detections at finer spatial resolutions (i.e., 1/3 km and 1 km)

These additional parameters are expected to provide [new insights into surface type](#) (e.g., distinguishing between ice, liquid water and land) and, for measurements over oceans, total column optical depths at both 532 nm and 1064 nm.

Cloud and Aerosol Layer Detection

The CALIOP V4.10 level 1 (L1) data, first released in April 2014, significantly improved the calibration of the CALIOP attenuated backscatter coefficients at 532 nm ([Kar et al., 2018](#); [Getzewich et al., 2018](#)) and especially at 1064 nm ([Vaughan et al., 2019](#)). In particular, the magnitude of the calibration coefficients at 532 nm decreased by ~3% to ~8%, depending on latitude and season, resulting in the concomitant increase in the 532 nm attenuated backscatter coefficients. This increase in backscatter magnitude translates directly into a slightly greater layer detection frequency. When combined with the layer detection increases obtained from the new surface detection algorithm, the V4.10 data products show a net cloud fraction gain of ~5% relative to V3.

Cloud Aerosol Discrimination (CAD)

The magnitude of the calibration changes introduced in the CALIOP V4.10 L1 data necessitated substantial revisions to the [V3 level 2 \(L2\) CAD algorithm](#). Accordingly, a new set of CAD probability distribution functions (PDFs) was developed and subsequently used to generate the V4.10 L2 data. The V4.10 CAD PDFs are still 5-dimensional, but now have increased latitude resolution (5° intervals vs. 10° in V3) which has led to an overall improvement in CAD reliability. The revised PDFs were specifically designed to be more sensitive to the presence of lofted aerosols. As a consequence, the V4.10 data products show significant improvements in the classification of high-altitude smoke plumes and Asian dust layers, which in earlier versions were often classified as cirrus clouds.

Application of the [V4.10 CAD algorithm](#) differs from previous versions in these important aspects:

1. In V3 and earlier, the CAD algorithm was applied only to tropospheric layers, and layers detected above the tropopause were classified as “stratospheric” features. In V4.10 the “stratospheric” feature type has been eliminated. Instead, the CAD algorithm is applied everywhere, to all layers detected. The CAD scores for stratospheric clouds and aerosols are generally robust within a few kilometers of the tropopause. However, at very high altitudes, the general paucity of samples available for the training set as well as falling SNR may affect the reliability of the CAD.

For in-depth scientific analyses of polar stratospheric clouds (PSCs), users are strongly advised to use CALIPSO’s dedicated PSC products. For less demanding applications, PSCs are also reported in the standard L2 data products. While the V4.10 CAD algorithm classifies the majority of the polar stratospheric layers as clouds, some aerosol layers are also identified. The spatial distribution of these polar stratospheric aerosol layers is similar to the distribution of STS (i.e., the supercooled ternary solution of nitric acid, sulfuric acid and water) obtained from the dedicated CALIPSO PSC product.

2. Unlike V3, the V4.10 CAD algorithm is also applied to those strongly scattering layers that can be detected at single shot resolution (333 m). In the past these layers were classified as clouds by default and were systematically removed before averaging over the weaker signals. In V4.10, layers detected at single shot resolution that are classified as aerosols are no longer removed from coarser resolution averages, and thus can be expected to increase peak aerosol optical depths in the regions where they occur. The bulk of the single shot layers classified as aerosols in V4.10 are found within the dust belt region of the globe. However, it should

be noted that optical properties of these layers were not used in building the V4.10 CAD PDFs, which may affect the overall CAD performance when classifying single shot layers.

While the CAD algorithm is applied to all layers detected, there are two anomalous situations where layers are subsequently reclassified using additional analysis. The first occurs when dense smoke plumes extend over stratus decks and other water clouds. The differential attenuation of the signals at 1064 nm and 532 nm by the smoke can lead to very high color ratios in the clouds below, which in turn can result in artificially low CAD scores. In such cases, the color ratio of the underlying clouds is reset to an empirically derived mean value and the CAD scores are recalculated. Both the original CAD score and the revised CAD score are recorded in the layer products. In the second case, the similarity of the scattering signatures of faint, isolated layers of lofted dust and weakly depolarizing cloud fragments makes them largely indistinguishable in the CAD domain. To achieve reliable separation, a sequence of spatial proximity tests is applied to identify those layers which may in fact be “fringes” of previously identified large scale ice clouds. Layers identified as “cirrus fringes” are assigned a special CAD score of 106.

Figure 1 shows the pattern of changes in CAD scores from V3 to V4.10. Most of the high confidence samples in V3 are also classified as the same type (cloud or aerosol) in V4.10 with similar high confidence. However, as seen in the lower right quadrant of Figure 1, a small fraction of layers classified as clouds in V3 are classified as aerosols in V4.10. Some of these have optical properties that fall in the grey zone between aerosols and clouds and may actually be misclassified clouds. These cases occur most often over the polar regions. Because they typically have low CAD scores, they can be identified and removed at the users’ discretion.

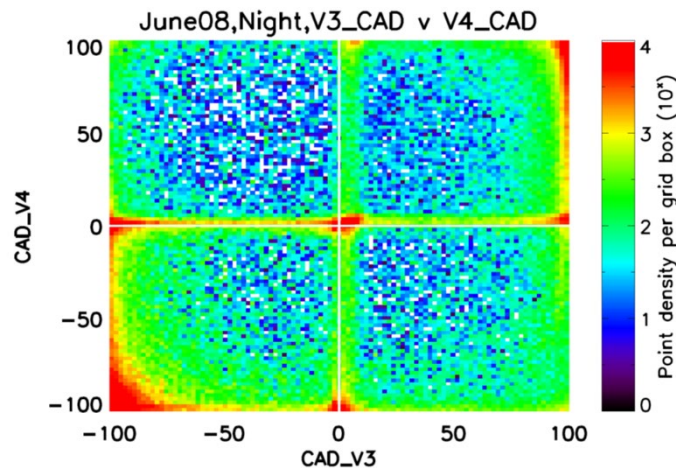


Figure 1: Comparison of CAD scores of the same samples between V3.30 and V4.10 using the L2 profile products.

After acquisition and analysis of over 10 years of space-based lidar data, the CALIPSO team has gained a much improved understanding of the physical and optical properties of the different types of aerosols and clouds that occur in different altitude regimes. As a result, the V4.10 PDFs are more representative and more physically realistic than earlier versions, in which the occurrence frequency of aerosols at higher altitudes was noticeably underestimated. One result of modifying the PDFs to achieve more accurate aerosol identification is an across the board decrease in the magnitude of the CAD scores reported in V4.10; i.e., the mean magnitude of CAD scores for all aerosols detected in V4.10 is lower than the mean magnitude in V3. Likewise, the mean magnitude of the cloud CAD scores is lower in V4.10 than in V3. In retrospect, the higher CAD scores in V3 should be seen as overly optimistic; the slightly lower V4.10 scores now provide a more realistic assessment of CAD classification confidence.

Aerosol Subtyping Changes

Several improvements to aerosol subtyping have been implemented in V4.10. The most fundamental change is that aerosol layers are now classified as either tropospheric aerosol or stratospheric aerosol feature types, depending on the location of the attenuated backscatter centroid relative to the MERRA2 reanalysis tropopause height. In previous versions, aerosol was only identified below the tropopause. Given that the CAD algorithm is applied at all altitudes in V4.10, aerosol layers detected above the tropopause are classified as stratospheric

aerosols and are assigned subtypes commonly found in the stratosphere. Figure 2 compares distributions of tropospheric aerosol subtypes between V3 and V4.10.

Tropospheric aerosol subtyping improvements

1. A new “dusty marine” aerosol subtype has been added. Dusty marine layers are mixtures of dust and marine aerosol identified as moderately depolarizing aerosol layers having base altitudes within the marine boundary layer (assumed to be at 2.5 km). In previous versions these layers would have been classified as polluted dust. The dusty marine lidar ratio is more representative of a dust/marine aerosol mixture and its characteristic lidar ratio is ~33% smaller than that of polluted dust. The geographic distribution of dusty marine layers agrees well with known locations of dust subsidence into the marine boundary layer, though some ambiguity occurs in regions where anthropogenic pollution, dust, and marine aerosol co-exist. These layers are classified as dusty marine, yet it is not always clear whether they should be typed instead as polluted dust.
2. Smoke layer identification and nomenclature has been revised. As in previous versions, elevated non-depolarizing aerosols are assumed to be smoke which is injected above the planetary boundary layer (PBL) due to combustion-induced buoyancy. The definition for “elevated” is revised in V4.10 to mean layers with tops higher than 2.5 km above ground level (i.e., a simple PBL approximation). For clarity, the nomenclature for the smoke aerosol subtype is changed to “elevated smoke”. Owing to the revised “elevated” definition and the introduction of a new algorithm to vertically homogenize aerosol subtyping for weakly scattering fringes detected at the base of extended plumes, elevated smoke layers which were misclassified as marine aerosol in V3 are now correctly classified as elevated smoke.
3. Within the PBL, it is difficult to discriminate smoke due to biomass burning from polluted continental aerosol arising from anthropogenic pollution using CALIOP measurements. Therefore, the description of the polluted continental subtype is revised to “polluted continental/smoke” to clarify that either aerosol type could be present.
4. In previous versions, [aerosol detected over snow, ice, or tundra were subtyped as either clean continental or polluted continental](#). Given that transport pathways exist for smoke, dust and other aerosol types to reach the Arctic, this condition has been removed in V4.10 and all species are allowed. Users are cautioned to treat aerosol detected over Antarctica carefully and to exercise prudence when interpreting aerosol subtyping in this region. Often aerosol layers in the Antarctic are classified as dust or polluted dust due to their elevated depolarization. Despite that transport pathways do exist for dust to reach Antarctica (from Patagonia for example), data users are cautioned that layers classified as aerosol may actually be misclassified clouds or blowing snow rather than true dust.
5. Calculation of the particulate depolarization ratio estimates using in the aerosol subtyping scheme now correctly accounts for signal attenuation due to overlying layers. Making this change greatly reduces [the over-abundance of polluted dust in identified in V3](#).
6. Tropospheric aerosol lidar ratios and lidar ratio uncertainties have been updated for the marine, dust, clean continental, and elevated smoke subtypes to reflect the current state of knowledge based on observations by [NASA Langley Airborne High Spectral Resolution Lidar](#), [EARLINET](#), [AERONET](#), CALIPSO and [synergistic multi-sensor retrievals](#).

Stratospheric aerosol subtypes introduced

Stratospheric aerosol subtypes have been introduced in V4.10 for ash, sulfate/other, smoke and polar stratospheric aerosol. The [V4.10 stratospheric aerosol subtyping algorithm](#) performs well at identifying volcanic ash and sulfate above the tropopause based on manual verification. Note that below the tropopause, ash and sulfate plumes are given tropospheric aerosol subtypes: volcanic ash is often classified as dust or polluted dust and volcanic sulfate is often classified as elevated smoke. As a result, contiguous aerosol features crossing the tropopause will have aerosol subtypes which switch from tropospheric to stratospheric subtypes, depending on the relationship between the attenuated backscatter centroid altitude of the layer identified by the feature finder and the tropopause altitude. Weakly scattering stratospheric aerosol layers which are not classified as polar stratospheric

aerosol are classified as “sulfate/other”. Therefore, layers that are, in fact, ash and/or smoke could be misclassified as “sulfate/other” if they are weakly scattering (layer integrated attenuated backscatter less than 0.001 sr^{-1}).

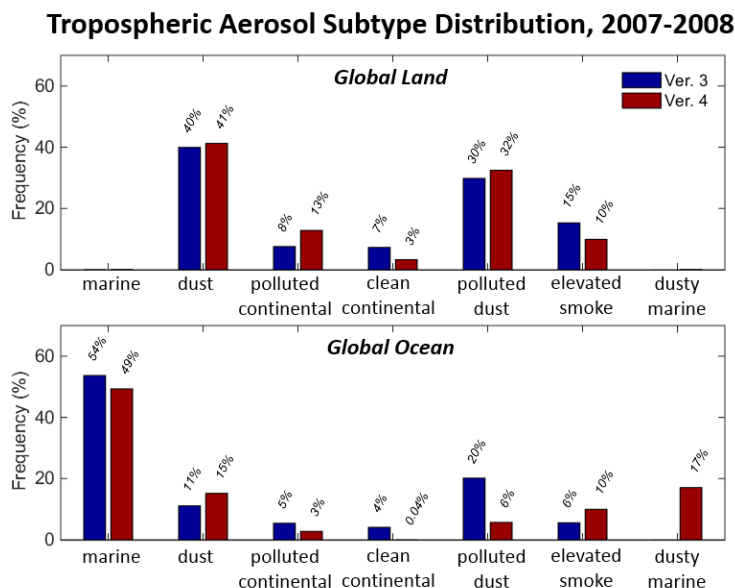


Figure 2: Comparison of global tropospheric aerosol subtype distributions between V3 and V4.10 for 2007-2008, day and night. Over land, elevated smoke is reduced in favor of polluted continental/smoke as a consequence of revised “elevated” definition. Over ocean, dusty marine replaces a substantial portion of polluted dust classifications.

Cloud Subtyping Changes

The CALIPSO cloud subtyping algorithm uses cloud top pressure, cloud opacity and cloud fraction to identify eight cloud types. A bug in the V3 analysis code caused a systematic underestimate of all categories of opaque clouds; in fact, no low overcast opaque clouds were reported in any of the V3 data products. As seen in Figure 3, this defect has been remedied in V4.10, and thus, relative to V3, the V4.10 data products show a large increase in the fraction of low opaque cloud types and a corresponding decrease in the fraction of low transparent clouds.

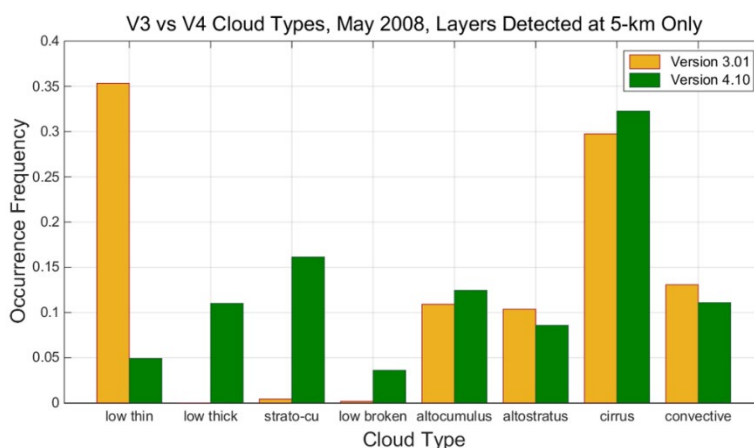


Figure 3: distribution of cloud subtypes in V3 (orange) and V4.10 (green) for all layers detected at a 5-km horizontal averaging resolution during May 2008

Cloud Ice-Water Phase Discrimination Changes

Layers identified as clouds by the CAD algorithm are further classified according to thermodynamic phase as either water, randomly oriented ice (ROI), horizontally oriented ice (HOI) or unknown phase. The phase algorithm

primarily uses an objective sorting algorithm based on [the clustering of relationships between the layer-integrated attenuated backscatter \(IAB\) and the layer-averaged depolarization](#). This technique relies on fundamental CALIOP L1 measurements, and in V4.10 confidently identifies the thermodynamic phase (ice vs. water) of at least 75% (nadir pointing) and 85% (tilted) of cloud layers, globally.

On November 28, 2007, the initial CALIOP viewing angle of 0.3° (nadir) was permanently changed to 3° (tilted), to repress specular reflections from hexagonal plates. These plates, with crystal faces perpendicular to the CALIOP laser beam, cause specular reflections which can be identified in nadir viewing data by abnormally large integrated attenuated backscatter with essentially zero depolarization. The V3 phase algorithm included a scheme for recognizing HOI that identified numerous instances of these ice clouds. However, in-depth comparisons of the V3 nadir and tilted data determined that very few true specular reflections were occurring in the tilted data, and so HOI testing of ice clouds initially identified as ROI was eliminated. In the V4.10 phase algorithm only water clouds observed in the nadir view are tested. Clouds that mainly consist of ROI may also have water or HOI occurring at warmer temperatures at the bottom of the layer, and these are now identified by the dominant cloud particle phase, which is ROI. Additional details about the change of off-nadir angle from 0.3° to 3.0° are given in Appendix 1 at the end of this document. Table 1 characterizes V3 to V4.10 changes in the volume of cloud phases globally, for both nadir and tilted viewing angles.

Table 1: Cloud volume occurrence frequency (5 km x 60 m bins) in percent; nadir statistics computed using all data from January through November 2007 (excluding off-nadir tests); tilted statistics computed using all data from January through November 2008 (MC = mid-confidence).

Cloud Phase	Phase Flag	Confidence Flag	V3 Nadir (0.3°)	V4.10 Nadir (0.3°)	V3 Tilted (3.0°)	V4.10 Tilted (3.0°)
ROI	1	3	48	53	64	67
Water	2	3	18	20	18	19
HOI	3	3	6	5	< 1	< 1
Unknown	0	0	9	13	6	10
Fringe	1	0	N/A	3	N/A	3
MC-HOI	3	2	17	5	10	N/A
MC-ROI	1	2	3	< 1	< 1	< 1

A non-zero, but negligible, amount of low- and mid-confidence water layers are also identified at each viewing angle. As these phase classifications account for less than 1% of all cloud bins, they are not shown in this table.

In V4.10, between 65-70% of the range bins identified as atmospheric features by CALIOP are classified as clouds. The population of water clouds identified at horizontal averages of 5 km or more remains very stable between V3 and V4.10, at about 18%. The ROI population is larger in tilted data than in nadir data and is 10-15% larger in V4.10 than in V3. The additional V4.10 ROI bins were mainly classified as clear air, mid-confidence HOI or stratospheric features in V3. Unknown phase clouds increase in V4.10 due to generally lower CAD scores and the detection of more thin cloud layers with weak backscatter and depolarization signals. The reduction in V4.10 HOI is due to the elimination of a spatial coherence test in the phase algorithm. About 3% of the cloud population in V4.10 are identified as “cirrus fringes”. Since the composition of cloud populations varies regionally and seasonally, these numbers should be used only for guidance in understanding the changes between V3 and V4.10.

Lidar Ratios and Multiple Scattering Factors for Ice Clouds

In V3 and earlier, ice clouds were assigned a constant multiple scattering factor of $\eta_{532} = 0.6$. In V4.10, [the multiple scattering factor is instead implemented as a sigmoid approximation function of the layer attenuated backscatter centroid temperature](#), with η_{532} increasing from 0.46 at 270 K to 0.76 at 190 K.

This approximation function was derived from extensive analysis of collocated measurements acquired by the CALIPSO lidar and the CALIPSO IIR, [which reconciled observed and theoretical ratios](#) of 532 nm optical depths

derived from V3 CALIOP measured two-way transmittances to the absorption optical depth retrieved from IIR measurements at 12.05 μm . The theoretical ratios are computed assuming [severely roughened aggregated columns](#).

In V3 and earlier, ice cloud extinction retrievals that could not be constrained by the direct measurement of the two-way transmittance (i.e., “unconstrained” retrievals) were assigned an initial default lidar ratio of 25 sr. For semi-transparent clouds, comparisons with IIR absorption optical depth at 12.05 μm and a [radiative closure experiment using MODIS 11 \$\mu\text{m}\$ radiances](#) both showed, on average, quite good agreement with V3 CALIOP constrained retrievals, but substantially worse agreement with unconstrained retrievals, thus demonstrating that the initial default lidar ratio was generally too small.

To ensure full consistency between unconstrained and constrained retrievals in semi-transparent clouds, initial ice cloud lidar ratios in V4.10 are derived from the statistical analysis of several years of constrained retrievals, using only those clouds identified as high-confidence randomly oriented ice. Like the multiple scattering factor, the V4.10 initial ice cloud lidar ratio is estimated using a sigmoid approximation function based on the layer attenuated backscatter centroid temperature. Default lidar ratio values [decrease from ~35 sr to ~20 sr as the cloud centroid temperature decreases](#). This initial lidar ratio is only used for semi-transparent ice clouds when constrained retrievals are not possible. For opaque clouds and constrained retrievals of semi-transparent clouds, the extinction retrievals are initialized using a lidar ratio derived directly from the CALIOP L1 measurements and the temperature-dependent multiple scattering factor.

Multiple Scattering Factors for Water Clouds

In V3 and earlier, all water clouds were assigned a constant multiple scattering factor of $\eta_{532} = 0.6$. In V4.10, η_{532} for transparent water clouds remains fixed at 0.6. For opaque layers, however, layer-effective [water cloud multiple scattering factors are computed from the measured layer integrated volume depolarization ratios](#). As a consequence, under the appropriate conditions (e.g., single layer clouds in otherwise clear skies), estimates of water cloud lidar ratios can now be obtained from the multiple scattering factors and the 532 nm layer integrated attenuated backscatter estimates.

Extinction and Optical Depths

The particulate backscatter and extinction profiles and layer optical depths reported in the CALIOP V4.10 data products are produced by a modified and substantially enhanced version of the [hybrid extinction retrieval algorithm](#) used in earlier releases. Several developments are particularly noteworthy.

- Analysis of Opaque Layers

[The extinction retrieval used for opaque layers is entirely different](#). In V3 and earlier, the lidar ratios used for opaque layers were assigned by the scene classification algorithms based on layer type (i.e., cloud vs. aerosol) and subtype (e.g., ice vs. water, dust vs. smoke, etc.). In V4.10, initial estimates of the lidar ratios for opaque layers are [computed directly from the measured integrated attenuated backscatter](#), and refined as necessary within the extinction solver to ensure that extinction coefficients are calculated through the full vertical extent of the layer. This procedure yields highly precise and accurate layer-effective lidar ratios, which translate directly into more realistic extinction coefficient estimates and eliminate many artifacts previously seen in CALIOP optical depth distributions.

- Increased Number of Constrained Retrievals

[Constrained retrievals](#) use measurements of clear air above and below a lofted layer to directly estimate layer optical depth. These optical depths provide a constraint on the solution of the lidar equation, allowing the layer lidar ratio to be retrieved from the data rather than estimated a priori. In retrospect, the approach used in V3 and earlier was perhaps too timid, in that constrained solutions were only attempted for lofted layers with optical depths greater than ~0.3. In V4.10 constrained solutions (and hence lidar ratio estimates) are derived for all layers having valid two-way transmittance measurements. Uncertainties in the lidar ratio estimates are

now reported for all retrievals. While lidar ratios derived from layers with small optical depths can have large random uncertainties, the extinction retrievals are unbiased.

- More Precise Reporting of Retrieval Success

For each extinction profile retrieved, information about the termination state of the extinction algorithm is provided in the extinction QC flags. These flags are implemented as 16-bit unsigned integers. Multiple bits can be toggled within each extinction QC flag, with each bit conveying a specific piece of information. In V3, 10 of the 16 bits were used. The V4.10 algorithm uses 14 bits and is both more verbose and more rigorous in its assessment of retrieval quality. As a consequence, users will encounter many more distinct QC flags in V4.10 than in V3. For example, for all data collected in 2008 V3 reported only 19 different extinction QC flags at 532 nm. By contrast, V4.10 is expected to report in the neighborhood of 75 different values for the same time period. The most reliable retrievals have extinction QC flags of 0, 1, 2, 16 or 18. Data flagged with other values should be treated with varying degrees of suspicion. In aberrant cases, the extinction retrieval can fail. The backscatter and extinction coefficients reported for these failed retrievals are set to a fill value of -333.

- Improved Estimates of Extinction Uncertainties

During the V4.10 development, considerable attention was given to providing [more accurate estimates of the uncertainties](#) reported for the CALIOP extinction coefficients and optical depths. In particular, V4.10 lidar ratio uncertainty estimates are now verified and adjusted as appropriate on a layer-by-layer basis. In the V3 processing these uncertainty estimates were always specified a priori and never varied thereafter.

While layer-effective multiple scattering factors for opaque water clouds can be reliably estimated, the known range dependence of water cloud multiple scattering is not accounted for in the V4.10 CALIOP retrieval algorithm. Furthermore, the V4.10 extinction retrieval does not attempt to compensate for the loss of ranging information introduced by pulse stretching. As a result, beyond the first range bin (and frequently within the first range bin) the V4.10 CALIOP extinction retrievals in opaque water clouds should be considered entirely unreliable. To reinforce this notion, the uncertainties for opaque water clouds are not calculated, but instead are assigned a uniform fill value of -29.

- Summary of Extinction Changes from V3 to V4.10

The changes described above will have considerable impact on the magnitude of the V4.10 backscatter and extinction coefficients, their attendant uncertainties, and in those parameters subsequently derived from these values. However, it is critically important for data users to understand that the extinction and optical depth changes from V3 to V4.10 cannot be attributed wholly to changes in the extinction algorithm. Changes in the a priori specifications of layer multiple scattering factors and/or layer lidar ratios can by themselves introduce considerable changes in the retrieved values of extinction and optical depth. Similarly, changes in the calibration coefficients from V3 to V4.10 result in small increases in the L1 attenuated backscatter coefficients, which in turn yield concomitant but nonlinear increases in particulate backscatter and extinction coefficients.

Revised Ice-Water Content Algorithm

Cloud ice water content (IWC) is reported for all ice clouds detected by CALIOP. As in V3, IWC is a provisional data product calculated as [a parameterized function](#) of the CALIOP 532 nm extinction coefficients retrieved within ice clouds. In V4.10, the parameterization has been modified to include [a temperature-dependent particle size relationship](#) that approximates the observations compiled in an expanded set of aircraft microphysical data. Due to the cumulative impact of multiple factors, including the new ice mass parameterization and improved V4.10 calibration and extinction coefficient retrievals, users can expect V4.10 IWC to be significantly larger than V3 IWC; e.g., up to 6-8 times as large for thick ice clouds at warm temperatures. At cold temperatures, the V4.10 IWC calculated for a given extinction coefficient is smaller than in V3. However, since the extinction coefficients are larger in V4.10, the resulting change in IWC from V3 to V4.10 is relatively small.

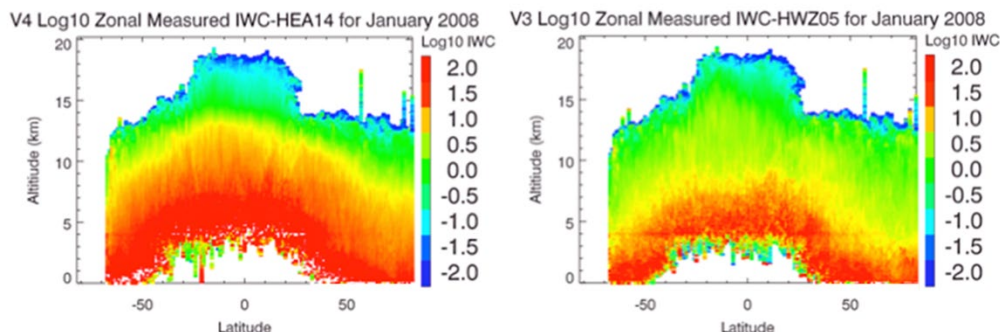


Figure 4: zonal mean IWC for January 2008 calculated from V4.10 data (left panel) and V3.01 data (right panel).

CALIPSO IWC is a highly derived data product. Besides the cloud particle area-to-mass parameterization, it relies on cloud feature determination (CAD), cloud phase determination, specification of lidar ratios and multiple scattering factors and the ensuing extinction retrieval. Uncertainty in cloud ice water content is affected by the [accuracy of the microphysical parameterization](#). However, the IWC uncertainty reported in the CALIPSO data products reflects only the uncertainty in the extinction coefficient retrieval. Because IWC is parameterized from ice particle extinction, it follows that data screening criteria for valid IWC should be similar to those used to identify valid extinction coefficients. Best results will likely be obtained by using only those data with high CAD scores that have also been classified as ice with high confidence.

New Data Product: 5-km Merged Layer Product

In response to numerous end-user requests, the V4.10 data release includes a new 5-km merged layer product that aggregates all of the information found in the existing 5-km cloud layer product and 5-km aerosol layer product and packages it into a single file. The 5-km merged layer product also contains a comprehensive subset of the data reported in the single shot layer product (as do the V4.10 5-km cloud and aerosol layer products), so that unambiguous cloud clearing information will always be immediately available. This new product offers several advantages to users of the CALIPSO layer products. In particular, (a) the spatial relationships between clouds and aerosols detected at varying averaging resolution in any column are fully specified and (b) the optical influences between layers of different types (e.g., the uncertainties in cloud optical depth retrievals for cirrus clouds lying above aerosol layers) can be readily appreciated and fully characterized. A complete specification of all parameters included in the 5-km merged layer product is given in the latest release of the CALIPSO Data Products Catalog.

Browse Image Improvements

The CALIPSO browse images have been augmented in the V4.10 release with new plots showing the cloud subtypes identified within each granule. The aerosol subtyping plots have been updated to reflect changes in aerosol subtyping and the addition of the stratospheric aerosol subtypes.

New Version 4.10 Data File Parameters

Table 2 lists all new parameters that have been added to the V4.10 data products. Of particular note is the inclusion of single shot layer detection information in all 5-km layer products.

Table 2: new scientific data sets reported in the CALIPSO V4.10 L2 data products

SDS name	VFM	Layer				Profile	
		1/3kmM	1kmC	5kmA	5kmC	5kmA	5kmC
Lidar Surface Detection (Vgroup)		✓	✓	✓	✓	✓	✓
Single Shot Detection (Vgroup)	✓			✓	✓		
Profile ID	✓					✓	✓
CAD Score		✓					
“Was Cleared” Flag		✓					
Opacity Flag		✓	✓				

	VFM	Layer				Profile	
SDS name		1/3kmM	1kmC	5kmA	5kmC	5kmA	5kmC
Layer Centroid Temperature		✓	✓		✓		
Initial CAD Score		✓	✓		✓		
Attenuated Scattering Ratio Statistics, 532 nm		✓	✓	✓	✓		
High Resolution Layers Cleared				✓	✓		
Final Lidar Ratio Uncertainty, 532 nm				✓	✓		
Final Lidar Ratio Uncertainty, 1064 nm					✓		
Ozone Number Density						✓	✓
IGBP Surface Type						✓	✓

Data Quality Statement for CALIPSO's Version 3.41 Lidar Level 2 Data Product Release

Data Version: 3.41

Data Release Date: October 02, 2020

Data Date Range: October 01, 2020 to present

Version 3.41 marks a change in the data products due to a required upgrade of the operating system on the cluster computer used to generate CALIPSO's publicly distributed data products. All program executables were re-compiled to process in this new environment with no changes made to the underlying science algorithms or inputs.

Data Quality Statement for CALIPSO's Version 3.40 Lidar Level 2 Data Product Release

Data Version: 3.40

Data Release Date: December 14, 2016

Data Date Range: December 01, 2016 to September 30, 2020

Version 3.40 release reflects an update of the Forward Processing – Instrument Teams (FP-IT) meteorological data provided by the Global Modeling and Assimilation Office (GMAO) from version 5.9.1 to version 5.12.4. No changes were made to the program executables.

Data Quality Statement for CALIPSO's Version 3.30 Lidar Level 2 Data Product Release

Data Version: 3.30

Data Release Date: April 19, 2013

Data Date Range: March 1, 2013 to November 30, 2016

Version 3.30 data products incorporate new versions of two important ancillary data products: (1) updated GMAO FP-IT meteorological data and (2) the enhanced Air Force Weather Authority (AFWA) snow and ice data set as ancillary inputs. Based on comparisons of CALIOP V3.02 data to the newly generated CALIOP V3.30 products, the transition to the new GEOS-5 FP-IT data is predicted to have only minimal effects on the science data products. Production of the V3.30 data set began with March 1, 2013.

Layer Detection

GEOS-5 molecular number densities increased in the CALIOP night and day calibration regions, which lowered the calibration coefficients and increased the attenuated backscatter coefficients, which in turn caused the number of layers detected to increase slightly. A two month of V3.02 to V3.30 showed that the number of aerosol and cloud layers increased by < 0.8% and < 0.2%, respectively.

Layer Classification

The GEOS-5 tropopause heights decreased by ~ 1 km between 30°S and 40°N . Since CALIOP classifies layers detected above the tropopause as stratospheric features, 3%–5% of the features formerly classified as stratospheric were reclassified as either cloud or aerosol. Over Antarctica in September 2011, tropopause heights decreased between 1.0 km and 1.5 km, causing all of cloud and aerosol layers with bases above the revised tropopause heights to be reclassified as stratospheric features. This effect may occur seasonally over Antarctica.

Data Quality Statement for CALIPSO's Version 3.02 Lidar Level 2 Data Product Release

Data Version: 3.02
Data Release Date: December 12, 2011
Data Date Range: November 1, 2011 to February 28, 2013

Version 3.02 represents a transition of the Lidar, IIR, and WFC science data processing and browse image production to a new cluster computing system. No algorithm changes were introduced, and only very minor changes were observed between V3.01 and V3.02 as a result of the compiler and computer architecture differences.

Data Quality Statement for CALIPSO's Version 3.01 Lidar Level 2 Data Product Release

Data Version: 3.01
Data Release Date: April 28, 2010
Data Date Range: June 13, 2006 to October 31, 2011

Version 3.01 of the Lidar Level 2 data products is a significant improvement over the previous version. Major code and algorithm improvements include:

- the elimination of a bug in the cloud clearing code that caused a substantial overestimate of low cloud fraction in earlier data releases (details given in [Vaughan et al., 2010](#));
- enhancements to the cloud-aerosol discrimination algorithm that increase the number of diagnostic parameters used to make classification decisions (details given in [Liu et al., 2010](#));
- improved daytime calibration procedures, resulting in more accurate estimates of layer spatial and optical properties (details given in [Powell et al., 2010](#)); and
- an entirely new algorithm for assessing cloud thermodynamic phase (details given in [Hu et al., 2009](#)).

Layer Detection

As in previous versions, the layer boundaries reported in the Lidar Level 2 Cloud and Aerosol Layer Products appear to be quite accurate. Some false positives are still found beneath optically thick layers; these, however, can generally be identified by their very low CAD scores (e.g., $|\text{CAD score}| \leq 20$). In opaque layers, the lowest altitude where signal is reliably observed is reported as the base. In actuality, this reported base may lie well above the true base. Opaque layers are denoted by an opacity flag. In this release, the layers which are reported represent a choice in favor of high reliability over maximum sensitivity. Weakly scattering layers sometimes will go unreported, in the interest of minimizing the number of false positives.

Cloud-Aerosol Discrimination

Figure 1 (below) compares the distributions of CAD scores derived from four months of version 3 test data to the corresponding version 2.01 data. The V3 curve shows a smoother distribution and generally has fewer low CAD values (i.e., values less than $\sim |95|$), reflecting the better separation of clouds and aerosols when using the version 3 5-D PDFs as compared to the separation provided by 3-D PDFs in previous versions. One notable exception to this observation is the bump between -10 and 20 in the V3 test curve, which accounts for $\sim 6\%$ of the total features.

The CAD scores in this region identify both outlier features whose optical/physical properties are not correctly measured or derived, and those features whose attributes fall within the overlap region between the cloud and aerosol PDFs. In contrast, these outliers are populated over the entire CAD span in the V2 release.

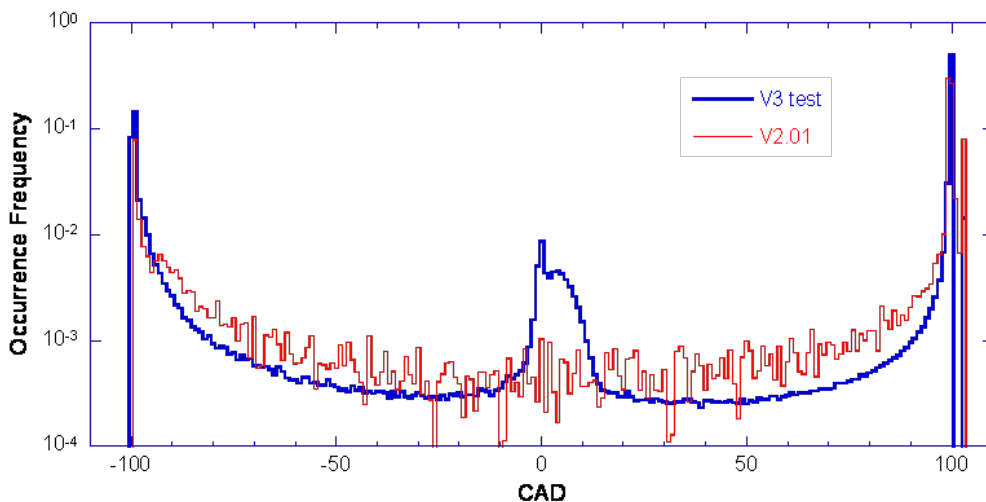


Figure 1: Histograms of CAD scores for Version 2 (red) and Version 3 (blue).

Figure 2 (below) presents the relationship between the CAD score and the layer IAB QA factor, which provides a measure of the integrated attenuated backscatter overlying a cloud or an aerosol layer. A layer IAB QA factor close to 1 indicates that the atmosphere above the layer under is clear. Decreasing values indicate the increasing likelihood of overlying layers that have attenuated the signal within the layer under consideration, and thus decreased the SNR of the measurement. A layer IAB QA factor of 0 would indicate total attenuation of the signal. As seen in the figure, the IAB QA is highest for high magnitude CAD scores and slopes down gradually for small CAD score magnitudes. This relationship reflects the fact that the presence of overlying features tends to add difficulty to the cloud-aerosol classification task, and therefore reduces the confidence of the classifications made. The dip between -10 and 20 represents features that are outliers in the 5-D CAD PDFs and indicates that these outliers most often lie beneath other relatively dense features. The cloud layers with special CAD scores (103 and 104) have the smallest IAB QA values. The relatively big value at CAD = 0 corresponds to the features having zero CAD values at high altitudes where the probability of the presence of overlying features is low. At high altitudes the separation of clouds and aerosols is not as good as at low altitudes because of the presence of subvisible cirrus clouds.

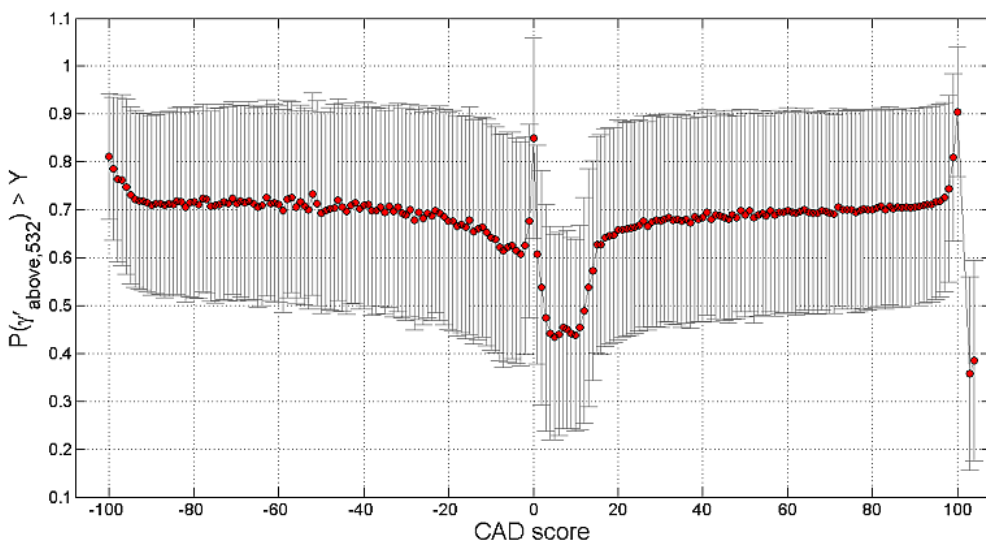


Figure 2: Relationship between CAD score and Layer IAB QA Factor

Overall, because of the better separation between clouds and aerosols in the 5D space, the 5D CAD algorithm significantly improves the reliability of the CAD scores. These improvements include:

1. Dense aerosol layers (primarily very dense dust and smoke over and close to the source regions), which are sometimes labeled as cloud in the V2 release, are now correctly identified as aerosol, largely because of the addition of the integrated volume depolarization ratio to the diagnostic parameters used for cloud-aerosol discrimination. In addition, in the open oceans, dense aerosols that were previously classified as clouds are now frequently observed in the marine boundary layer. Improvements are also seen for these maritime aerosols. Note, however, dense dust/smoke layers found at single-shot (0.333 km) resolution will be classified as cloud by default. This issue will be revisited for post-V3 releases.
2. Because the V2 CAD algorithm used a latitude-independent set of 3D PDFs, a class of optically thin clouds encountered in the polar regions that can extend from the surface to several kilometers were sometimes misclassified as aerosols. In version 3, these features are now correctly classified as cloud.
3. Correct classification of heterogeneous layers is always difficult. An example of a heterogeneous layer would be an aerosol layer that is vertically adjacent to a cloud or contains an embedded cloud, but which is nonetheless detected by the feature finder as a single entity in the V2 release. By convention, heterogeneous layers should be classified as clouds. The version 3 feature finding algorithm has also been improved greatly and can now much better separate the embedded or adjacent single-shot cloud layers from the surrounding aerosol. This improvement in layer detection contributes significantly to the improvement of the CAD performance.
4. Some so-called features identified by the layer detection scheme are not legitimate layers, but instead are artifacts due to the noise in the signal, multiple scattering effects, or to artificial signal enhancements caused by non-ideal detector transient response or an overestimate of the attenuation due to overlying layers. These erroneous "pseudo-features" are neither cloud nor aerosol and are distributed outside of the cloud and aerosol clusters in the PDF space. The V3 CAD algorithm can better identify these outlier features by assigning a small CAD score (the bump between -10 and 20 in the V3 CAD histogram) and classify most of them as cloud by convention. A CAD threshold of 20 can effectively filter out these outliers.

Some misclassifications may still occur with the 5D algorithm. For example, dust aerosols can be transported long distance to the Arctic. When moderately dense dust layers are occasionally transported to high latitudes, where cirrus clouds can present even in the low altitudes, they may be misclassified. This is also the case for moderately dense smoke aerosols occasionally transported to the high latitudes. Smoke can be mixed with ice particles during the long range transport, which makes the smoke identification even more difficult. When moderately dense dust and smoke are transported vertically to high altitudes, even at low latitudes, misclassifications can occur due to the presence of cirrus clouds. Volcanic aerosol that is newly injected into the high altitudes may have a large cross-polarized backscatter signal and thus may be misclassified as cloud.

Aerosol Type Identification

The main objective of the aerosol subtyping scheme is to estimate the appropriate value of the aerosol extinction-to-backscatter ratio (S_a) to within 30% of the true value. S_a is an important parameter used in the determination of the aerosol extinction and subsequently the optical depth from CALIOP backscatter measurements. S_a is an intensive aerosol property, i.e., a property that does not depend on the number density of the aerosol but rather on such physical and chemical properties as size distribution, shape, and composition. These properties depend primarily on the source of the aerosol and such factors as mixing, transport, and, in the case of hygroscopic aerosols, hydration.

The extinction products are produced by first identifying an aerosol type and then using the appropriate values of S_a and the multiple scattering factor, $\eta(z)$. Note that multiple scattering corrections have not yet been implemented for the current data release, so that $\eta(z) = 1$ for all aerosol types. The accuracy of the S_a value used in the lidar inversions depends on the correct identification of the type of aerosol. In turn, the accuracy of the subsequent optical depth estimate depends on the accuracy of S_a .

The underlying paradigm of the type classification is that a variety of emission sources and atmospheric processes will act to produce air masses with a typical, identifiable aerosol type. This is an idealization, but one that allows us to classify aerosols based on observations and location in a way to gain insight into the geographic distribution of aerosol types and constrain the possible values of S_a for use in aerosol extinction retrievals.

The aerosol subtype product is generated downstream of the cloud-aerosol discrimination (CAD) scheme and, therefore, depends on the cloud-aerosol classification scheme in a very fundamental way. If a cloud feature is misclassified as aerosol, the aerosol subtype algorithm will identify this 'aerosol' as one of the aerosol subtypes. The user must exercise caution where the aerosol subtype looks suspicious or unreasonable. Such situations can occur with some frequency in the southern oceans and the polar regions.

Cloud Ice/Water Phase Discrimination

The cloud phase algorithm used in Version 2 has been replaced with a new, completely different approach. The V3 algorithm classifies detected cloud layers as water, randomly-oriented ice (ROI), or horizontally-oriented ice (HOI) based on relations between depolarization, backscatter, and color ratio ([Hu et al. 2009](#)). These classifications have not yet been rigorously validated, which is difficult, but many of the obvious artifacts found in the V2 data have been eliminated.

The V2 algorithm included a rudimentary ability to identify a specific subset of high confidence instances of HOI. These clouds were classified as ice clouds and flagged with a 'special CAD score' of 102, indicating that they had been further classified as HOI. The new version 3 algorithm implements a much more sophisticated scheme for recognizing HOI that correctly identifies many more instances of these clouds. The special CAD score of 102 is no longer used to identify these layers. Instead, the "ice cloud" and "mixed phase cloud" classifications have been eliminated and replaced as shown in Table 1 below. Associated QC flags are given in Table 2.

Table 1: Updated Ice/Water Phase Flags

Value	V2 Interpretation	V3 Interpretation
0	unknown/not determined	unknown/not determined
1	ice	randomly oriented ice (ROI)
2	water	water
3	mixed phase	horizontally oriented ice (HOI)

Table 2: Updated Ice/Water Phase QC Flags

Value	V2 Interpretation	V3 Interpretation
0	no confidence	no/low confidence
1	low confidence	phase based on temperature only
2	medium confidence	medium confidence
3	high confidence	high confidence

A confidence flag of QA=1 indicates the phase classification is based on temperature. Initial classification tests are based on layer depolarization, layer-integrated backscatter, and layer-average attenuated backscatter color ratio. Layers classified as water with temperatures less than -40 C are forced to ROI and given confidence flags of QA=1. Layers classified as ROI or HOI with temperatures greater than 0 C are forced to water and also given confidence flags of QA=1. Clouds for which the phase is 'unknown/not determined' are assigned confidence values of 0 (no/low confidence).

Layers classified as HOI based on anomalously high backscatter and low depolarization are assigned QA=3. These layer characteristics are rarely detected after the CALIOP viewing angle was changed to 3° in November 2007. The V3 algorithm computes the spatial correlation of depolarization and integrated backscatter and uses this as an additional test of cloud phase. Layers classified as HOI using this test are assigned QA=2. The spatial correlation test is responsible for the majority of the layers classified as HOI. These layers typically have higher backscatter than ROI but similar depolarization and are common even at a viewing angle of 3°. We interpret this as clouds with

significant perpendicular backscatter from ROI but containing enough HOI to produce enhanced backscatter. These layers tend to be found at much colder temperatures than the high confidence HOI (see [Hu et al. 2009](#)).

Cloud and Aerosol Optical Depths

The reliability of cloud and aerosol optical depths reported in the V3 data products is considerably improved over the V2 release. Whereas the V2 optical depths were designated as a beta quality product, and not yet suitable for use in scientific publications, the maturity level of the V3 optical depths has been upgraded to provisional. Several algorithm improvements and bugs fixes factored into the decision to upgrade the maturity level. Among these were the addition of the [aerosol layer base extension algorithm](#), which greatly improves AOD estimates in the planetary boundary layer (PBL), and several significant improvements to the code responsible for rescaling the attenuated backscatter coefficients in lower layers to compensate for the beam attenuation that occurs when traversing transparent upper layers.

Data Quality Statement for CALIPSO's Version 2.02 Lidar Level 2 Data Product Release

Data Version: 2.02
Data Release Date: October 2008
Data Date Range: September 14, 2008 to October 29, 2009

Version 2.02 of the Level 2 data products is a maintenance release that implements the following changes.

- Corrections were made to the code used to interpolate the GMAO meteorological data products to the CALIPSO orbit tracks.
- The Cabanes backscattering cross-sections used to derive the molecular scattering models used for the Level 1 and Level 2 analyses were revised downward by ~0.8%.
- A typographical error was identified in the runtime script that controls the behavior of the aerosol subtyping algorithm in the Level 2 analyses.

The impacts of these changes on the Level 2 data products are as follows.

Layer Detection

As a result of the first two changes, the 532 nm and 1064 nm calibration constants are larger, on average, by ~1%, resulting in corresponding decreases in the magnitudes of the attenuated backscatter coefficients at both wavelengths. These changes in the level 1 data result in only small changes to the layer detection statistics. For example, the difference in the total number of layers detected by the two different versions on August 12, 2006 was 4: 9680 layers were detected by the V2.01 code versus 9676 layers detected by the V2.02 code.

Cloud-Aerosol Discrimination

With one exception, there were only minimal changes in cloud-aerosol discrimination results. The exception occurs in the polar regions when PSCs are present. For the August 12, 2006 test case, corrections to the interpolation algorithms applied to the GMAO data result in a slight upward shift in the tropopause heights and hence more clouds and fewer stratospheric layers are identified in the V2.02 results.

Cloud Ice/Water Phase Discrimination

Because this classification is based on depolarization ratio and temperature no substantial changes, there were no substantial changes in the assessments of cloud thermodynamic state.

Aerosol Subtype Identification

Correcting the level 2 runtime script error will reduce the number of layers identified as smoke and increase the number of layers identified as sea salt.

Cloud and aerosol extinction profiles and optical properties

Changes in backscatter and extinction coefficients at the tops of layers are small and proportional to the changes in the calibration coefficients. However, due to the cumulative nature of error propagation in the extinction retrieval, differences between V2.02 and V2.01 increase with increasing penetration depths, and can grow large when optical depths are large (i.e., > 3).

Data Quality Statement for CALIPSO's Version 2.01 Lidar Level 2 Data Product Release

Data Version: 2.01
Data Release Date: January 2008
Data Date Range: June 13, 2006 to September 13, 2008

Layer Detection

Given the accuracy of the CALIPSO altitude registration, the layer heights reported in the Lidar Level 2 Cloud and Aerosol Layer Products appear to be quite accurate. In optically dense layers, the lowest altitude where signal is reliably observed is reported as the base. In actuality, this reported base may lie well above the true base. In this release, the layers which are reported represent a choice in favor of high reliability over maximum sensitivity. Weakly scattering layers sometimes will go unreported, in the interest of minimizing the number of false positives.

Cloud-Aerosol Discrimination

Based on the initial CALIOP measurements, an improved version of the cloud-aerosol discrimination (CAD) algorithm has been implemented for this release. Overall, the updated algorithm works well in most cases; manual verification of the classifications for a full day of data suggests that the success rate is in the neighborhood of 90% or better. Nevertheless, several types of misclassifications are still occurred with some frequency. Among these, the most prevalent are:

- Dense aerosol layers (primarily very dense dust and smoke over and close to the source regions) are sometimes labeled as cloud. Because the CAD algorithm operates on individual layers, without a contextual awareness of any surrounding features, it can happen that small but strongly scattering regions within an extended aerosol layer can occasionally be labeled as cloud. This occurs because the optical properties (backscatter and color ratio) within the region are similar to what would be expected for the relatively faint clouds that fall within the PDF overlap region. These misclassifications are often apparent from studying the Level 1 browse images. Based on the initial analysis of the CALIOP measurements, the cloud and aerosol distributions show variabilities that depend on season and on geophysical location. The globally averaged PDFs used in the current release will have a larger overlap between the cloud and aerosol than would occur for more regionally specific statistics. For future versions of the CAD algorithm, we expect to develop and deploy PDFs that will correctly reflect both seasonal and latitudinal variations.
- Many optically thin clouds, both ice and water, are encountered in the polar regions. The current CAD PDFs do not work as well in the polar regions as at lower latitudes and misclassifications of clouds as aerosol are more common. In particular, thin ice clouds which can extend from the surface to several kilometers in altitude, are sometimes misclassified as aerosol.
- Correct classification of heterogeneous layers is always difficult, and the process can easily go awry. An example of a heterogeneous layer would be an aerosol layer that is vertically adjacent to a cloud or contains an embedded cloud, but which is nonetheless detected by the feature finder as a single entity. By convention, heterogeneous layers should be classified as clouds. However, depending on the relative strengths of the components, these layers are sometimes erroneously identified as aerosol.

Some so-called features identified by the layer detection scheme are not legitimate layers, but instead are artifacts due to the noise in the signal, multiple scattering effects, or to artificial signal enhancements caused by non-ideal detector transient response or an overestimate of the attenuation due to overlying layers. These erroneous

"pseudo-features" are neither cloud nor aerosol; however, because they are not properly interdicted in the processing stream, the CAD algorithm nonetheless attempts to assign them to one class or the other. Very frequently these layers can be identified by their very low CAD scores (typically less than 20).

Cloud Ice/Water Phase Discrimination

Cloud phase is determined using a depolarization/backscatter relation, together with temperature and backscatter thresholds. Complete descriptions of the algorithm mechanics and underlying theory are given in Section 6 of the CALIPSO Scene Classification ATBD. The algorithm implemented for the version 2.01 release identifies obvious water and ice clouds and clear cases of oriented ice crystals. Improvements for recognizing mixed phase clouds are planned for future release.

Aerosol Subtype Identification

The main objective of the aerosol subtyping scheme is to estimate the appropriate value of the aerosol extinction-to-backscatter ratio (S_a) to within 30% of the true value. S_a is an important parameter used in the determination of the aerosol extinction and subsequently the optical depth from CALIOP backscatter measurements. S_a is an intensive aerosol property, i.e., a property that does not depend on the number density of the aerosol but rather on such physical and chemical properties as size distribution, shape and composition. These properties depend primarily on the source of the aerosol and such factors as mixing, transport, and in the case of hygroscopic aerosols, hydration.

The extinction products are produced by first identifying an aerosol type and then using the appropriate values of S_a and the multiple scattering factor, $\eta(z)$. Note that multiple scattering corrections have not yet been implemented for the current data release, so that $\eta(z) = 1$ for all aerosol types. The accuracy of the S_a value used in the lidar inversions depends on the correct identification of the type of aerosol. In turn, the accuracy of the subsequent optical depth estimate depends on the accuracy of S_a . The underlying paradigm of the type classification is that a variety of emission sources and atmospheric processes will act to produce air masses with a typical, identifiable aerosol 'type'. This is an idealization, but one that allows us to classify aerosols based on observations and location in a way to gain insight into the geographic distribution of aerosol types and constrain the possible values of S_a for use in aerosol extinction retrievals. The aerosol subtype product is generated downstream of the cloud-aerosol discrimination (CAD) scheme and, therefore, depends on the cloud-aerosol classification scheme in a very fundamental way. If a cloud feature is misclassified as aerosol, the aerosol subtype algorithm will identify this 'aerosol' as one of the aerosol subtypes. The user must exercise caution where the aerosol subtype looks suspicious or unreasonable. Such situations can occur with some frequency in the southern oceans and the polar regions.

Cloud and aerosol extinction profiles

The CALIOP cloud and aerosol profiles of extinction and backscatter are released as beta products. Cloud profiles are reported at a horizontal resolution of 5 km; aerosol profiles are reported at a horizontal resolution of 40 km. These products contain a number of known errors and, in their current form, cannot be used as standalone products. The current products contain no data quality information, and hence must be used in conjunction with the Cloud and/or Aerosol Layer Products and/or the Vertical Feature Mask Product, which contain data quality parameters and confidence flags. Data assessment and screening procedures have not yet been developed. Because of this, the profile data product is considered to be not appropriate for scientific publication but is released to users for evaluation and to provide feedback to the CALIOP algorithm development team. PLEASE NOTE: users of the CALIOP extinction and backscatter profile data should read and thoroughly understand the information provided in the Profile Products Data Quality Summary. This summary contains an expanded description of the extinction retrieval process from which the layer optical depths are derived and provides essential guidance in the appropriate use of all CALIOP extinction-related data products. Validation and improvements to the profile products QA are ongoing efforts, and additional data quality information will be included with future releases.

Cloud and aerosol optical depths

Because comprehensive data assessment and screening procedures have not yet been developed, the CALIOP cloud and aerosol optical depths reported in the V2.01 data release are not considered appropriate for scientific publication. The data is being released as a beta quality product, for evaluation by the user community, and to provide feedback to the CALIOP algorithm development team.

Data Quality Statement for CALIPSO's Version 1.10 Lidar Level 2 Data Product Release

Data Version: 1.10
Data Release Date: December 8, 2006
Data Date Range: June 13, 2006 to November 11, 2007

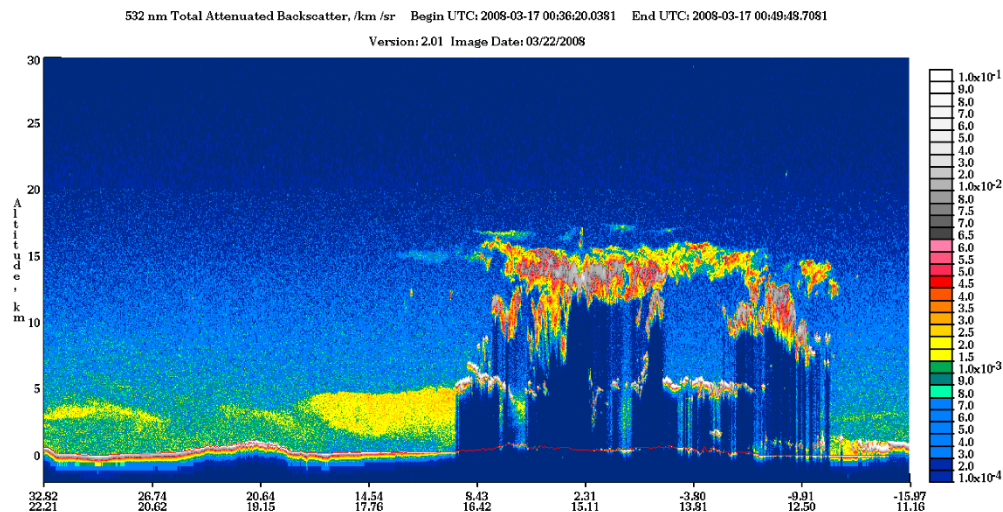
The CALIPSO vertical feature mask (VFM) data product reports a single 16-bit integer for each lidar altitude resolution element in the data stream downlinked from the satellite. Upon decoding each of these bit-mapped integers, users will obtain information describing layer location (both vertically and horizontally), layer type, and the amount of horizontal averaging required for the layer to be detected.

Given the accuracy of the CALIPSO altitude registration, the layer heights reported in the Lidar Level 2 Cloud and Aerosol Layer Products and the VFM appear to be quite accurate. In optically dense layers, the lowest altitude where signal is observed is reported as the base. In actuality, this point may lie well above the true base. In this release, the layers which are reported represent a choice in favor of high reliability over maximum sensitivity. Weakly scattering layers sometimes will go unreported, in the interest of minimizing the number of false positives.

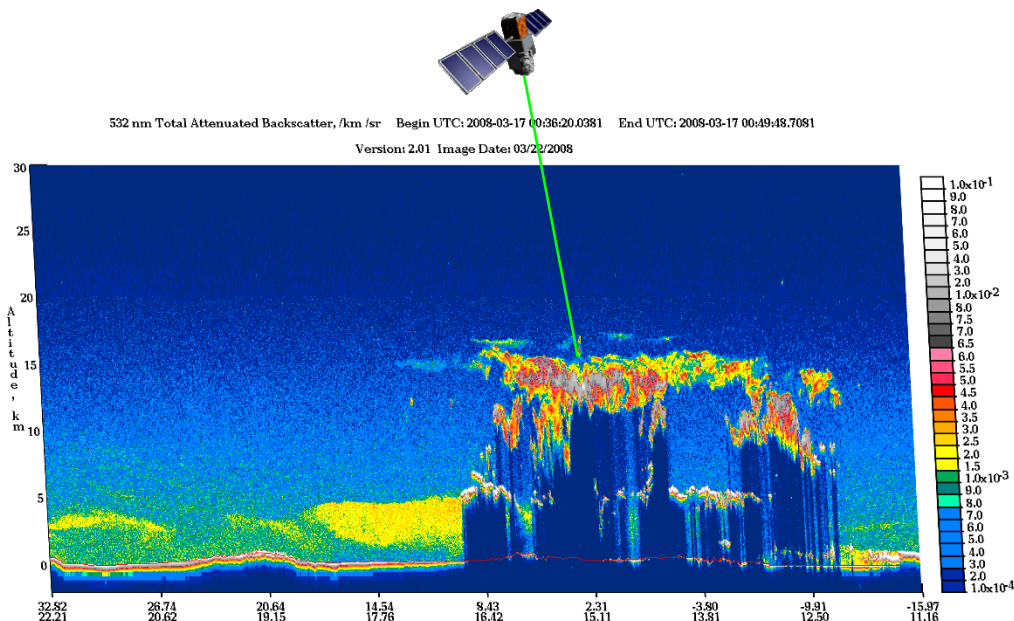
A preliminary version of the algorithm to discriminate cloud and aerosol has been used in this release. Overall, the algorithm performance is fairly good at labeling cloud as cloud and somewhat less successful in labeling aerosol as aerosol. Several types of misclassifications are fairly common and should be watched for. The most common misclassification is portions of dense aerosol layers being labeled as cloud. The algorithm operates on individual profiles, so small regions within an aerosol layer are sometimes labeled as cloud. These misclassifications are often apparent from study of Level 1 browse images. Actual clouds occurring within aerosol layers appear to be correctly classified as cloud most of the time. Additionally, portions of the bases of some cirrus clouds are mislabeled as aerosol, and some tropospheric polar clouds are erroneously labeled as aerosol. Improvements to the cloud/aerosol discrimination algorithm are underway and misclassifications should be greatly reduced in future data releases.

Appendix 1

Prior to November 28, 2007, CALIPSO was nominally pointed in a 'near nadir' direction (actually at $\sim 0.3^\circ$ off nadir, to avoid the full force of specular reflections from still waters and horizontally oriented ice crystals). In that pointing configuration, the CALIOP browse images – as shown below – correctly represented both the spatial distribution of clouds and aerosols, and the optical effects of overlying layers on the atmosphere below.



As a result of the change to pointing 3° off-nadir, with the tilt being in the same plane as the satellite velocity vector (i.e., along track, rather than cross track), the spatial distribution of layers is not exactly what is shown in the standard browse images. A more faithful representation might look like this...



There are several aspects of this change that could be of interest to data users:

1. While there is now a 3° vertical shear in the spatial distribution of clouds and aerosols (i.e., as shown above), the optical effects of overlying layers are still correctly represented by the original, upright images that are being shown on our web pages.
2. The altitudes reported in all products are still measured with respect to a nadir viewing instrument, and thus users need not (and should not) make any corrections for pointing angle.
3. The laser footprint locations reported in the data products give the latitude and longitude coordinates of the beam location on the Earth at mean sea level.
4. The horizontal offset between any two points in the vertical can be computed using 'triangle trig'. If the vertical distance is V , the horizontal offset, Δh , between the upper and lower points is $\Delta h = V \cdot \tan(3^\circ)$.
5. Version 2 of the data products includes a new 'Spacecraft_Position' SDS that contains all of the spacecraft attitude information required to vertically collocate the CALIPSO and CloudSat profiles. This was included at the request of the CloudSat team, specifically for the continued production of their GeoProf products.

6. In general, the optical properties reported for measurements of aerosols and water clouds are not expected to change as a function of the change in pointing angle. However, the properties reported for individual ice clouds will change by some varying amount, depending on the concentration of horizontally aligned ice crystals present in the cloud. Among the changes that can be anticipated are
- a reduction in the maximum values of integrated attenuated backscatter measured at both wavelengths;
 - an increase in the minimum depolarization ratios associated with strongly scattering ice clouds;
 - a small change in the proportion of clouds classified as ice versus those classified as water; and
 - an increase in the minimum lidar ratios retrieved for strongly scattering ice clouds.

References

- Burton, S. P., R. A. Ferrare, M. A. Vaughan, A. H. Omar, R. R. Rogers, C. A. Hostetler, and J. W. Hair, 2013: Aerosol Classification from Airborne HSRL and Comparisons with the CALIPSO Vertical Feature Mask, *Atmos. Meas. Tech.*, **6**, 1397–1412, <https://doi.org/10.5194/amt-6-1397-2013>.
- Chand, D., T. L. Anderson, R. Wood, R. J. Charlson, Y. Hu, Z. Liu, and M. Vaughan, 2008: Quantifying above-cloud aerosol using spaceborne lidar for improved understanding of cloudy-sky direct climate forcing, *J. Geophys. Res.*, **113**, D13206, <https://doi.org/10.1029/2007JD009433>.
- Garnier, A., J. Pelon, M. A. Vaughan, D. M. Winker, C. R. Trepte, and P. Dubuisson, 2015: Lidar multiple scattering factors inferred from CALIPSO lidar and IIR retrievals of semi-transparent cirrus cloud optical depths over oceans, *Atmos. Meas. Tech.*, **8**, 2759–2774, <https://doi.org/10.5194/amt-8-2759-2015>.
- Getzewich, B. J., M. A. Vaughan, W. H. Hunt, M. A. Avery, K. A. Powell, J. L. Tackett, D. M. Winker, J. Kar, K.-P. Lee, and T. Toth, 2018: CALIPSO Lidar Calibration at 532-nm: Version 4 Daytime Algorithm, *Atmos. Meas. Tech.*, **11**, 6309–6326, <https://doi.org/10.5194/amt-11-6309-2018>.
- Haarig, M., R. Engelmann, H. Baars, B. Gast, D. Althausen and A. Ansmann, 2025: Discussion of the spectral slope of the lidar ratio between 355 nm and 1064 nm from multiwavelength Raman lidar observations, *Atmos. Chem. Phys.*, **25**, 7741–7763, <https://doi.org/10.5194/acp-25-7741-2025>.
- Heymsfield, A. J., D. Winker, and G.-J. van Zadelhoff, 2005: Extinction-ice water content-effective radius algorithms for CALIPSO, *Geophys. Res. Lett.*, **32**, L10807, <https://doi.org/10.1029/2005GL022742>.
- Heymsfield, A., D. Winker, M. Avery, M. Vaughan, G. Diskin, M. Deng, V. Mitev, and R. Matthey, 2014: Relationships between Ice Water Content and Volume Extinction Coefficient from In Situ Observations for Temperatures from 0° to -86°C: Implications for Spaceborne Lidar Retrievals, *J. Appl. Meteor. Climatol.*, **53**, 479–505, <https://doi.org/10.1175/JAMC-D-13-087.1>.
- Holz, R. E., S. Platnick, K. Meyer, M. Vaughan, A. Heidinger, P. Yang, G. Wind, S. Dutcher, S. Ackerman, N. Amarasinghe, F. Nagle, and C. Wang, 2016: Resolving ice cloud optical thickness biases between CALIOP and MODIS using infrared retrievals, *Atmos. Chem. Phys.*, **16**, 5075–5090, <https://doi.org/10.5194/acp-16-5075-2016>.
- Hu, Y. M. Vaughan, Z. Liu, B. Lin, P. Yang, D. Flittner, W. Hunt, R. Kuehn, J. Huang, D. Wu, S. Rodier, K. Powell, C. Trepte, and D. Winker, 2007: The depolarization-attenuated backscatter relation: CALIPSO lidar measurements vs. theory, *Opt. Express*, **15**, 5327–5332, <https://doi.org/10.1364/OE.15.005327>.
- Hu, Y., M. Vaughan, Z. Liu, K. Powell, and S. Rodier, 2007: Retrieving Optical Depths and Lidar Ratios for Transparent Layers Above Opaque Water Clouds From CALIPSO Lidar Measurements, *IEEE Geosci. Remote Sens. Lett.*, **4**, 523–526, <https://doi.org/10.1109/LGRS.2007.901085>.
- Hu, Y., D. Winker, M. Vaughan, B. Lin, A. Omar, C. Trepte, D. Flittner, P. Yang, W. Sun, Z. Liu, Z. Wang, S. Young, K. Stamnes, J. Huang, R. Kuehn, B. Baum, and R. Holz, 2009: CALIPSO/CALIOP Cloud Phase Discrimination Algorithm, *J. Atmos. Oceanic Technol.*, **26**, 2293–2309, <https://doi.org/10.1175/2009JTECHA1280.1>.

- Hunt, W. H, D. M. Winker, M. A. Vaughan, K. A. Powell, P. L. Lucker, and C. Weimer, 2009: CALIPSO Lidar Description and Performance Assessment, *J. Atmos. Oceanic Technol.*, **26**, 1214–1228, <https://doi.org/10.1175/2009JTECHA1223.1>.
- Kar, J., M. A. Vaughan, K. P. Lee, J. Tackett, M. Avery, A. Garnier, B. Getzewich, W. Hunt, D. Josset, Z. Liu, P. Lucker, B. Magill, A. Omar, J. Pelon, R. Rogers, T. D. Toth, C. Trepte, J.-P. Vernier, D. Winker, and S. Young, 2018: CALIPSO Lidar Calibration at 532 nm: Version 4 Nighttime Algorithm, *Atmos. Meas. Tech.*, **11**, 1459–1479, <https://doi.org/10.5194/amt-11-1459-2018>.
- Kim, M.-H., A. H. Omar, J. L. Tackett, M. A. Vaughan, D. M. Winker, C. R. Trepte, Y. Hu, Z. Liu, L. R. Poole, M. C. Pitts, J. Kar, and B. E. Magill, 2018: The CALIPSO Version 4 Automated Aerosol Classification and Lidar Ratio Selection Algorithm, *Atmos. Meas. Tech.*, **11**, 6107–6135, <https://doi.org/10.5194/amt-11-6107-2018>.
- Liu, Z., R. Kuehn, M. Vaughan, D. Winker, A. Omar, K. Powell, C. Trepte, Y. Hu, and C. Hostetler, 2010: The CALIPSO Cloud And Aerosol Discrimination: Version 3 Algorithm and Test Results, 25th International Laser Radar Conference (ILRC), 5–9 July 2010, St. Petersburg, Russia; see <https://www.researchgate.net/publication/285685007>.
- Liu, Z., J. Kar, S. Zeng, J. Tackett, M. Vaughan, M. Avery, J. Pelon, B. Getzewich, K.-P. Lee, B. Magill, A. Omar, P. Lucker, C. Trepte, and D. Winker, 2019: Discriminating Between Clouds and Aerosols in the CALIOP Version 4.1 Data Products, *Atmos. Meas. Tech.*, **12**, 703–734, <https://doi.org/10.5194/amt-12-703-2019>.
- Liu, Z., R. Kuehn, M. Vaughan, D. Winker, A. Omar, K. Powell, C. Trepte, Y. Hu, and C. Hostetler, 2010: The CALIPSO Cloud And Aerosol Discrimination: Version 3 Algorithm and Test Results, 25th International Laser Radar Conference (ILRC), 5–9 July 2010, St. Petersburg, Russia; see <https://www.researchgate.net/publication/285685007> The CALIPSO cloud and aerosol discrimination Version 3 algorithm and test results.
- Liu, Z., J. Kar, S. Zeng, J. Tackett, M. Vaughan, M. Avery, J. Pelon, B. Getzewich, K.-P. Lee, B. Magill, A. Omar, P. Lucker, C. Trepte, and D. Winker, 2019: Discriminating Between Clouds and Aerosols in the CALIOP Version 4.1 Data Products, *Atmos. Meas. Tech.*, **12**, 703–734, <https://doi.org/10.5194/amt-12-703-2019>.
- Lopes, F. J. S., E. Landulfo, and M. A. Vaughan, 2013: Evaluating CALIPSO's 532 nm lidar ratio selection algorithm using AERONET sun photometers in Brazil, *Atmos. Meas. Tech.*, **6**, 3281–3299, <https://doi.org/10.5194/amt-6-3281-2013>.
- Lu, X., Y. Hu, Z. Liu, S. Rodier, M. Vaughan, C. Trepte, and J. Pelon, 2017: Observations of Arctic snow and sea ice cover from CALIOP lidar measurements, *Remote Sens. Environ.*, **194**, 248–263, <https://doi.org/10.1016/j.rse.2017.03.046>.
- Lu, Z., X. Liu, Z. Zhang, C. Zhao, K. Meyer, C. Rajapakshe, C. Wu, Z. Yang and J. E. Penner, 2018: Biomass smoke from southern Africa can significantly enhance the brightness of stratocumulus over the southeastern Atlantic Ocean, *PNAS*, **115**, 2924–2929, <https://doi.org/10.1073/pnas.1713703115>.
- Miller, S. D. and G. L. Stephens, 1999: Multiple scattering effects in the lidar pulse stretching problem, *J. Geophys. Res. Atmos.*, **104**, 22205–22219, <https://doi.org/10.1029/1999JD900481>.
- Mioche, G., D. Josset, J.-F. Gayet, J. Pelon, A. Garnier, A. Minikin and A. Schwarzenboeck. 2010: Validation of the CALIPSO-CALIOP extinction coefficients from in situ observations in midlatitude cirrus clouds during the CIRCLE-2 experiment, *J. Geophys. Res. Atmos.*, **115**, D00H25, <https://doi.org/10.1029/2009JD012376>.
- Omar, A., D. Winker, C. Kittaka, M. Vaughan, Z. Liu, Y. Hu, C. Trepte, R. Rogers, R. Ferrare, R. Kuehn, and C. Hostetler, 2009: The CALIPSO Automated Aerosol Classification and Lidar Ratio Selection Algorithm, *J. Atmos. Oceanic Technol.*, **26**, 1994–2014, <https://doi.org/10.1175/2009JTECHA1231.1>.
- Papagiannopoulos, N. and 15 coauthors, 2016: CALIPSO climatological products: evaluation and suggestions from EARLINET, *Atmos. Chem. Phys.*, **16**, 2341–2357, <https://doi.org/10.5194/acp-16-2341-2016>.

- Platt, C. M. R., D. M. Winker, M. A. Vaughan and S. D. Miller, 1999: Backscatter-to-Extinction Ratios in the Top Layers of Tropical Mesoscale Convective Systems and in Isolated Cirrus from LITE Observations, *J. Appl. Meteor. Climatol.*, **38**, 1330–1345, [https://doi.org/10.1175/1520-0450\(1999\)038<1330:BTERIT>2.0.CO;2](https://doi.org/10.1175/1520-0450(1999)038<1330:BTERIT>2.0.CO;2).
- Powell, K. A., C. A. Hostetler, Z. Liu, M. A. Vaughan, R. E. Kuehn, W. H. Hunt, K. Lee, C. R. Trepte, R. R. Rogers, S. A. Young, and D. M. Winker, 2009: CALIPSO Lidar Calibration Algorithms: Part I - Nighttime 532 nm Parallel Channel and 532 nm Perpendicular Channel, *J. Atmos. Oceanic Technol.*, **26**, 2015–2033, <https://doi.org/10.1175/2009JTECHA1242.1>.
- Powell, K. A., M. A. Vaughan, R. R. Rogers, R. E. Kuehn, W. H. Hunt, K-P. Lee, and T. D. Murray, 2010: The CALIOP 532-nm Channel Daytime Calibration: Version 3 Algorithm, 25th International Laser Radar Conference (ILRC), 5–9 July 2010, St. Petersburg, Russia; see <https://www.researchgate.net/publication/391011856>.
- Rajapakshe, C., Z. Zhang, J. E. Yorks, H. Yu, Q. Tan, K. Meyer, S. Platnick and D. M. Winker, 2017: Seasonally Transported Aerosol Layers over Southeast Atlantic are Closer to Underlying Clouds than Previously Reported, *Geophys. Res. Lett.*, **44**, <https://doi.org/10.1002/2017GL073559>.
- Redemann, J. and 68 coauthors, 2021: An overview of the ORACLES (ObseRvations of Aerosols above CLouds and their intEractionS) project: aerosol–cloud–radiation interactions in the southeast Atlantic basin, *Atmos. Chem. Phys.*, **21**, 1507–1563, <https://doi.org/10.5194/acp-21-1507-2021>.
- Rodriguez, J. V., R. C. Verhappen, C. Weimer, C. R. Trepte and T. E. Cayton, 2022: Charged Particle Fluxes Associated with CALIPSO Low Laser Energy Shots, *IEEE T. Nucl. Sci.*, **69**, 2146–2153, <https://doi.org/10.1109/TNS.2022.3204715>.
- Ryan, R. A., M. A. Vaughan, S. D. Rodier, J. L. Tackett, J. A. Reagan, R. A. Ferrare, J. W. Hair, and B. J. Getzewich, 2024: Total Column Optical Depths Retrieved from CALIPSO Lidar Ocean Surface Backscatter, *Atmos. Meas. Tech.*, **17**, 6517–6545, <https://doi.org/10.5194/amt-17-6517-2024>.
- Tackett, J., M. Vaughan, J. Lambeth, and A., Garnier, 2022: Critical Improvements to CALIOP Boundary Layer Cloud-Clearing in Version 4.5, 2022 CALIPSO/CloudSat Science Team Meeting, 12–14 September 2022, Fort Collins, CO USA, <https://ntrs.nasa.gov/citations/20220013563>.
- Tackett, J. L., J. Kar, M. A. Vaughan, B. Getzewich, M.-H. Kim, J.-P. Vernier, A. H. Omar, B. Magill, M. C. Pitts, and D. Winker, 2023: The CALIPSO version 4.5 stratospheric aerosol subtyping algorithm, *Atmos. Meas. Tech.*, **16**, 745–768, <https://doi.org/10.5194/amt-16-745-2023>.
- Tackett, J. L., R. A. Ryan, A. E. Garnier, J. Kar, B. Getzewich, X. Cai, M. A. Vaughan, C. R. Trepte, R. Verhappen, D. M. Winker and K.-P. A. Lee, 2025: Mitigating Impacts of Low Energy Laser Pulses on CALIOP Data Products, *EGUsphere* [AMTD], <https://doi.org/10.5194/egusphere-2025-2376>, accepted for publication.
- Toth, T. D., J. Zhang, J. R. Campbell, J. S. Reid, Y. Shi, R. S. Johnson, A. Smirnov, M. A. Vaughan, and D. M. Winker, 2013: Investigating Enhanced Aqua MODIS Aerosol Optical Depth Retrievals over the Mid-to-High Latitude Southern Oceans through Intercomparison with Co-Located CALIOP, MAN, and AERONET Datasets, *J. Geophys. Res. Atmos.*, **118**, 4700–4714, <https://doi.org/10.1002/jgrd.50311>.
- Toth, T. D., J. R. Campbell, J. S. Reid, J. L. Tackett, M. A. Vaughan, J. Zhang, and J. W. Marquis, 2018: Minimum Aerosol Layer Detection Sensitivities and their Subsequent Impacts on Aerosol Optical Thickness Retrievals in CALIPSO Level 2 Data Products, *Atmos. Meas. Tech.*, **11**, 499–514, <https://doi.org/10.5194/amt-11-499-2018>.
- Toth, T. D., M. Clayton, Z. Li, D. Painemal, S. Rodier, J. Kar, T. Thorsen, R. Ferrare, M. Vaughan, J. Tackett, H. Bian, M. Chin, A. Garnier, E. Welton, R. Ryan, C. Trepte and D. Winker, 2025: Mapping CALIPSO Marine and Dusty Marine Aerosol Lidar Ratios using MODIS AOD Constrained Retrievals and GOCART Model Simulations, *EGUsphere* [AMTD], <https://doi.org/10.5194/egusphere-2025-2832>, accepted for publication.
- Vaughan, M., K. Powell, R. Kuehn, S. Young, D. Winker, C. Hostetler, W. Hunt, Z. Liu, M. McGill, and B. Getzewich, 2009: Fully Automated Detection of Cloud and Aerosol Layers in the CALIPSO Lidar Measurements, *J. Atmos. Oceanic Technol.*, **26**, 2034–2050, <https://doi.org/10.1175/2009JTECHA1228.1>.

- Vaughan, M., R. Kuehn, J. Tackett, R. Rogers, Z. Liu, A. Omar, B. Getzewich, K. Powell, Y. Hu, S. Young, M. Avery, D. Winker, and C. Trepte, 2010: Strategies for Improved CALIPSO Aerosol Optical Depth Estimates, 25th International Laser Radar Conference (ILRC), 5–9 July 2010, St. Petersburg, Russia, <https://ntrs.nasa.gov/citations/20100026019>.
- Vaughan, M., K.-P. Lee, A. Garnier and B. Getzewich, 2016: Improvements to the CALIOP Surface Detection Algorithm, 2016 CALIPSO CloudSat Science Team Meeting, 1-3 March 2016, Newport News, VA USA, <https://doi.org/10.13140/RG.2.2.21628.04481>.
- Vaughan, M., A. Garnier, D. Josset, M. Avery, K.-P. Lee, Z. Liu, W. Hunt, J. Pelon, Y. Hu, S. Burton, J. Hair, J. Tackett, B. Getzewich, J. Kar, and S. Rodier, 2019: CALIPSO Lidar Calibration at 1064 nm: Version 4 Algorithm, *Atmos. Meas. Tech.*, **12**, 51–82, <https://doi.org/10.5194/amt-12-51-2019>.
- Venkata, S. L. and J. A. Reagan, 2016: Aerosol Retrievals from CALIPSO Lidar Ocean Surface Returns, *Remote Sens.*, **8**, 1006, <https://doi.org/10.3390/rs8121006>.
- Yang, P., L. Bi, B. A. Baum, K.-N. Liou, G. W. Kattawar, M. I. Mishchenko, and B. Cole, 2013: Spectrally Consistent Scattering, Absorption, and Polarization Properties of Atmospheric Ice Crystals at Wavelengths from 0.2 to 100 μm , *J. Atmos. Sci.*, **70**, 330–347, <https://doi.org/10.1175/JAS-D-12-039.1>.
- Young, S. A. and M. A. Vaughan, 2009: The retrieval of profiles of particulate extinction from Cloud Aerosol Lidar Infrared Pathfinder Satellite Observations (CALIPSO) data: Algorithm description, *J. Atmos. Oceanic Technol.*, **26**, 1105–1119, <https://doi.org/10.1175/2008JTECHA1221.1>.
- Young, S. A., M. A. Vaughan, J. L. Tackett, A. Garnier, J. B. Lambeth, and K. A. Powell, 2018: Extinction and Optical Depth Retrievals for CALIPSO's Version 4 Data Release, *Atmos. Meas. Tech.*, **11**, 5701–5727, <https://doi.org/10.5194/amt-11-5701-2018>.